Osseointegrated system for fixation of upper leg protheses

Tomaszewski, Pawel Krzysztof

Osseointegrated system for fixation of upper leg prostheses

Paweł Krzysztof Tomaszewski

The research described in this thesis was primarily performed at the Department of Biomedical Engineering of the University Medical Center Groningen and the Orthopaedic Research Lab at the Radboud University Nijmegen Medical Centre.

This work was supported by Fonds NutsOhra

Financial support for the publication of this thesis was provided by:

Anna Foundation|NOREF	Anna Foundation|NOREF
Cadmes BV	Cadmes BV
IMDI-CoRE SPRINT	IMDI-CoRE SPRINT
Implantcast Benelux BV	Implantcast Benelux BV
Prothese-en Orthese-Makerij Nijmegen	Prothese-en Orthese-Makerij Nijmegen
RMS Foundation, Bettlach, Switzerland	RMS Foundation, Bettlach, Switzerland
Stichting Business Generator Groningen	Stichting Business Generator Groningen
University of Groningen	University of Groningen
University Medical Center Groningen	University Medical Center Groningen
Vereenigde	Vereenigde
W.J. Kolff Institute	W.J. Kolff Institute

ISBN
978-90-367-5729-4 (printed version)
978-90-367-5730-0 (digital version)

Printing
Printed by IMGRAFIA, ul. Piłkarska 44, 94-121 Łódź, Poland

Cover
Cover designed by Małgorzata Miller-Tomaszewska

RIJKSUNIVERSITEIT GRONINGEN

Osseointegrated system for fixation of upper leg prostheses

Proefschrift

ter verkrijging van het doctoraat in de

Medische Wetenschapen

aan de Rijksuniversiteit Groningen

op gezag van de

Rector Magnificus, dr. E. Sterken,

in het openbaar te verdedigen op

woensdag 31 oktober 2012

om 11.00 uur

door

Paweł Krzysztof Tomaszewski

geboren op 7 maart 1982

te Łódź, Polen

Promotores:	Prof. dr. ir. G.J. Verkerke
	Prof. dr. ir. N. Verdonschot
	Prof. dr. S.K. Bulstra
Beoordelingscommissie:	Prof. dr. ir. H.F.J.M. Koopman
	Prof. dr. G.M. Raghoebar
	Prof. dr. G. Rakhorst

Contents

Chapter 1.	Introduction.	7
Chapter 2.	A comparative finite-element analysis of bone failure and load transfer of osseointegrated prostheses fixations.	17
Chapter 3.	Simulated bone remodeling around two types of osseointegrated implants for direct fixation of upper-leg prostheses.	31
Chapter 4.	Numerical analysis of an osseointegrated prosthesis fixation with reduced bone failure risk and periprosthetic bone loss.	47
Chapter 5.	Experimental assessment of a new direct fixation implant for artificial limbs.	61
Chapter 6.	Analysis of different material couples for an optimal wear performance in a new design of a direct fixation implant.	75
Chapter 7.	Potential improvement of tribological performance of PEEK polymers by application of diamond-like carbon coating.	85
Chapter 8.	In-vivo experiment with the new direct fixation implant.	97
Chapter 9.	General discussions and concluding remarks.	105
	Summary.	111
	Patent summary.	117
	Samenvatting.	119
	Streszczenie.	125
	Acknowledgements / Dankwoord / Podziękowania.	131

Chapter 1

Introduction

Background

The two most common causes of limb amputation are trauma and vascular disorders. Globally, trauma is a major cause of amputation and it accounts for approximately 30% of new amputations in developed countries (industry and transport related accidents) and substantially more in developing nations with up to 94% new amputations in countries with a recent history of war and civil turmoil (Lucas, 2004). Together with vascular diseases, diabetes and tumors cause approximately 65% of all amputations in industrialized countries. Among all, above knee (transfemoral) amputation is the second most frequent level of amputation (31% of all limb amputations) after below knee (transtibial) amputation (47%).

In The Netherlands around 600 patients undergo transfemoral amputation each year, which gives an average of 3.7 amputations per 100,000 inhabitants (Rommers, 2008). The transfemoral amputation is a permanent disfigurement, which has a big impact on patients' mobility, professional activity, lifestyle and quality of life.

Leg prostheses

To overcome the loss of a part of the leg, prostheses are available. A standard method of fixation of such external leg prosthesis to the limb remnant is using a prosthetic socket, which embraces the soft tissues of the upper leg remnant. This prosthesis fixation method is often reported as unsatisfactory due to stump pain, soft-tissue damage, lack of appropriate control and fitting problems (Lyon et al., 2000; Hagberg and Branemark, 2001; Dudek et al., 2005; Meulenbelt et al., 2011). All these problems arise at the stump-socket interface and are attributed to the fact that the soft tissues of the residual limb are not appropriately suited for support and transfer of the patients' body weight.

Direct fixation of external prosthesis

An alternative solution to the conventional stump-socket attachment of external leg prostheses is to fixate the prosthesis directly to the bone of the remnant of the leg, commonly referred to as osseointegration (Hansson et al., 1983). Currently, two direct trans-femoral limb fixation devices are available for clinical use, namely the OPRA system (Integrum AB, Göteborg, Sweden) and the ISP Endo/Exo prosthesis (ESKA Implants AG, Lübeck, Germany). Both devices follow a similar general concept of a metal-based intramedullary stem connected with a coupling element, which protrudes the soft tissue layer of the stump to provide an attachment for an external artificial limb (0a). The fixation of the intramedullary stem with the bone remnant is realized by a different method for both implants. The OPRA device has a threaded stem made of a commercially pure titanium and the ISP implant uses a cobalt-chromium-molybdenum stem covered with a highly porous metal structure (Branemark et al., 2001; Staubach and Grundei, 2001; Klinbeil, 2006) (0b,c). Both surfaces enable bony ingrowth and formation of a durable bone-implant interface; this is the so-called osseointegration, which provides long-term fixation of the prosthesis.

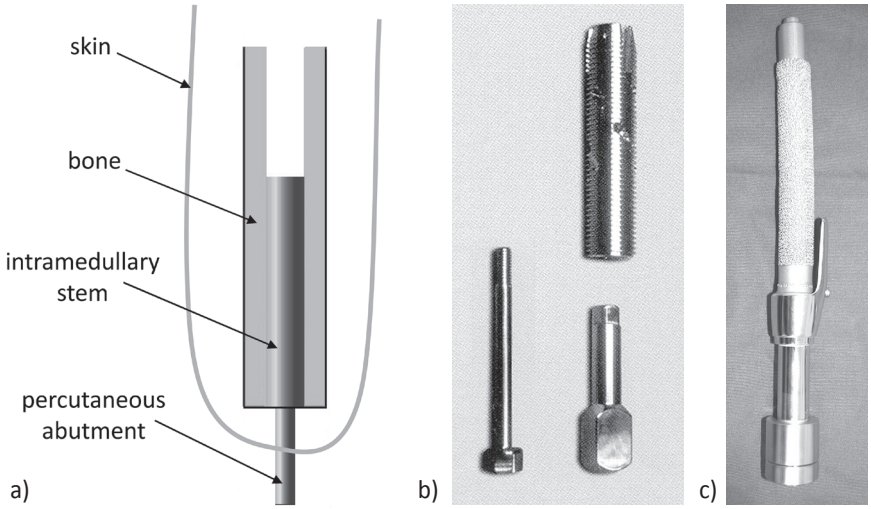

Figure 1. Schematic representation of direct prosthesis fixation implant; b) the OPRA system (Integrum AB, Göteborg, Sweden), source: (Ward, 2005); c) the ISP Endo/Exo prosthesis (ESKA Implants AG, Lübeck, Germany), source: (Aschoff, 2010).

Surgical technique

The surgical procedure for implantation of the direct fixation implants consists of two stages. During the first surgery, the implant is introduced into the medullary cavity and left unloaded for 6 to 8 weeks for the ISP implant, and for 6 months in case of the OPRA device (Ward, 2005; Büll, 2006). During that time bone-implant integration is expected to occur and the patient is usually able to use a traditional prosthetic system (although some adjustments might be needed). In the second stage the skin penetrating shaft is attached to the intramedullary fixation. After wound healing, the patient takes part in a rehabilitation program, during which loading of the implant is gradually increased and after 1 month (for the ISP patients) to 6 months (for the OPRA patients) full load bearing is allowed (Ward, 2005; Hagberg and Branemark, 2009; Aschoff, 2010).

Physical and prosthetic benefits of the direct fixation prostheses

Between 1990 and 2008, 100 patients were treated with the OPRA implant (Hagberg and Branemark, 2009). The ISP device was implanted in 37 patients from year 1999 till 2009 (Aschoff, 2010). The patient population consists mainly of middle-aged men (mean of 43 years old at implantation with a 91/46 male to female ratio), who underwent transfemoral amputation due to trauma (71%) or tumor (18%). The clinical results showed that direct attachment of an artificial limb to the skeletal system allows overcoming skin problems and fitting difficulties characteristic to the conventional socket fixation (Bergkvist, 1998). Furthermore, it provides a better control of the prosthetic

limb including sensory feedback from the ground surface (Gunterberg, 1998; Ward, 2005). Additionally, the range of the hip joint motion and sitting comfort is increased relative to socket prostheses (Hagberg et al., 2005; Hagberg et al., 2008; Tranberg et al., 2011). All these benefits lead to increased prosthetic use, better mobility and lower energy consumption that in consequence considerably increase quality of life of the amputated patients.

Direct fixation implant issues

The two principal challenges with a percutaneous transfemoral fixation implants are: secure and durable fixation of the prosthetic shaft in the medullary canal of the bone; and reliable shielding of the implant against possible ascending infections arising from the dermal interface (Aschoff, 2010). The overall rate of revisions in the group of patients treated with the ISP implant of 20/37 (Aschoff, 2010) and the OPRA implant removal rate of 20/97 (Hagberg and Branemark, 2009), clearly indicates that the rehabilitation with the direct fixation implants remains still a challenging treatment. Examples of the direct fixation implant related issues described in the clinical and mechanical evaluations are:

Infections

The percutaneous part of a direct fixation implant is a potential site for infectious complications. These occur in approximately 40% of patients (Aschoff et al., 2009; Tillander et al., 2010). Most infection related to the direct fixation implant are superficial ones in the skin penetration area. However, severe implant infections are also present at a considerable rate of 18% (Tillander et al., 2010). These are relatively difficult to treat and ultimately might lead to implant removal, which was reported in 1 out of 37 (Aschoff, 2010) and 1 out of 33 (Tillander et al., 2010) cases for the ISP and the OPRA device, respectively.

Periprosthetic bone loss

The intramedullary fixation is obtained by means of direct bone ingrowth into the titanium implant surface (OPRA) or the highly porous CoCrMo-alloy structure (ISP). These materials enable to achieve a stable interface with bone tissue, which was demonstrated in case of dental and uncemented hip implants. However, as the stiffness of these metal-based implants is relatively higher than that of the periprosthetic bone, these implants are expected to change bone loading as compared to the intact situation. This inevitably leads to a bone remodeling response, which was reported in a clinical follow-up study with the OPRA implant (Xu and Robinson, 2008). The radiographs of 11 patients with an average 8 years of socket use prior to implantation presented considerable progressive bone loss around the distal end of the femur and bone deposition at the proximal end of the implant. This, in general, reduces prosthetic support, decreases bone strength and ultimately may lead to implant loosening as was previously observed in case of total hip implants (Petersen et al., 1995; Spittlehouse et al., 1998; Kobayashi et al., 2000). Although up to now no clinical report of bone

changes around the ISP prosthesis has been published, the same concept of cobalt-chromium alloy stem with a highly porous metal layer did not eliminate periprosthetic bone loss of hip implants (Götze et al., 2006).

The bone remodeling issue might be even more pronounced for direct fixation implant users as in the current rehabilitation programs percutaneous implants are mostly fitted in patients who have experienced problems with socket fixation. Reported mean time of socket prosthesis use prior to treatment with direct fixation devices is about 11 years (Hagberg and Branemark, 2009; Aschoff, 2010). Hence, the bone has not been loaded to physiological levels for considerable time, resulting in considerable bone loss (Sherk et al., 2008). The decreased bone quality and its subsequent strength, prior to the implantation, might make the issue of periprosthetic bone remodeling even more critical for direct-fixation implants.

Bone failure

The stiffness mismatch between direct fixation implant and bone, which in addition usually has a deteriorated strength due to prolonged socket-prosthesis use, the geometry of the intramedullary shaft that provokes peak stresses at the distal ends, combined with high loading arising during walking, and even more critical falling accidents, occasionally leads to pertrochanteric femur fractures. Two such fractures have been reported for the ISP implant (Büll, 2006; Aschoff, 2010; Lunow et al., 2010). These result either in discontinuation of the treatment or require further complicated fracture stabilization.

Implant failures

Excessive or fatigue loading sometimes leads to bending or fracture of the skin penetrating part of the OPRA implant (3 cases) (Gunterberg, 1998; Sullivan et al., 2003; Hagberg and Branemark, 2009) and was reported to lead once (out of 37) to fracture of the ISP stem (Aschoff, 2010; Lunow et al., 2010). The former case required a relatively easy replacement of the implant's part, whereas the latter lead to surgical removal of the implant.

Limitations

Current rehabilitation programs with the direct fixation implants require thorough pre-assessment of candidates. An obvious exclusion criteria are medical conditions which might compromise osseointegration of the implant, i.e. diabetes, vascular disease, risk of bone sepsis, skeletal immaturity or patient's age exceeding 70 years.

A clear shortcoming of the percutaneous method is a two-stage surgical procedure and the length of the rehabilitation period, which spans from 10-14 weeks for the ISP device up to 12-18 months for the OPRA implant (Hagberg and Branemark, 2009; Aschoff, 2010). As a result patients' mobility is impaired and bone tissue stays unloaded for a considerable time. That can promote bone resorption and thus lead to an increased risk of bone fracture.

An anatomical limitation for treatment with direct transfemoral prosthesis fixation is a minimum necessary length of the femoral remnant's midshaft of

12-15 cm for the ISP stem and 10-12 cm for the OPRA stem (Ward, 2005; Aschoff, 2010). Additionally current selection protocols include a body mass limit of 100 kg, as high loads as a consequence of high body mass are considered to be unsafe.

All these restraining issues make percutaneous implants a secondary choice in transfemoral prosthetics, leaving only amputees who have experienced major difficulties with socket-type prosthesis as the primary target group (Sullivan et al., 2003; Aschoff, 2010).

Aim of the thesis

The aim of the thesis was threefold. The first aim was to evaluate issues listed above with potential mechanical underlying conditions to gain insight in these problems. The second aim was to use results of these analyses to design a new concept of transfemoral direct prosthesis fixation to overcome limiting issues of the current implants. The third aim was to verify numerically and experimentally if the proposed implant could increase mechanical safety and enable more patients to benefit from rehabilitation with osseointegrated direct fixation implants.

New design requirements

Based on the literature study and analysis of mechanical safety and influence of load transfer on the long term bone turnover around the current osseointegrated implants (Chapter 2 and 3), the following requirements for an improved design were formulated:

I. The intramedullary stem should be fixed in the bone by means of direct bone ingrowth into implant surface (cementless fixation). Moreover, all used materials must be biocompatible and suitable for a long-term application inside human body.
II. A close fitting of the stem and bone must be obtained to enable osseointegration, thus the implant must be available in different sizes covering a range of typical intramedullary canal diameters, that is from 10 mm in the lateromedial to 23 mm in anteroposterior direction (Bulstra et al., 1996).
III. The new design must be suitable for patients with short residual femur meaning that a maximum of 8 cm of intramedullary canal is enough for implant fixation.
IV. The stem must provide better, than existing designs, mechanical safety to the periprosthetic bone both during normal walking and falling accidents, meaning that bone overload by implant must be avoided.
V. The implant should provide stress distribution as close as possible to physiological in order to minimize adverse periprosthetic bone remodeling.
VI. The intramedullary stem should provide a long-term performance, thus withstand fatigue loads characteristic for standard walking. An estimate based on an average of 5000 steps per day (Tudor-Locke et al., 2011) and desired 20 years of performance leads to approximately 36.5 million cycles.
VII. The improved fixation system should be safe for patients with body mass of up to 100 kg.

VIII. Formation of wear debris should be minimized, that is not exceeding amounts present in the contemporary orthopaedic implants, as it could lead to aseptic loosening of the implant (Brown et al., 2009; Golish and Anderson, 2011).
IX. The percutaneous connector should be designed to enable minimum infection risk.
X. Implantation of the prosthesis must be possible by means of a surgical procedure, which should not be more complex than in case of total hip arthroplasty.
XI. It must be possible to manufacture the new implant with commercially available biomaterials and processes so that the implant is equally or more economical to manufacture than contemporary joint replacement implants.

Thesis outline

The first issue addressed in this thesis was to investigate the biomechanical interaction of the current osseointegrated direct fixation implants with the periprosthetic bone.

Chapter 2 describes a finite element analysis of the stress distribution and bone failure risk around the OPRA and the ISP direct fixation implants during normal walking activity.

Chapter 3 concerns the long term bone response to the OPRA and the ISP type of direct fixation implants. Strain adaptive bone remodeling simulations are used to investigate the influence of the implant properties and delay time between amputation and implantation on bone loss and premature fracture risk.

In Chapter 4 the design of the new concept of direct fixation implant is presented. FE analyses of periprosthetic bone failure risk and adverse bone remodeling related to the developed concept are performed and compared to the results obtained for the currently used osseointegrated implants.

Chapter 5 presents an experimental and numerical comparison of the cortical strains induced by the standard titanium (OPRA-like) stem and the new implant.

Chapters 6 and 7 focus on tribological aspects related to the new implant design and the requirement to minimize potential wear debris formation. Chapter 6 presents results of tribological measurements of the fretting performance of various combinations of PEEK, CoCrMo and Ti6Al4V biomaterials to assess the potential of these materials for use in the new implant. In Chapter 7 it was investigated if a diamond-like carbon coating can improve tribological performance and reduce wear debris formation of a sliding interface between Ti6Al4V and different PEEK polymers.

In Chapter 8 an in-vivo experiment is described that evaluates the overall biological response and verifies FE predictions relative to strain adaptive bone remodeling around the new implant.

Chapter 9 discusses the results as described in the current thesis and relates the current state of development of the new direct fixation implant to the design requirements defined in the Chapter 1. Furthermore, suggestions for future research and development steps are formulated.

Additionally, as appendix an abstract of the filled patent application summarizing patent claims on the new osseointegrated direct fixation implant developed within frame of this thesis is presented.

References

Aschoff, H. H., et al. (2009). "The endo-exo femur prosthesis-a new concept of bone-guided, prosthetic rehabilitation following above-knee amputation." Zeitschrift für Orthopädie und Unfallchirurgie 147(5): 610-615.

Aschoff, H. H., Kennon, R.E., Keggi, J.M., Rubin, L.E. (2010). "Transcutaneous, Distal Femoral, Intramedullary Attachment for Above-the-Knee Prostheses: An Endo-Exo Device." Journal of Bone and Joint Surgery 92(Suppl 2): 180-186.

Bergkvist, R. (1998). Osseointegration: case report on prosthetic treatment in transfemoral amputation. IXth World Congress ISPO, Amsterdam.

Branemark, R., et al. (2001). "Osseointegration in skeletal reconstruction and rehabilitation: a review." Journal of Rehabilitation Research and Development 38(2): 175-181.

Brown, T. D., et al. (2009). "2009 Nicolas Andry Award: clinical biomechanics of third body acceleration of total hip wear." Clin Orthop Relat Res 467(7): 1885-1897.

Büll, O. (2006). Theoretische aspekte und erste praktische ergebnisse von perkutanen exoprothesen bei oberschenkelamputationen. Munich, Ludwig-Maximilians-University.

Bulstra, S. K., et al. (1996). "Femoral canal occlusion in total hip replacement using a resorbable and flexible cement restrictor." J Bone Joint Surg Br 78(6): 892-898.

Dudek, N. L., et al. (2005). "Dermatologic conditions associated with use of a lower-extremity prosthesis." Arch Phys Med Rehabil 86(4): 659-663.

Golish, S. R., et al. (2011). "Bearing surfaces for total disc arthroplasty: metal-on-metal versus metal-on-polyethylene and other biomaterials." Spine J.

Götze, C., et al. (2006). "Long-term influence of the spongiosa metal surface prosthesis on the periprosthetic bone. A radiological and osteodensitometric analysis of implantation of the S&G (ESKA) hip prosthesis." Zeitschrift fur Orthopadie und ihre Grenzgebiete 144(2): 192-198.

Gunterberg, B., Branemark, P-I., Branemark, R., Bergh, P. and Rydevik, B. (1998). Osseointegrated prosthesis in lower limb amputation: the development of a new concept. IX-th World Congress ISPO, Copenhagen, ISPO.

Hagberg, K., et al. (2001). "Consequences of non-vascular trans-femoral amputation: a survey of quality of life, prosthetic use and problems." Prosthetics and Orthotics International 25(3): 186-194.

Hagberg, K., et al. (2009). "One hundred patients treated with osseointegrated transfemoral amputation prostheses-rehabilitation perspective." Journal of Rehabilitation Research and Development 46(3): 331-344.

Hagberg, K., et al. (2008). "Osseointegrated trans-femoral amputation prostheses: prospective results of general and condition-specific quality of life in 18 patients at 2-year follow-up." Prosthetics and Orthotics International 32(1): 29-41.

Hagberg, K., et al. (2005). "Socket versus bone-anchored trans-femoral prostheses: hip range of motion and sitting comfort." Prosthetics and Orthotics International 29(2): 153-163.

Hansson, H. A., et al. (1983). "Structural aspects of the interface between tissue and titanium implants." J Prosthet Dent 50(1): 108-113.

Klinbeil, K. (2006). Metallurgische Grundlagen für die gusstechnische Herstellung einer räumlichen Oberflächenstruktur. Ossärre Integration. R. Gradinger and H. Gollwitzer. Heidelberg, Springer Medizin Verlag: 46-52.

Kobayashi, S., et al. (2000). "Poor bone quality or hip structure as risk factors affecting survival of total-hip arthroplasty." Lancet 355(9214): 1499-1504.

Lucas, M., Wikoff, E., DiGiacomo, R., Kahn, S., Kellenberger, N., Esquenazi, R., Mostaccio, F., Kalstein, R. (2004). Causes and Prevention. The Rehabilitation of People with Amputations, World Health Organization, United States Department of Defense, MossRehab Amputee Rehabilitation Program, MossRehab Hospital, USA: 1-3.

Lunow, C., et al. (2010). "Endo-exo femoral prosthesis: clinical course after primary implantation of an intramedullary percutaneous endo-exo femoral prosthesis following upper leg amputation." Der Unfallchirurg 113(7): 589-593.

Lyon, C. C., et al. (2000). "Skin disorders in amputees." J Am Acad Dermatol 42(3): 501-507.

Meulenbelt, H. E., et al. (2011). "Skin problems of the stump in lower limb amputees: 1. A clinical study." Acta Dermato Venereologica 91(2): 173-177.

Petersen, M. M., et al. (1995). "Changes in bone mineral density of the distal femur following uncemented total knee arthroplasty." Journal of Arthroplasty 10(1): 7-11.

Rommers, G. M. (2008). Epidemiologie van amputaties aan de onderste extremiteit. Amputatie en prosthesiologie van de onderste extremiteit. J. H. B. Geertzen, Rietman J.S., Lemma: 53.

Sherk, V. D., et al. (2008). "BMD and bone geometry in transtibial and transfemoral amputees." Journal of Bone and Mineral Research 23(9): 1449-1457.

Spittlehouse, A. J., et al. (1998). "Bone loss around 2 different types of hip prostheses." Journal of Arthroplasty 13(4): 422-427.

Staubach, K. H., et al. (2001). "The first osseointegrated percutaneous prosthesis anchor for above-knee amputees." Biomedizinische Technik Biomedical engineering 46(12): 355-361.

Sullivan, J., et al. (2003). "Rehabilitation of the trans-femoral amputee with an osseointegrated prosthesis: the United Kingdom experience." Prosthetics and Orthotics International 27(2): 114-120.

Tillander, J., et al. (2010). "Osseointegrated Titanium Implants for Limb Prostheses Attachments: Infectious Complications." Clin Orthop Relat Res.

Tranberg, R., et al. (2011). "Improvements in hip- and pelvic motion for patients with osseointegrated trans-femoral prostheses." Gait Posture 33(2): 165-168.

Tudor-Locke, C., et al. (2011). "How many steps/day are enough? For older adults and special populations." Int J Behav Nutr Phys Act 8(1): 80.

Ward, D. A., Robinson, K.P. (2005). Osseointegration for the skeletal fixation of limb prostheses in amputations at the trans-femoral level. The osseointegration book. P.-I. Branemark, Quintessenz Verlags: 463-476.

Xu, W., et al. (2008). "X-ray image review of the bone remodeling around an osseointegrated trans-femoral implant and a finite element simulation case study." Annals of Biomedical Engineering 36(3): 435-443.

Chapter 2

A comparative finite element analysis of bone failure and load transfer of osseointegrated prostheses fixations

P.K. Tomaszewski [1], N. Verdonschot [2,3], S.K. Bulstra [4], G.J. Verkerke [1,3]

[1] University Medical Center Groningen, University of Groningen, The Netherlands.
[2] Radboud University Nijmegen Medical Centre, Orthopaedic Research Laboratory, Nijmegen, The Netherlands.
[3] Department of Biomechanical Engineering, University of Twente, Enschede, The Netherlands.
[4] Department of Orthopaedics, University Medical Center Groningen, University of Groningen, The Netherlands.

Annals of Biomedical Engineering, 2010, Volume 38, Issue 7, pp. 2418-27.

Introduction

Each year around 600 patients undergo transfemoral amputation in the Netherlands, which gives an average of 3.7 amputations per 100,000 inhabitants (Rommers, 2008). The conventional prosthetic limb attachment is realized by a stump fitting socket to which the artificial limb is fixed. Decades of development of socket technology has led to a more optimal coupling between stump and socket. However, performance of this fixation method is often reported as unsatisfactory (Hagberg and Branemark, 2001). Pain, soft tissue irritation and breakdown (Sullivan et al., 2003) and lack of appropriate control of the prosthetic limb (Hagberg et al., 2005) arise due to the fact that the soft tissues of the residual limb are not appropriately suited for body weight support. Moreover, the fixation is affected by volumetric variations of the stump due to swelling (Bergkvist, 1998).

For two decades an alternative solution has been offered by attachment of the artificial limb directly to the femur via a percutaneous implant. Long-term fixation is achieved by osseointegration (Branemark et al., 2001).

Currently, two trans-femoral limb fixation devices are available on the market: the OPRA system (Integrum AB, Göteborg, Sweden) and the ISP Endo/Exo prosthesis (ESKA Implants AG, Lübeck, Germany). Both devices follow a similar general concept: a metal-based intramedullary stem is connected with a coupling element, which protrudes the soft tissue layer of the stump to provide an attachment for an external artificial limb. However, the fixation of the intramedullary stem with the bone is realized by different method in both implants. The OPRA device has a form of titanium stem with a thread and the ISP implant uses a cobalt-chromium-molybdenum stem covered with a porous metal (Branemark, 2001; Staubach and Grundei, 2001).

The surgical procedure for implantation consists of two stages. First, the implant is introduced into the medullary cavity and left unloaded for 6 to 8 weeks for the ISP implant, and up to 6 months for the OPRA device (Ward, 2005; Büll, 2006). During that time bone-implant integration is expected to occur. In the second surgery the skin penetrating shaft is attached to the intramedullary fixation. After wound healing, loading of the system is gradually increased and 3-6 months later full load bearing is allowed (Ward, 2005).

Direct attachment of an artificial limb to the skeletal system allows overcoming the conventional socket system problems and provides a better control of the prosthetic limb including sensory feedback from the ground surface (Ward, 2005). Finally, the range of the hip joint motion is unrestricted and sitting comfort is increased relative to socket prostheses (Hagberg et al., 2005; Hagberg et al., 2008).

However, infection problems may occur (Gunterberg, 1998; Ward, 2005; Büll, 2006) and there is a risk of fracture (either of the implant or the bone) or bone-implant interface disruption and implant loosening. Because the stiffness of the intramedullary stem is much higher than that of bone, high loads could cause bone fractures around the tip of the intramedullary stem or close to the osteotomy. The reported cases of failure include intertrochanteric femur fracture and bending fractures of the skin-penetrating part of the devices, usually as a result of a falling accident (Sullivan et al., 2003; Ward, 2005; Büll, 2006).

Moreover, it is generally known in endoprosthetics that after implantation the local loading condition in the periprosthetic region changes considerably in comparison to the intact situation leading to bone resorption around the implant. Obviously direct skeletal attachment of prosthetic component is also expected to provoke a bone remodeling response (Gunterberg, 1998; Xu et al., 2006), which could promote bone fracture.

An obvious shortcoming of the percutaneous method is the length of the rehabilitation period, which spans up to 18 months. As a result bone tissue stays unloaded for a considerable time. This, again, could promote bone resorption and thus lead to an increased risk of bone fracture.

Current protocols of patient selection for treatment with direct transfemoral prosthesis fixation include a body mass limit of 100 kg, as high loads as a consequence of high body mass are considered to be unsafe. All these restraining issues make percutaneous implants a secondary choice in transfemoral prosthetics, leaving only trauma-amputation patients, who have experienced major difficulties with socket-type prosthesis as the primary target group (Hagberg and Branemark, 2001; Sullivan et al., 2003).

If these restraining issues could be resolved more patients could benefit from the advantages of direct fixation. In this study we hypothesized that current percutaneous devices could be considerably improved when a thorough biomechanical analysis was available. Finite element (FE) analyses techniques are highly suitable for this purpose. In the field of the transfemoral skeletal attachment the finite element modeling was previously used to study the influence of various geometric parameters on stress and strain distribution in the region of the bone-implant interface (Xu et al., 2000; Zheng, 2005; Xu and Robinson, 2008). More recently, FE modeling compared stress distribution within bone adjacent to the OPRA implant subjected to different loading conditions that may occur during weight bearing exercises (Lee et al., 2008) and searched for the correlations between FE simulated stress/strain distributions and the bone turnover observed on clinical radiographs (Xu et al., 2006). Helgason et al. (Helgason et al., 2009) analyzed with a general model the failure risk of direct skeletal attachment.

However, none of these studies assessed the risk of bone-implant interface failure nor reported any results about the ISP device. So a more detailed mechanical analysis of both implants will improve our understanding of the biomechanical issues that are involved with respect to prosthetic limb attachment devices.

The purpose of this study was to assess the mechanical consequences of the changed loading pattern within the bone and its potential consequences on long-term bone remodeling. In particular, we analyzed if the normal walking activity can cause any risk to the femur of the amputee using direct prosthesis fixation. Furthermore, we investigated if the application of the porous metal on the cobalt-chromium-molybdenum alloy stem of the ISP prosthesis is more beneficial to the bone-implant load transfer than the titanium stem of the OPRA system either early post-operative (before bony ingrowth) or after bone ingrowth had occurred.

Materials and methods

Three FE models were created, one representing a femur amputated at the metaphyseal level and provided with OPRA prosthesis, one representing the same femur bone with an ISP device and a third model representing the intact femoral bone (Figure 1).

The geometry of the bone was determined from CT scans (slice thickness 3 mm) of a male femur bone with normal bone mineral density (DEXA T-score: 0.1).

The amputated femur model represented the most common osteotomy level of 250 mm above the knee. The surface-shape contours of the two implants (Figure 2) were fitted in the femoral bone and implemented into the FE models. The implants with the same outer diameter of the intramedullary part were assumed to be in close contact to the bone. Firstly, using frictional contact (friction coefficient of 0.4 (Shirazi-Adl et al., 1993)), which models the direct post-operative case. Secondly, the implant and bone were bonded to represent full osseointegration.

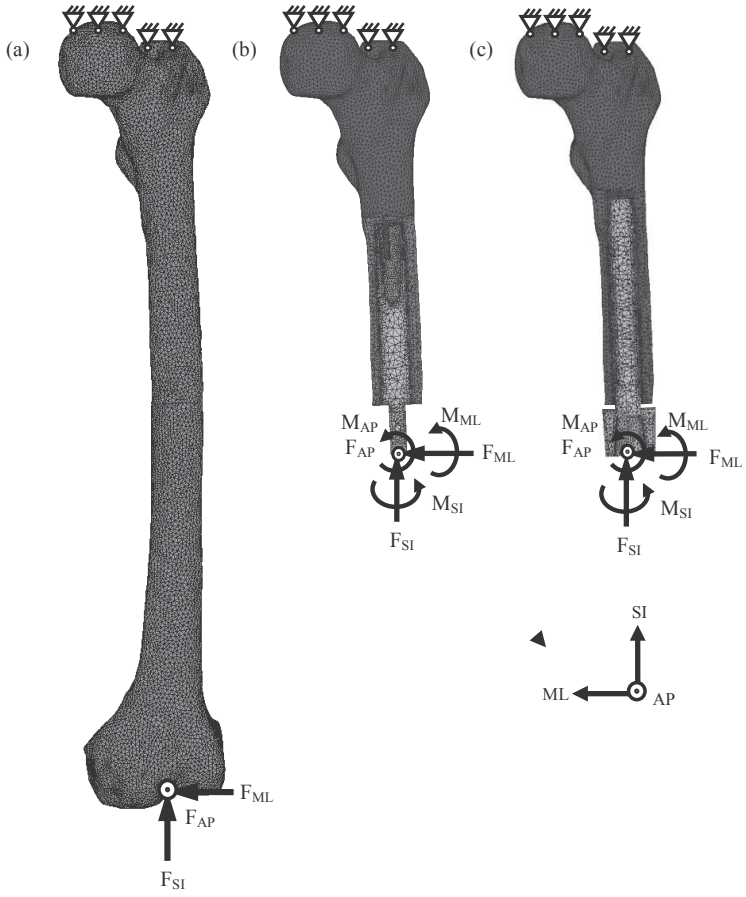

Figure 1. Finite element mesh and boundary conditions applied to the intact bone (a), the OPRA implant (b) and the ISP implant model. The axes are denoted as antero-posterior (AP), medio-lateral (ML) and superior-inferior (SI).

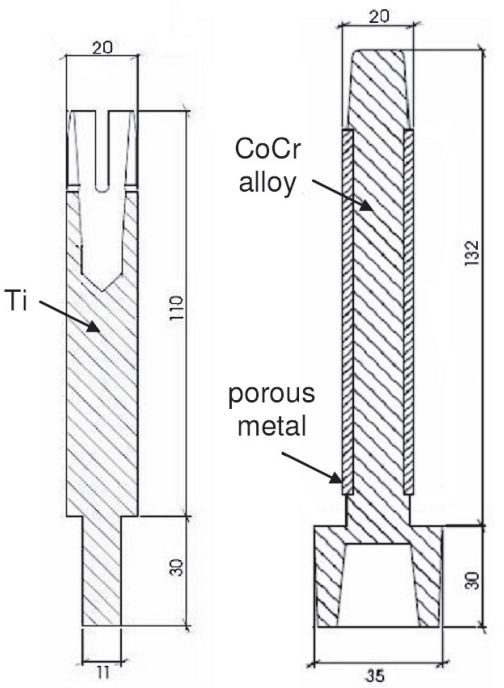

Figure 2. Geometry of the OPRA (a) and the ISP implant (b), all dimensions in [mm].

The optimal mesh size for the bone model was determined by a mesh refinement test with 5% convergence error for the peak equivalent von Misses stress. The edge length for all meshes was 3 mm except for the interface region where it was further refined, leading to meshes in the range of 150,000 to 190,000 of four-noded tetrahedral elements.

The Young's moduli of the bone elements were derived from their ash densities (Keyak and Falkinstein, 2003): $E = 33900\rho_{ash}^{2.20}$ for $\rho_{ash} \le 0.27$ (trabecular bone); $E = 10200\rho_{ash}^{2.01}$ for $\rho_{ash} \ge 0.6$ (cortical bone); $E = 5307\rho_{ash} + 469$ for $0.27 < \rho_{ash} < 0.6$ (transition); where ρ_{ash} was calculated from calcium hydroxyapatite (CHA) - calibrated CT scan data using the relationship (Keyak et al., 2005): $\rho_{ash} = 0.0633 + 0.887\rho_{CHA}$. Poisson's ratio for all bone elements was 0.4. Characteristic elastic moduli for implant materials was taken as follows: ISP prosthesis stem (cobalt-chromium-molybdenum) $2.1 \cdot 10^5$ MPa and the porous metal layer (Spongiosa metal with assumed partial bone ingrowth) $1.0 \cdot 10^3$ MPa (Klinbeil, 2006); the OPRA implant (commercially pure titanium) $1.1 \cdot 10^5$ MPa. Poisson's ratio for all implant materials was set to 0.3.

Two loading cases from a normal walking cycle at 25% (heel strike) and 55% (shortly before toe-off) were considered. The loading of the implants was taken from the measurements performed with amputees using the OPRA device (Lee et al., 2007). The set of forces at the condyles of the intact femur were measured in vivo with an instrumented knee implant (D'Lima et al., 2007). The latter was used as a reference situation when all muscle forces were present, since a normal walking activity in this

case is safe for the bone. Firstly, the intact loads (D'Lima et al., 2007) were linearly scaled to correspond to the implant loads (Lee et al., 2007), reported for a patient with 61 kg body mass. Secondly, both loads were linearly rescaled to represent a body mass of 100 kg. The loading conditions are presented in Table 1. In all simulations the bone was fixed at the proximal end and load was applied distally (Figure 1.).

Load case	Intact knee joint			Implanted					
	F_{SI} [N]	F_{AP} [N]	F_{ML} [N]	F_{SI} [N]	F_{AP} [N]	F_{ML} [N]	M_{SI} [Nm]	M_{AP} [Nm]	M_{ML} [Nm]
1	1302	244	-180	780	100	-20	-2.0	-7.2	30.8
2	1170	44	-60	180	120	40	4.1	37.3	0.0
	(1914)	(73)	(-99)	(295)	(196)	(66)	(6.7)	(61.0)	(0.0)

Table 1. Overview of two different load cases applied to the FE models. All values are given for body mass of 61 kg and 100 kg (values in brackets). FSI, FAP, FML are the superior-interior axis (superior being positive), antero-posterior (anterior being positive) and medio-lateral (lateral being positive) respectively.

Periprosthetic bone failure risk was evaluated by the von Mises stress (σ_{VM}) criterion, previously used in related research (Keyak et al., 1998; Keyak, 2001; Keyak and Falkinstein, 2003; Keyak et al., 2005). The bone strength (S) was calculated for each bone element from ρ_{ash} (Keyak and Falkinstein, 2003): $S = 137 \cdot \rho_{ash}^{1.88}$ for $\rho_{ash} < 0.317$ (trabecular bone); $S = 114 \cdot \rho_{ash}^{1.72}$ for $\rho_{ash} \geq 0.317$ (cortical bone). Bone failure risk was identified when $\sigma_{VM} / S \geq 1$.

The assessment of interface stresses was taken from Huiskes et al. (Huiskes and van Rietbergen, 1995). Interface stresses were based upon nodal contact forces extracted from a contact algorithm provided by Marc (MSC Software Corporation, Santa Ana, CA, USA). The interface area associated with the node in contact was calculated by dividing the interface normal force by the interface normal stress. To relate interface stresses (normal and shear stresses) to the probability of mechanical failure we used a criterion defined by Hoffman (Hoffman, 1967). Each nodal point at the interface was assigned a Hoffman number calculated from the normal and shear stress and the interface-bone density as: $H = \frac{1}{S_c S_t}\sigma_n^2 + (\frac{1}{S_t} - \frac{1}{S_c})\sigma_n + \frac{1}{S_s^2}\sigma_s^2$ where S_c, S_t and S_s are the interface uniaxial compressive, tensile and shear strength, respectively. All strengths depend on the apparent density of the interface bone as (Stone et al., 1983; Kaplan et al., 1985): $S_c = 32.4\rho^{1.85}$, $S_t = 14.5\rho^{1.71}$, $S_s = 21.6\rho^{1.65}$. The regression equation relating apparent density to ash density was (Keyak et al., 1994): $\rho = 1.79\rho_{ash} + 0.0119$. The Hoffman criterion transforms the local interface stresses to a value referred to as the Hoffman number (H), which represents the probability of interface failure. The interface disruption is assumed to occur when $H > 1$, for lower H no interface failure is expected.

According to the adaptive bone-remodeling theory (Weinans et al., 1992; Van Rietbergen et al., 1993), the bone mass is regulated by the elastic strain energy

per unit mass (Carter, 1987). Following this theory our study examined strain energy density (SED) distribution in the intact and amputated bones to predict the long-term bone remodeling.

Comparing the peak values of any stress or strain quantity obtained with the FEM is often unreliable due to mesh dependency, especially in contact problems. In this study we therefore chose to determine the peak stress threshold beyond which one percent of the interface area was exposed to (Figure 3).

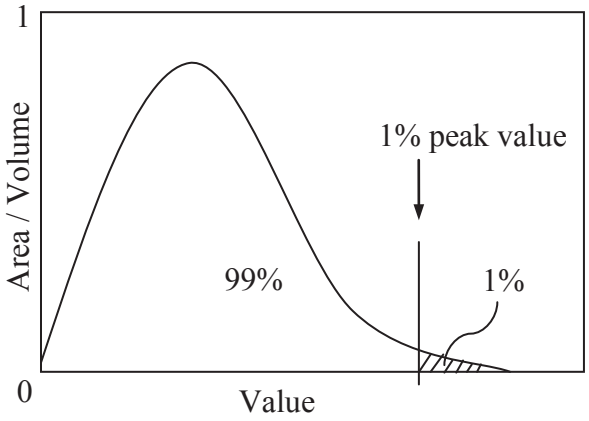

Figure 3. The 1% peak value determined from the volumetric / areal distribution of analyzed quantity.

As the two different prosthetic systems led to a different interfacial area, the data on the plots was normalized with total interface area equal to $6.0 \cdot 10^3$ mm^2 for the ISP and $6.0 \cdot 10^3$ mm^2 for the OPRA implant. Similar analyses (1% peak threshold values) were performed to quantify peak values for strain energy density and bone failure ratio values in the volumes of the bone adjacent to the implants. The bone volumes were selected from the osteotomy up to 10 mm above the proximal implants' end and were $81.1 \cdot 10^3$ mm^3 and $62.7 \cdot 10^3$ mm^3 for the ISP and the OPRA implants, respectively.

Results

The stress pattern in the bone changed considerably after implantation of direct fixation prostheses. In both load cases the equivalent von Mises stresses in the diaphysis of the intact femur was uniformly distributed along the cortex (Figure 4a). After introduction of the implants high stress concentration in the bone region close to the proximal end of the implant was found and much lower stresses were present in the distal part located close to the osteotomy. The stresses were slightly more evenly distributed in the bone around the ISP than the OPRA implant. Overall levels of the von Mises stress were higher in the intact than in the implanted bones.

Introduction of the direct fixation prostheses caused redistribution of the strain energy density in the bone. Similarly as in case of the von Mises stress, high values of the SED were present in the proximity of the implants' proximal tips and relatively low

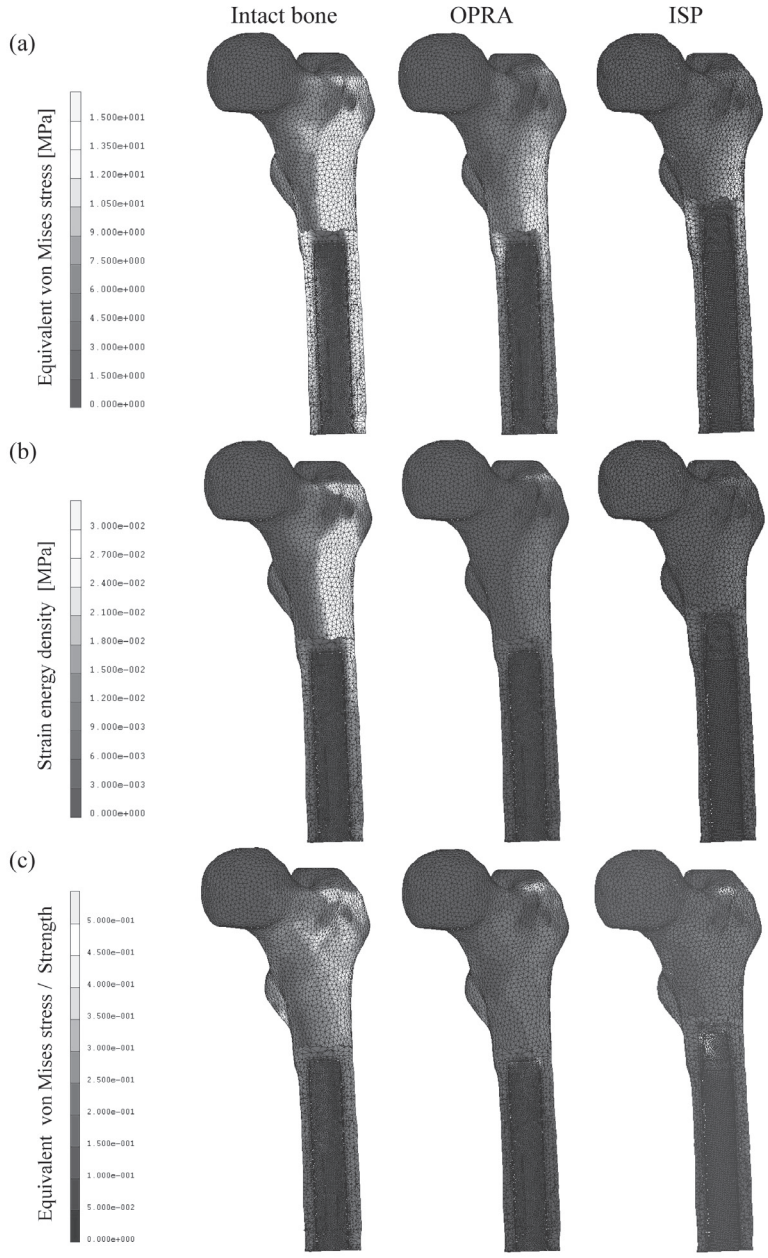

Figure 4. Von Mises stress (a), strain energy density (b) and von Mises stress / Strength distribution (c) in the periprosthetic bone obtained for the load case 1. Part of the bone removed to facilitate the direct comparison of intact bone with the implanted cases

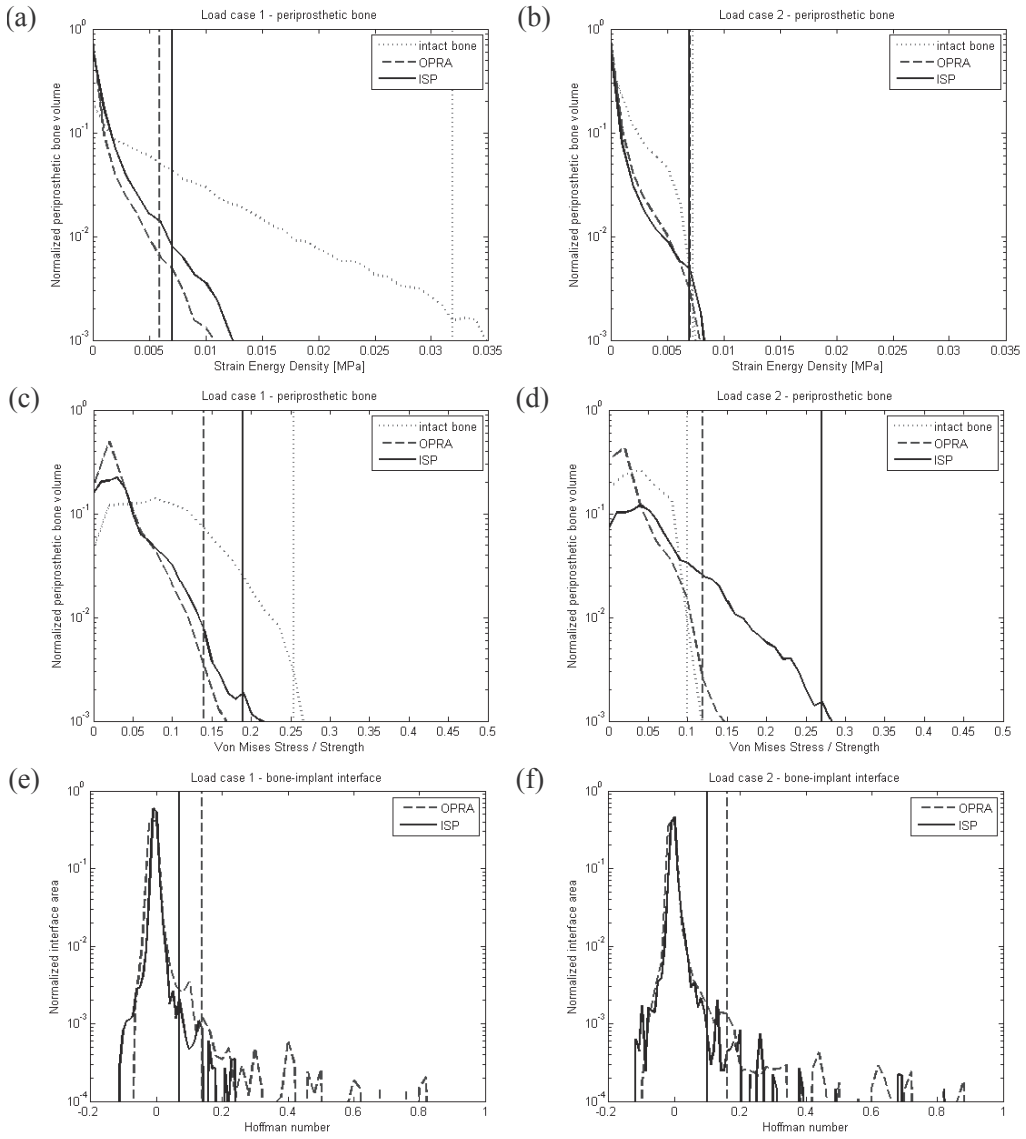

Figure 5. Area/volume distribution of the strain energy density (a, b), the von Mises stress/ Strength (c, d) in the periprosthetic bone region and the Hoffman number (e, f) at the bone-implant interface obtained from the simulations with bonded interface for the load case 1- (a, c, e) and load case 2- (b, d, f). Vertical lines mark 1% peak thresholds.

values more distally. In both considered load configurations the overall levels of the SED were higher in the intact bone, however, the difference was much larger in the first load case representing heel strike phase of the gait cycle (Figure 5 a, b). Relative to bone remodeling stimulus, the ISP prosthesis induced higher SED levels that the OPRA design.

Normal walking activity did not cause considerable risks to the bone fitted with the direct fixation implants. Loads for a person with the body mass of 61 kg (Table 1) did not indicate any direct bone damage ($\sigma_{VM}/S < 1$) neither directly post-operative nor after complete bone ingrowth. The highest failure ratio was always found in the bone region in contact with the proximal end of the implant (Figure 4c). The probability of the bone failure was higher for the ISP than for the OPRA implant (Figure 5 c, d).

The interface load transfer varied between both studied implants. In the debonded simulation, the OPRA device showed higher compressive and shear stresses at the interface. When the implants were bonded to the bone, values of shear stresses were still higher for the OPRA prosthesis but tensile stresses as well as compressive stresses were lower than in case of the ISP prosthesis. This was reflected in much lower Hoffman values found at the ISP implant bone interface (Figure 5 e, f).

The increase in the body mass of the patient over the limit of 100 kg is assumed to be dangerous for the bone-implant integrity. As the second load case appeared to be more demanding for the interface, it was chosen for the additional simulation with the loads corresponding to the patient's mass of 100 kg (Table 1). As expected the increased failure risk of periprosthetic bone and bone-implant interface was found for both implants (Table 2). However, direct interface failure was indicated only for the OPRA prosthesis.

		Load case 1			Load case 2					
		intact bone	OPRA	ISP	intact bone		OPRA		ISP	
bonded	**Bone volume**									
	von Mises stress strength	0.26	0.14	0.16	0.10	(0.18)	0.12	(0.20)	0.18	(0.40)
	strain energy density	0.032	0.006	0.008	0.007	(0.018)	0.006	(0.017)	0.007	(0.021)
	Interface area									
	Hoffman value		0.14	0.08			0.16	(0.50)	0.10	(0.16)
	shear stress		7.20	1.40			5.20	(8.40)	1.98	(2.42)
	compressive stress		2.38	4.98			4.38	(4.20)	5.39	(6.82)
	tensile stress		2.00	2.79			2.40	(3.81)	2.85	(5.42)
debonded	**Bone volume**									
	von Mises stress strength		0.16	0.26			0.12		0.24	
	strain energy density		0.009	0.009			0.008		0.009	
	Interface area									
	shear stress		1.80	2.10			1.80		1.84	
	compressive stress		5.03	6.40			5.40		5.20	

Table 2. 1% peak values calculated for body mass of 61 kg and 100 kg (values in brackets).

Discussion

Our study aimed to identify the mechanical situation after implantations of direct skeletal fixations for upper-leg prostheses. For this purpose we used the finite element method to analyze the intact femur and transected femora fitted with two different implants. The normal bone density assumed for the implanted femora represented a case of a patient fitted with direct fixation prosthesis shortly after trauma amputation. In this way, the bone properties in both analyzed cases are the same and the results are not biased by any individual factors such as level of activity and time between amputation and prosthesis implantation. The FE modeling demonstrated considerable difference in magnitude and distribution of stresses between the healthy and implanted femora. This effect is induced by the altered loading conditions of the amputated bone as well as by the introduction of the intramedullary implant. The muscle activity in the amputated leg is considerably impaired, therefore the remaining bone experiences less loading from the muscular system. This finding correlates well with lower bone mineral densities measured in post-amputation femora (Sherk et al., 2008).

The influence of the implant on the surrounding bone is an important aspect in contemporary endoprosthetics. The notable variation in stress patterns in the bone around both direct fixation implants originates from their different geometric and elastic properties. The ISP stem promotes slightly more uniform load transfer than the threaded OPRA device. The observed stress patterns for the latter prosthesis were similar to those recently reported by Xu and Robinson (Xu et al., 2006). The more favorable bone-implant interface stress transfer was found in case of the ISP implant, in which the low stiffness porous structure at the stem appears to reduce shear stresses at the bone-implant interface.

The considerable difference of strain energy distribution between intact and implanted femora suggests new bone formation in the regions adjacent to the proximal end of the implants and bone resorption in the distal part of the bone. This stays in agreement with published clinical data of the OPRA patients (Xu et al., 2006). Bone stock preservation and minimization of the bone failure risk appear to be incompatible design goals. The direct comparison of the SED levels around both implants predicts less adverse bone remodeling around the ISP stem. On the other hand, analyzing the periprosthetic bone failure probability around fixations suggests that less bone damage is likely to appear around the OPRA device.

In our study we used load data reported from two different measurement setups, that could also introduce inaccuracy in the analysis, but it obviously is very difficult to get a consistent loading data set (intact and amputated) of the same person. Furthermore, it should be realized that this loading configuration does not represent a worst case scenario; staircase climbing or stumbling would be better suitable for that. However, for the amputated patient these loading configurations are unknown. Estimating these loads from the healthy situation is not possible due to the absence of muscle forces in amputated patients. However, we believe that the qualitative differences in both systems will remain as found in this study for these higher load cases.

For analyzing the two prosthetic systems analyzed in this study some assumptions were made. The trabecular metal was assumed to have only some stiffening due to bone ingrowth and omitting the threading of the OPRA system was thought to be of minor influence for the global stress transfer patterns. Furthermore, bony ingrowth was assumed to be either fully absent or fully completed, which is obviously a simplification of reality. Nevertheless, we believe that we have simulated the most important features of the two prosthetic systems to an adequate degree in order to get an estimation of the load-transfer mechanisms that are involved in the short and longer-term fixation of these types of implants. Based on these assumptions, we would like to emphasize that the results of this study should be considered from a global point of view rather than trusting the exact figures.

From a mechanical perspective loading of the implant directly post-operative does not considerably increase bone failure risk. Therefore assuming an accurate fit between the implant and prosthesis, a shorter delay period between implantation and loading of the stem may be considered. However, whether early loading would jeopardize bony ingrowth due to dynamic motions at the implant-bone interface was not analyzed in this study and would require further analyses.

A considerable increase in the failure risk of the bone-implant integrity was found with a body mass increase to 100 kg, which justifies the limitation used in clinical practice. It furthermore highlights that the factor of safety against mechanical failure of these reconstructions is relatively low, which corresponds to the reported in-vivo literature (Sullivan et al., 2003; Ward, 2005; Büll, 2006).

In conclusion, we found some general differences between the two designs analyzed in this study. The ISP design seemed to have a slightly more physiological SED distribution (favoring long-term bone maintenance), but the OPRA design generated lower bone stresses (reducing the risk of bone fracture). The application of a low-stiffness porous layer on the ISP stem's surface appears to be very favorable for bone-implant interface safety. With this respect we would recommend this method for the intramedullary fixation.

In a more general sense, implantation of a percutaneous amputation prosthesis had considerable effects on the stress and strain energy density levels in the bone. This was caused by the implant itself, but also by the changed loading conditions. The safety factor against periprosthetic bone failure of the two percutaneous designs was relatively low. In order to increase it, we recommend to use a porous metal layer on the entire intramedullary part of a stem. The performed analysis is currently used to develop an alternative implant design with increased safety factor against mechanical failure.

References

Bergkvist, R. (1998). Osseointegration: case report on prosthetic treatment in transfemoral amputation. IXth World Congress ISPO, Amsterdam.

Branemark, P.-I. (2001). Bone-anchored amputation prostheses for the upper limb. The osseointegration book. P.-I. Branemark, Quintessenz Verlags: 443--462.

Branemark, R., et al. (2001). "Osseointegration in skeletal reconstruction and rehabilitation: a review." Journal of Rehabilitation Research and Development 38(2): 175-181.

Büll, O. (2006). Theoretische aspekte und erste praktische ergebnisse von perkutanen exoprothesen bei oberschenkelamputationen. Munich, Ludwig-Maximilians-University.

Carter, D. R. (1987). "Mechanical loading history and skeletal biology." J Biomech 20(11-12): 1095-1109.

D'Lima, D. D., et al. (2007). "In vivo knee moments and shear after total knee arthroplasty." J Biomech 40 Suppl 1: S11-17.

Gunterberg, B., Branemark, P-I., Branemark, R., Bergh, P. and Rydevik, B. (1998). Osseointegrated prosthesis in lower limb amputation: the development of a new concept. IXth World Congress ISPO, Copenhagen, ISPO.

Hagberg, K., et al. (2001). "Consequences of non-vascular trans-femoral amputation: a survey of quality of life, prosthetic use and problems." Prosthetics and Orthotics International 25(3): 186-194.

Hagberg, K., et al. (2008). "Osseointegrated trans-femoral amputation prostheses: prospective results of general and condition-specific quality of life in 18 patients at 2-year follow-up." Prosthetics and Orthotics International 32(1): 29-41.

Hagberg, K., et al. (2005). "Socket versus bone-anchored trans-femoral prostheses: hip range of motion and sitting comfort." Prosthetics and Orthotics International 29(2): 153-163.

Helgason, B., et al. (2009). "Risk of failure during gait for direct skeletal attachment of a femoral prosthesis: a finite element study." Med Eng Phys 31(5): 595-600.

Hoffman, O. (1967). "The brittle strength of orthotropic materials." Journal of Composite Materials 1: 200-206.

Huiskes, R., et al. (1995). "Preclinical testing of total hip stems. The effects of coating placement." Clin Orthop Relat Res(319): 64-76.

Kaplan, S. J., et al. (1985). "Tensile strength of bovine trabecular bone." J Biomech 18(9): 723-727.

Keyak, J. H. (2001). "Improved prediction of proximal femoral fracture load using nonlinear finite element models." Med Eng Phys 23(3): 165-173.

Keyak, J. H., et al. (2003). "Comparison of in situ and in vitro CT scan-based finite element model predictions of proximal femoral fracture load." Medical Engineering & Physics 25(9): 781-787.

Keyak, J. H., et al. (2005). "Predicting proximal femoral strength using structural engineering models." Clinical Orthopaedics and Related Research 437: 219-228.

Keyak, J. H., et al. (1994). "Correlations between orthogonal mechanical properties and density of trabecular bone: use of different densitometric measures." Journal of Biomedical Materials Research 28(11): 1329-1336.

Keyak, J. H., et al. (1998). "Prediction of femoral fracture load using automated finite element modeling." Journal of Biomechanics 31(2): 125-133.

Klinbeil, K. (2006). Metallurgische Grundlagen für die gusstechnische Herstellung einer räumlichen Oberflächenstruktur. Ossärre Integration. R. Gradinger and H. Gollwitzer. Heidelberg, Springer Medizin Verlag: 46-52.

Lee, W. C., et al. (2007). "Kinetics of transfemoral amputees with osseointegrated fixation performing common activities of daily living." Clinical Biomechanics 22(6): 665-673.

Lee, W. C., et al. (2008). "Magnitude and variability of loading on the osseointegrated implant of transfemoral amputees during walking." Med Eng Phys 30(7): 825-833.

Rommers, G. M. (2008). Epidemiologie van amputaties aan de onderste extremiteit. Amputatie en prosthesiologie van de onderste extremiteit. J. H. B. Geertzen, Rietman J.S., Lemma: 53.

Sherk, V. D., et al. (2008). "BMD and bone geometry in transtibial and transfemoral amputees." Journal of Bone and Mineral Research 23(9): 1449-1457.

Shirazi-Adl, A., et al. (1993). “Experimental determination of friction characteristics at the trabecular bone/porous-coated metal interface in cementless implants.” J Biomed Mater Res 27(2): 167-175.

Staubach, K. H., et al. (2001). “The first osseointegrated percutaneous prosthesis anchor for above-knee amputees.” Biomedizinische Technik Biomedical engineering 46(12): 355-361.

Stone, J. L., et al. (1983). “Multiaxial strength characteristics of trabecular bone.” J Biomech 16(9): 743-752.

Sullivan, J., et al. (2003). “Rehabilitation of the trans-femoral amputee with an osseointegrated prosthesis: the United Kingdom experience.” Prosthetics and Orthotics International 27(2): 114-120.

Van Rietbergen, B., et al. (1993). “ESB Research Award 1992. The mechanism of bone remodeling and resorption around press-fitted THA stems.” J Biomech 26(4-5): 369-382.

Ward, D. A., Robinson, K.P. (2005). Osseointegration for the skeletal fixation of limb prostheses in amputations at the trans-femoral level. The osseointegration book. P.-I. Branemark, Quintessenz Verlags: 463-476.

Weinans, H., et al. (1992). “The behavior of adaptive bone-remodeling simulation models.” J Biomech 25(12): 1425-1441.

Xu, W., et al. (2000). “Finite element analysis of bone stress and strain around a distal osseointegrated implant for prosthetic limb attachment.” Proc Inst Mech Eng H 214(6): 595-602.

Xu, W., et al. (2008). “X-ray image review of the bone remodeling around an osseointegrated trans-femoral implant and a finite element simulation case study.” Annals of Biomedical Engineering 36(3): 435-443.

Xu, W., et al. (2006). “Three-dimensional finite element stress and strain analysis of a transfemoral osseointegration implant.” Proceedings of the Institution of Mechanical Engineers, Part H: Journal of Engineering in Medicine 220(6): 661-670.

Zheng, L., Luo, J., Wang, X., Chen, J., Gu, Z., Zhang, X (2005). “3D finite element analysis of bone stress around distally osseointegrated implant for artificial limb attachment.” Key Engineering Materials (288-289): 653-656.

Chapter 3

Simulated bone remodeling around two types of osseointegrated implants for direct fixation of upper-leg prostheses

P.K. Tomaszewski[1], N. Verdonschot[2,3], S.K. Bulstra[4], J.S. Rietman[3,5], G.J. Verkerke[1,3]

[1] Departments of Biomedical Engineering and [1]Orthopaedics, University Medical Center Groningen, University of Groningen, Groningen, The Netherlands.
[2] Radboud University Nijmegen Medical Centre, Orthopaedic Research Laboratory, P.O. Box 9101, 6500 HB Nijmegen, The Netherlands.
[3] Department of Biomechanical Engineering, University of Twente, Enschede, The Netherlands.
[4] Department of Orthopaedics, University Medical Center Groningen, University of Groningen, The Netherlands.
[5] Roessingh Research and Development, Enschede, The Netherlands.

Journal of Mechanical Behavior of Biomedical Materials, in press, 2012.

Introduction

After upper leg amputation patients are conventionally fitted with a prosthetic socket that embraces the residual limb and connects the external leg prosthesis to the body. An alternative solution is a direct attachment of the leg prosthesis to the skeletal system by an osseointegrated percutaneous implant fitted in the medullary canal of the femur remnant. As a result, a connection of the artificial limb directly to the skeletal system is achieved.

Currently, two types of trans-femoral percutaneous implants are in clinical use, the OPRA system (Integrum AB, Göteborg, Sweden) and the ISP Endo/Exo prosthesis (ESKA Implants AG, Lübeck, Germany). Both implants differ in composition and structure. The OPRA implant has a form of a threaded titanium pin, which is screwed in the medullary cavity during an implantation (Branemark et al., 2001). The ISP prosthesis, a press-fit implant, is composed of a cobalt-chromium-molybdenum (CoCrMo) stem covered with a porous trabecular metal (Aschoff, 2010).

These implants overcome disturbing soft tissue problems present with conventional socket systems and provide a better control of the prosthetic limb (Ward, 2005). Consequently, they increase a patient's activity levels and offer a larger range of hip joint motion and sitting comfort compared to socket prostheses (Hagberg et al., 2005; Hagberg et al., 2008).

However, the percutaneous implants are exposed to infections (Gunterberg, 1998; Ward, 2005; Buell, 2006), and a risk of bone and implant fracture (Sullivan et al., 2003; Ward, 2005; Buell, 2006; Aschoff, 2010). Moreover, these implants are expected to change bone loading, as compared to the intact situation (Gunterberg, 1998; Xu and Robinson, 2008). Excessive reduction in bone stress around an implant often results in a progressive loss of bone mineral density (BMD). This bone remodeling reduces prosthesis support, decreases bone strength and ultimately may lead to implant loosening or a bone fracture if an adverse loading event occurs (Petersen et al., 1995; Spittlehouse et al., 1998; Kobayashi et al., 2000). Additionally, bone loss compromises bone stock when revision surgery is required. Several factors influencing bone remodeling have been identified, for example stem shape, material properties and interface bonding characteristics (Engh et al., 1987; Huiskes et al., 1992; Weinans et al., 1992; Engh et al., 1999), properties of the host bone, including geometry, bone mineral density and cortical thickness (Buckland et al., 2010).

Usually percutaneous implants are placed in patients that have utilized a standard socket prosthesis before (Aschoff et al., 2009; Hagberg and Branemark, 2009). Hence, the bone has not been loaded to physiological levels for some time, resulting in considerable bone loss (Sherk et al., 2008). This is confirmed in a clinical study showing substantial bone loss after mid-term usage of a socket prosthesis (Xu and Robinson, 2008). The decreased bone quality and its subsequent inferior strength, prior to the implantation of a percutaneous prosthesis, may make the issue of periprosthetic bone remodeling even more critical for direct-fixation implants. Alternatively, osseointegrated fixation prostheses can also be implanted in patients immediately after amputation (Büll, 2006); however this is not common clinical practice. The timing of implantation can seriously influence the long-term bone turnover.cx

The long-term bone turnover after implantation can be quantitatively predicted by an adaptive bone-remodeling simulation, which combines bone remodeling theory with finite element (FE) analysis. The developed numerical models have provided good predictions of adaptive changes in the periprosthetic bone (Van Rietbergen et al., 1993; Kerner et al., 1999). A good correlation of numerical results with animal experiments and clinical data has been reported in multiple studies (Weinans et al., 1993; Kerner et al., 1999; van Rietbergen and Huiskes, 2001). So far, no attempts have been made to predict bone turnover around trans-femoral direct fixation stems.

In the current paper, we compared long-term periprosthetic bone changes around two types of direct fixation implants considering two possible initial situations. First, we simulated immediate post-amputation implantation of the two different osseointegrated implants, which is represented by conventional bone remodeling simulation, the same as developed for hip stems. Secondly, a new approach was implemented, which takes into account post-socket bone degeneration as a starting point, thereby assuming that the prosthesis is implanted after a considerable amount of post-amputation time and bone loss. It might appear that due to the relative increase in direct bone loading, osseointegrated prostheses implanted after prolonged socket use can induce some bone formation, which is lost during the period of prosthetic socket use. Therefore we studied the influence of the delay between amputation and implantation on periprosthetic bone turnover around both direct fixation implants.

The main goal of the study was to investigate differences in long-term bone changes between the two types of osseointegrated implants and assess how the bone remodeling process was affected after implantation (either direct or long term post-amputation) of an upper-leg prosthesis. Moreover, we questioned if the implants is more likely to provoke excessive bone remodeling, thereby inducing premature bone fracture in the analyzed scenarios.

Materials and Methods

Finite element analysis

Generic FE models of intact femoral bone and amputated bones implanted with direct-fixation implants, with similar geometrical and mechanical characteristics as OPRA and ISP Endo/Exo prosthesis, were created for this study (Figure 1). The FE model of the bone was based on computed tomography (CT) data of a femoral bone of an 81 year old male with normal bone quality. However, to represent the typical young amputation patient, the density of the bone was linearly upscaled to obtain a bone mineral density in the femoral neck of (BMDneck=1.01 g/cm^2) (Sherk et al., 2008).

The Young's moduli of the bone elements were derived from their ash densities (Keyak and Falkinstein, 2003): $E = 33900\rho_{ash}^{2.20}$ for $\rho_{ash} \le 0.27$ (trabecular bone); $E = 10200\rho_{ash}^{2.01}$ for $\rho_{ash} \ge 0.6$ (cortical bone); $E = 5307\rho_{ash} + 469$ for $0.27 < \rho_{ash} < 0.6$ (transition); where ρ_{ash} was calculated from calcium hydroxyapatite (CHA) - calibrated CT scan data using the relationship (Keyak et al., 2005): $\rho_{ash} = 0.0633 + 0.887\rho_{CHA}$. Poisson's ratio for all bone elements was 0.35.

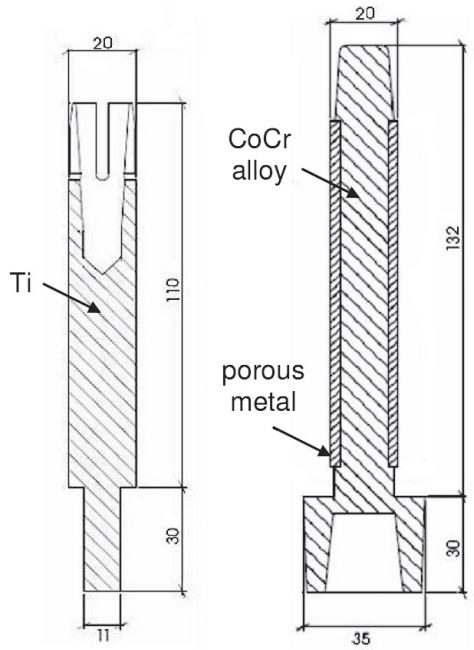

Figure 1. Schematic representation of the implants' models used in the study.

Load case	Load					
	F_{SI} [N]	F_{AP} [N]	F_{ML} [N]	M_{SI} [Nm]	M_{AP} [Nm]	M_{ML} [Nm]
1	780	100	-20	-2.0	30.8	-7.2
2	180	120	40	0.0	37.3	4.1

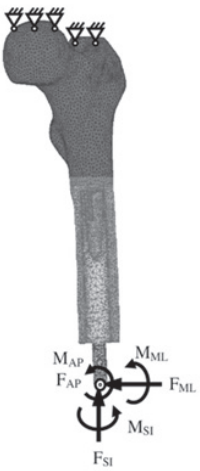

Figure 2. Left: Loads used in the simulations (Lee et al., 2007); Right: FE model and applied boundary conditions (periprosthetic bone volume used in failure risk analysis depicted in light color).

The optimal mesh size for the bone model was determined by a mesh refinement test with 5% convergence error for the peak von Mises stress. The edge length for all meshes was 3 mm except for the interface region where it was further refined, leading to meshes between 150,000 and 190,000 of four-noded tetrahedral elements.

The surface-shape contour models of the OPRA and the ISP implants were fitted in the femoral bone (amputated 250 mm above the knee) and implemented into the FE models. The implants of the same outer diameter (20 mm) were assumed to be bonded to represent full osseointegration.

Characteristic elastic moduli for implant materials was taken as follows: ISP prosthesis stem (cobalt-chromium-molybdenum) MPa and the porous metal layer MPa (Klinbeil, 2006); the OPRA implant (commercially pure titanium) MPa. Poisson's ratio for all implant materials was set to 0.3.

Two loading cases from a normal walking cycle at 25% (heel strike) and 55% (shortly before toe-off) were considered (Figure 2). The loading of the implants were taken from the experimental measurements with the OPRA device (Lee et al., 2007). In all simulations the bone was rigidly fixed at the proximal end away from the prosthetic tip to eliminate the effect on the peri-prosthetic stress distribution. The load was applied distally (Figure 2).

Bone failure risk assessment

Periprosthetic bone failure risk was evaluated by considering the von Mises stress (σ_{VM}) criterion (Keyak et al., 1998; Keyak and Falkinstein, 2003; Keyak et al., 2005). The bone strength (S) was calculated for each bone element (Keyak and Falkinstein, 2003) as: $S = 137 \cdot \rho_{ash}^{1.88}$ for $\rho_{ash} < 0.317$ (trabecular bone); $S = 114 \cdot \rho_{ash}^{1.72}$ for $\rho_{ash} \geq 0.317$ (cortical bone). Bone failure risk was identified when $\sigma_{VM} / S \geq 1$.

To minimize mesh dependency on the calculated results, we chose to define a 'failure risk parameter' (FRP). This defined the peak stress threshold beyond the one percent of the periprosthetic bone volume was exposed to (Figure 3). The periprosthetic bone volumes for stress assessment were selected from the osteotomy up to 10 mm above the proximal implants' end (Figure 2).

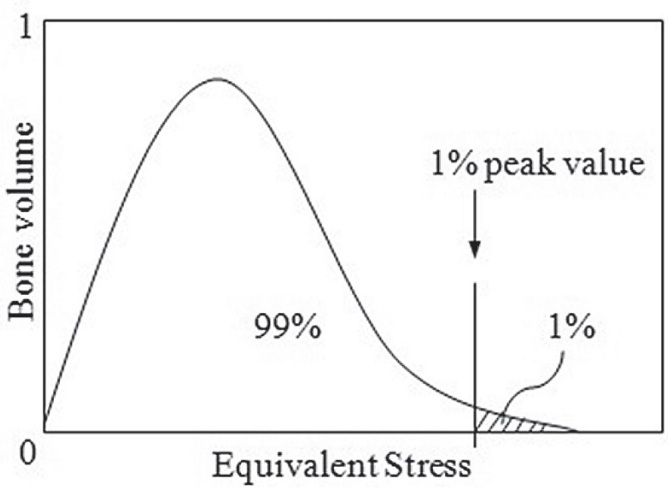

Figure 3. The 1% peak value determined from volumetric distribution of the equivalent stress.

Bone remodeling simulation

The strain adaptive bone remodeling theory was used to predict long-term changes in bone mineral density (BMD). The theory assumes that during representative loading cycles bone cells react to local changes in elastic strain energy, which were provoked by the prosthesis relative to the normal physiological situation. In the mathematical formulation, the bone remodeling signal (r), produced by two loads and subsequently averaged, was determined in each element as the average strain energy per unit of mass. In each time step the rates of bone density adaptation are determined by comparing the signal values in the implanted model (r) to the pre-operative reference values (rref). In the locations, where remodeling stimulus (r-rref) is positive, bone was formed (BMD increases). Consequently, a negative stimulus indicates local bone loss (BMD decreases). A threshold level r=0.35rref is assumed (Tarala et al., 2011), which leads to a stimulus zone where no reaction occurs. Furthermore, it was assumed that bone formation and loss occur more rapidly in bone with a higher amount of free surface. Typically, the free surface was low in case of low and very high bone density (Martin, 1972).

To calculate bone remodeling an iterative simulation procedure was integrated with the FE program MSC.Marc (MSC Software Corporation, Santa Ana, CA, USA).

Two different scenarios of bone remodeling around direct fixation prostheses were simulated, one being 'immediate implantation', the other assuming considerable time of socket prosthesis use – 'post-socket'. In the immediate scenario, similarly as in other studies (Weinans et al., 1993; van Rietbergen and Huiskes, 2001), the same intact bone density distributions (BMD_{neck}=1.01 g/cm^2) are assumed in the reference and implanted model. In the second scenario the reference model had the again intact BMD (BMD_{neck}=1.01 g/cm^2) and in the amputated femur model the BMD was reduced by 30% (BMD_{neck}=0.72 g/cm^2) due to bone disuse caused by socket prosthesis as reported for transfemoral amputees (Sherk et al., 2008).

The simulations predict bone remodeling as a function of computer time units (CTU). To relate the CTU to actual clinical time, the predictions were quantified by fitting a simulated case to clinical measurements of bone remodeling around the OPRA implant (post-socket scenario), reported by Xu and Robinson (Xu and Robinson, 2008), who measured bone remodeling around the OPRA implant (post-socket scenario). The remodeling period of 50 months was considered for this study as then the highest changes in bone remodeling are expected (Tarala et al., 2011), moreover a clinical evidence has suggested that bone suffers from 'memory loss' and the adaptive process stops after sixty months (Petersen et al., 1995; Saari et al., 2007).

Subsequently, the results were presented in the form of dual energy X-ray absorptiometry (DXA) scans. The BMD and bone mineral content (BMC) around implants were measured in 7 zones (Figure 5), corresponding to Gruen zones defined for hip stems (Gruen et al., 1979).

Figure 4. Bone changes around the OPRA implant: Left: clinical radiograph at 64 months; Right: simulated image ('post-socket' scenario) at 620 computer time units (CTU). Determined time factor: 1 month = 10CTU.

Results

General bone remodeling patterns observed after the 'immediate implantation' scenario were similar around both implants. They were characterized by a mild bone densification around the tip of the implants; medium bone loss in the middle regions and relatively large bone loss close to the osteotomy level. After 20 months both implants presented slight increase (+1%) in BMD in the proximal zone 4 and around -9% BMD decrease in the distal zones. In the middle zones the OPRA showed up to -9% bone loss and the ISP up to -7% (zone 2). The differences were more visible after 50 months of simulated time, when BMD loss in the distal zones was on average -21% around the OPRA and -24% around the ISP.

In the 'post-socket' simulation, high bone resorption was found around the distal end of the femur and a considerable bone deposition at the proximal tip of the OPRA implant. A close match between the simulated and the clinical bone contours enabled the simulations' time scale to be determined; according to which 10 CTU were equivalent to 1 month in-vivo (Figure 4).

The difference between both implants was much more pronounced in the 'post-socket' case, where the ISP implant showed considerably less bone loss during remodeling. The simulation of 'post-socket' implantation indicated similar levels of new bone formation around both implants (Figure 6); however not leading to overall improvement in bone stock preservation. Relatively higher BMD increase was found only

in the proximal zone 4 for both implants (OPRA +28%, ISP +27%) compared to 'immediate implantation' (OPRA +4%, ISP +2%) at 50 months post-operatively. Additionally a mild bone densification was visible in the femoral head and intertrochanteric region (Figure 6). The highest bone loss was found in the distal regions (zone 1 and 7) on average -15% OPRA, -17% ISP after 20 months and -42% ISP to -50% OPRA after 50 months. A moderate reduction of the bone stock occurred around the middle-part of

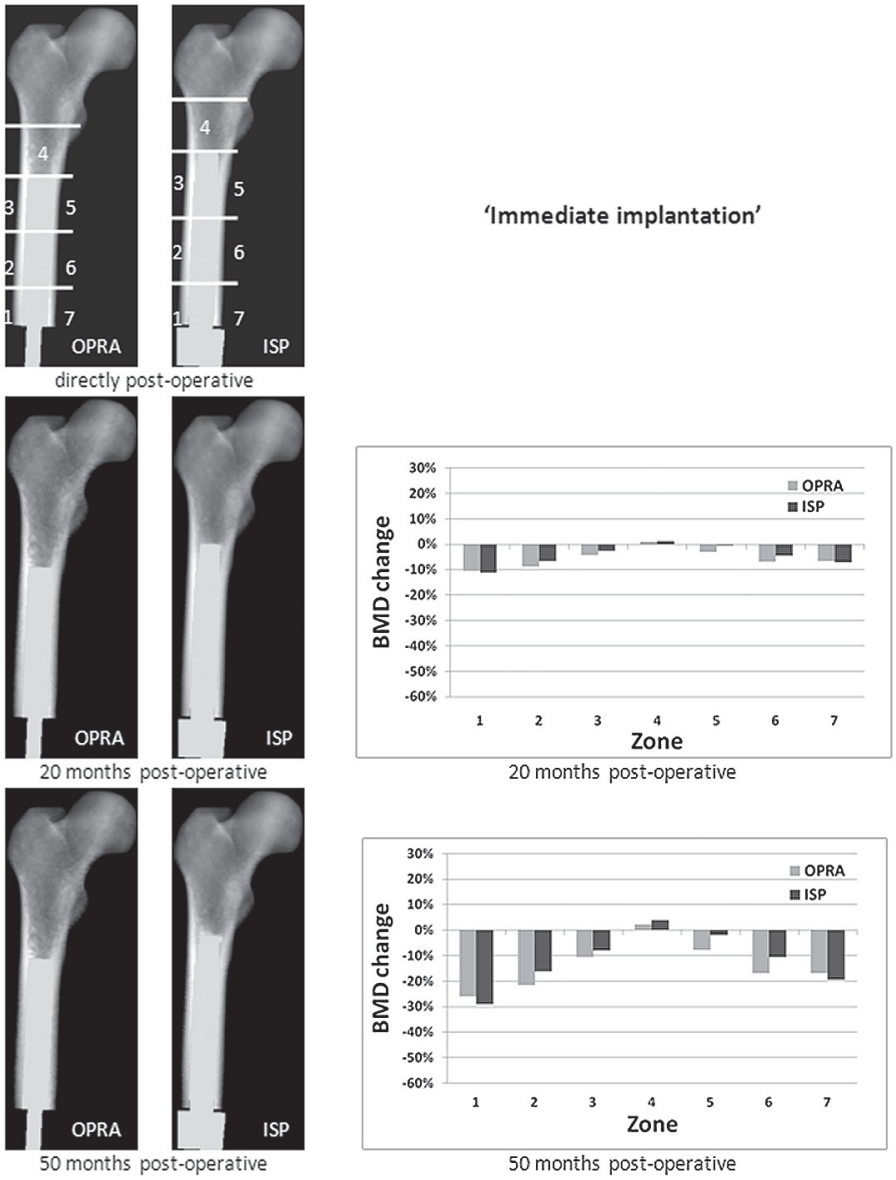

Figure 5. Comparison of bone remodeling around both implants at different time points ('immediate implantation' scenario). Left: Simulated radiographs; Right: Bone remodeling calculated in zones around implants.

the stems (zone 2 and 6), where the maximum bone loss was -14% and -44% for OPRA and -6% and -17% for ISP in 20 and 50 months, respectively. In the proximal region (zones 3 and 5) a slight bone loss was present for the OPRA implant (maximum of -2% at 20 months and -9% at 50 months) and a moderate bone densification for the ISP implant (maximum of +10% and +13 % at 20 and 50 months).

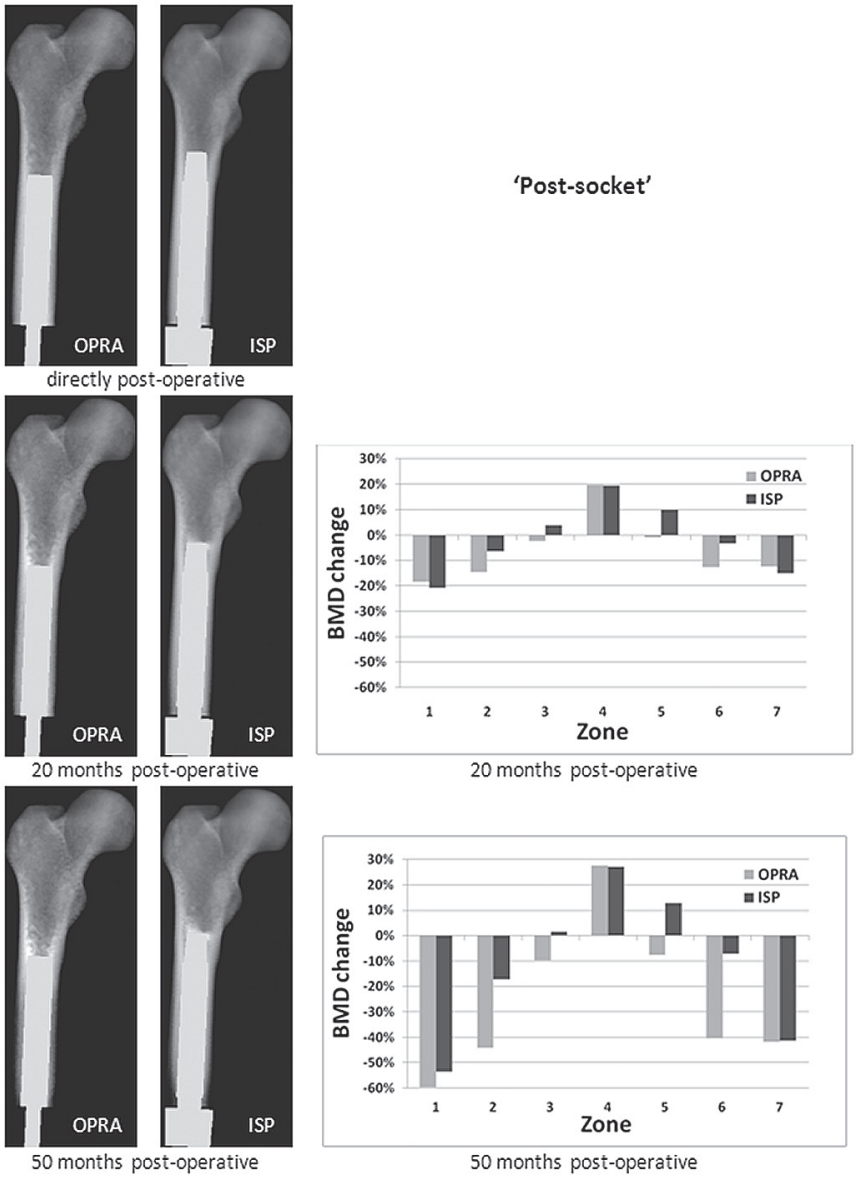

Figure 6. Comparison of bone remodeling around both implants at different time points ('post-socket' scenario) Left: Simulated radiographs; Right: Bone remodeling calculated in zones around implants

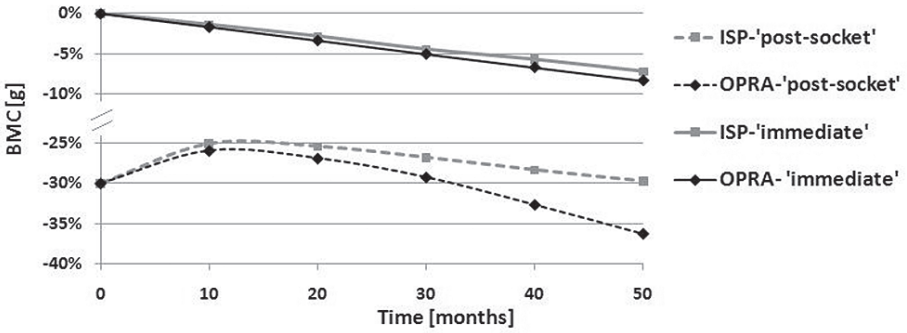

Figure 7. Change of total bone mineral content in all zones around implants obtained from 'immediate' (--) and 'post-socket' (–) implantation scenario.

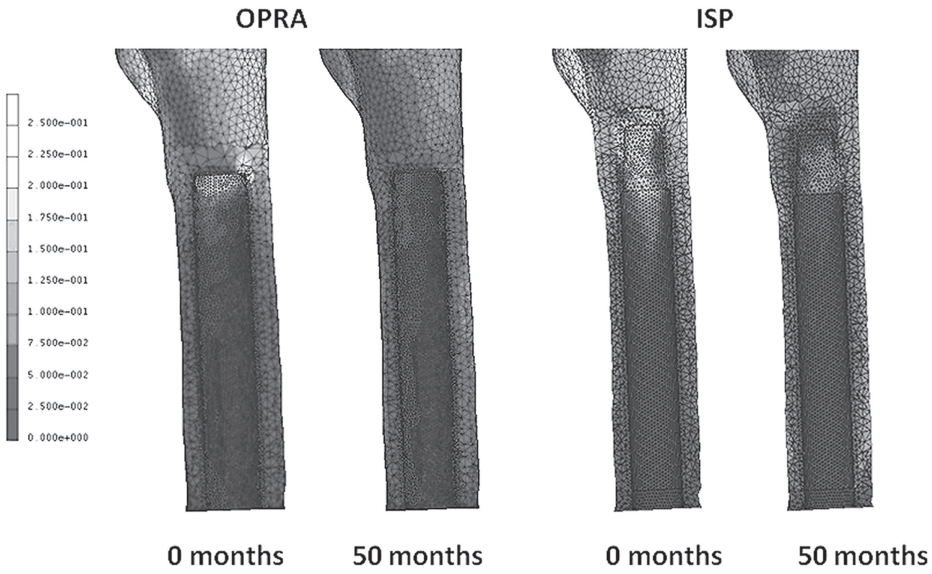

Figure 8. Periprosthetic bone failure risk (σ_{VM}/S) around implants in the 'post-socket' scenario, directly after implantation and after 50 months of bone remodeling.

Also in terms of total bone mineral content calculated around the stems, more bone loss was provoked by the OPRA implant than the ISP prosthesis. Despite the initial bone densification observed in the 'post-socket' scenario, the overall levels of the BMC for both implants remained considerably lower than in case of 'immediate implantation'. For the 'immediate implantation' scenario BMC the overall bone decrease was -3% for both implants after 20 months and -7% (ISP) to -8% (OPRA) after 50 months (Figure 7). For the 'post-socket' scenario an overall BMC increase was found in the first period, with a maximum of +5% for ISP and +4% for OPRA between 10 and 20 months. Afterwards, a slow decrease resulted in the BMC level comparable with the initial one for the ISP and -6% lower for the OPRA after 50 months.

Simulated bone remodeling did not indicate any direct risk of premature bone fracture as indicated by the 'failure risk parameter' (FRP<1.0). Generally, a lower periprosthetic bone failure risk was found for the OPRA implant as compared to the ISP prosthesis. In the 'immediate implantation' scenario FRP increased in a period of 50 months from 0.12 to 0.22 for the ISP and from 0.08 to 0.09 for the OPRA implant. On the other hand, loading of the 'post-socket' bone resulted in better maintained bone density and consequently decreased fracture risk. After 50 months the FRP decreased for both implants: 0.39 to 0.23 (ISP) and 0.17 to 0.12 (OPRA) (Figure 8). Nevertheless, the FRP at 50 months after 'post-socket' implantation remained higher than in case of 'immediate' implantation. Hence the probability of peri-prosthetic fractures remained higher for the post-socket case.

Discussion

In this study adaptive bone remodeling simulation was used to investigate long-term periprosthetic bone changes around two types of direct-fixation implants considering two different initial conditions. Considerable differences in bone remodeling were present for both implants and initial conditions. The simulation results were qualitatively compared with the clinical findings and consistent bone resorption patterns were observed. The bone turnover after implantation of direct-fixation implants is more complex than in case of hip arthroplasty due to post-amputation bone quality deterioration. Interestingly, in this case a rapid spatial redistribution of density, dominated by high density increase in the proximal zone, is visible in the initial period. Once the bone density reaches it saturation in this region (according to the free surface definition) the local rate of mass change is very low and the relatively slower bone loss in the distal regions becomes dominant as visible on BMC plot in Figure 8. The modified bone remodeling model, which accounts for this effect, in our opinion enables the prediction of realistic bone changes around the analyzed implants. The considerable bone strengthening in the region proximal to the implant can be explained by increased bone loading induced by direct skeletal fixation implants, as compared with conventional socket prostheses. Validation of the bone remodeling patterns as found in this study is not straightforward due to an uncommon way of bone change measurement around the OPRA implant in the clinical study (Xu and Robinson, 2008). Standard radiographs enabled only measurement of cortical thickness change instead of BMD as provided by standard DXA-scanning. Therefore simulated bone remodeling patterns could be only visually compared with the clinical results.

In the performed analysis the ISP prosthesis was observed to offer better bone stock preservation than the OPRA implant. The use of a porous flexible metal layer on the CoCrMo stem results in a much lower overall stiffness of the ISP-type implant as compared to solid titanium OPRA-type implant. Consequently a more physiological load transfer to the bone is obtained, what was also found in a previous study (Tomaszewski et al., 2010). This results also in a less-extensive bone remodeling response, which can be considered as an advantage. On the other hand, the ISP implant presented generally higher bone failure risk than the OPRA prosthesis. The highest values of the

FRP were always found at the tip of the ISP implant, which was in direct contact with the trabecular bone. It is not surprising as at this location the CoCrMo core of the ISP implant is not covered with the porous trabecular metal layer. Also the OPRA implant presented elevated FRP values at the proximal tip, even though the stiffness of the implant in this region is reduced by some material removal. This study used a stress based bone failure criterion (rather than strain based one), as it was demonstrated in numerous studies to provide accurate bone failure predictions (Keyak et al., 1998; Keyak and Rossi, 2000; Keyak et al., 2005; Tanck et al., 2009; Derikx et al., 2011).

Obviously the simulations embed several limitations which should be considered when interpreting the results. The bone remodeling algorithm does not take into account metabolic aspects related to vascularization or genetic differences, which are not crucial for the performed comparative analysis. Moreover the used adaptive bone remodeling algorithm modeled changes in the BMD without (internal remodeling) predicting modifications of the external bone geometry, which are present on the clinical radiographs (Xu and Robinson, 2008). The internal bone remodeling algorithm is capable to provide realistic predictions of the bone turnover as was demostrated in numerous studies (Huiskes et al., 1992; Van Lenthe et al., 1997; Kerner et al., 1999; Barink et al., 2003; Sharma et al., 2010; Chong et al., 2011; Tarala et al., 2011). The current study assumed the threshold of remodeling signal at the level of r=0.35r, similarly as a different study using the same bone model (Tarala et al., 2011), as sensitivity analysis of this parameter would require more extensive clinical data than currently available (Xu and Robinson, 2008).The bone model was based on CT-scans of an 81 year old male, which is not the common age for patients, treated with osseointegrated implants. The reason for using this CT-data was the fact that the model was based on a cadaver bone. As we have no access to younger donors, we had to re-scale the bone density to the typical young amputation patient. It should be noted that, the coefficients of calibration equation taken from literature data (Keyak et al., 2005) are dependent on number of factors such as for example the CT machine parameters. Although the bone properties in this case might not exactly represent the reality, the same method provided previously accurate predictions for bone failure strength (Tanck et al., 2009).

The rescaling of the original BMD enabled to fit the model with the clinical data, reported for younger patients (Xu and Robinson, 2008) and subsequently allowed determining the time constant, which was based, however, only on one time point.

Another shortcoming is the application of the same loading conditions for both intact and implanted models. In this manner, only the effect of the implant is modeled and changes in the muscle loading due to amputation are not considered. We are convinced that this does not influence the results of the performed qualitative relative comparison. This could be further improved by incorporating musculoskeletal modeling into bone remodeling simulations.

Remarkably, ‘post-socket’ implantation patients lose relatively less bone, however, as their initial BMD is about 30% lower than for ‘immediate implantation’, they remain at higher risk for implant failure. If these healthy younger patients receive a fixation implant immediately after trauma, less effect of the implant on the

periprosthetic bone is expected due to better initial bone quality (Engh et al., 1992), what also results in higher safety against mechanical failure.

The simulation included two peak values of all daily activities and assumed the same loading frequency before and after implantation. However, this frequency may decrease in case of a trauma patient immediately implanted with an osseointegrated prosthesis and increase for patients, who received implant after problems with socket prosthesis. On the other hand, if 'immediate implantation' patients are younger and more active, they might apply more adverse loads on the implant (or may fall more severely) which results in earlier loosening. Only a randomized long-term clinical study could identify differences between implants and patient groups, but due to the low number of patients per institute, this is very difficult to achieve. In fact the inability of clinical analysis makes these types of simulations especially valuable.

Models used in this study were generic, rather than subject-specific; nevertheless in our opinion they represent the most important geometrical and mechanical features of the implants and were suitable for comparison of the bone changes. Obviously adverse biological conditions caused by, for example, infections were not considered.

Apparently, bone adaptation induced by more direct loading of the bone remnant by both analyzed osseointegrated prostheses is not able to compensate for the severe bone loss induced by sub-physiological loads due to socket use after amputation. Therefore, from a mechanical perspective, it is safer to perform the implantation directly after amputation instead of after a period of socket usage.

Conclusion

In conclusion, the two implants for direct prostheses fixation provoke considerable bone resorption. Much more bone loss was found around the titanium screw implant (OPRA-type) as compared with the porous coated CoCrMo stem (ISP-type and bone loss was much more severe after a prolonged period of post-socket use. Hence, from a biomechanical perspective it is better to limit the post-socket time and to re-design direct fixation devices to reduce bone loss and the probability of peri-prosthetic bone fractures.

References

Aschoff, H. H., et al. (2009). "The endo-exo femur prosthesis-a new concept of bone-guided, prosthetic rehabilitation following above-knee amputation." Zeitschrift für Orthopädie und Unfallchirurgie 147(5): 610-615.

Aschoff, H. H., Kennon, R.E., Keggi, J.M., Rubin, L.E. (2010). "Transcutaneous, Distal Femoral, Intramedullary Attachment for Above-the-Knee Prostheses: An Endo-Exo Device." Journal of Bone and Joint Surgery 92(Suppl 2): 180-186.

Barink, M., et al. (2003). "A different fixation of the femoral component in total knee arthroplasty may lead to preservation of femoral bone stock." Proc Inst Mech Eng H 217(5): 325-332.

Brånemark, R., et al. (2001). "Osseointegration in skeletal reconstruction and rehabilitation: a review." Journal of Rehabilitation Research and Development 38(2): 175-181.

Buckland, A. J., et al. (2010). "Periprosthetic Bone Remodeling Using a Triple-Taper Polished Cemented Stem in Total Hip Arthroplasty." Journal of Arthroplasty 25(7): 1083-1090.

Buell, O. (2006). Theoretische aspekte und erste praktische ergebnisse von perkutanen exoprothesen bei oberschenkelamputationen. Munich, Ludwig-Maximilians-Universitaet.

Büll, O. (2006). Theoretische aspekte und erste praktische ergebnisse von perkutanen exoprothesen bei oberschenkelamputationen. Munich, Ludwig-Maximilians-University.

Chong, D. Y., et al. (2011). "The influence of tibial component fixation techniques on resorption of supporting bone stock after total knee replacement." J Biomech 44(5): 948-954.

Derikx, L. C., et al. (2011). "Implementation of asymmetric yielding in case-specific finite element models improves the prediction of femoral fractures." Comput Methods Biomech Biomed Engin 14(2): 183-193.

Engh, C. A., et al. (1987). "Porous-coated hip replacement. The factors governing bone ingrowth, stress shielding, and clinical results." Journal of Bone and Joint Surgery 69(1): 45-55.

Engh, C. A., Jr., et al. (1999). "Factors affecting femoral bone remodeling after cementless total hip arthroplasty." Journal of Arthroplasty 14(5): 637-644.

Engh, C. A., et al. (1992). "A quantitative evaluation of periprosthetic bone-remodeling after cementless total hip arthroplasty." Journal of Bone and Joint Surgery, American Volume 74(7): 1009-1020.

Gruen, T. A., et al. (1979). ""Modes of failure" of cemented stem-type femoral components: a radiographic analysis of loosening." Clinical Orthopaedics and Related Research 141: 17-27.

Gunterberg, B., Branemark, P-I., Branemark, R., Bergh, P. and Rydevik, B. (1998). Osseointegrated prosthesis in lower limb amputation: the development of a new concept. IXth World Congress ISPO, Copenhagen, ISPO.

Hagberg, K., et al. (2009). "One hundred patients treated with osseointegrated transfemoral amputation prostheses-rehabilitation perspective." Journal of Rehabilitation Research and Development 46(3): 331-344.

Hagberg, K., et al. (2008). "Osseointegrated trans-femoral amputation prostheses: prospective results of general and condition-specific quality of life in 18 patients at 2-year follow-up." Prosthet Orthot Int 32(1): 29-41.

Hagberg, K., et al. (2005). "Socket versus bone-anchored trans-femoral prostheses: hip range of motion and sitting comfort." Prosthet Orthot Int 29(2): 153-163.

Huiskes, R., et al. (1992). "The relationship between stress shielding and bone resorption around total hip stems and the effects of flexible materials." Clinical Orthopaedics and Related Research 274: 124-134.

Kerner, J., et al. (1999). "Correlation between pre-operative periprosthetic bone density and post-operative bone loss in THA can be explained by strain-adaptive remodelling." J Biomech 32(7): 695-703.

Keyak, J. H., et al. (2003). "Comparison of in situ and in vitro CT scan-based finite element model predictions of proximal femoral fracture load." Medical Engineering & Physics 25(9): 781-787.

Keyak, J. H., et al. (2005). "Predicting proximal femoral strength using structural engineering models." Clinical Orthopaedics and Related Research 437: 219-228.

Keyak, J. H., et al. (1994). "Correlations between orthogonal mechanical properties and density of trabecular bone: use of different densitometric measures." Journal of Biomedical Materials Research 28(11): 1329-1336.

Keyak, J. H., et al. (2000). "Prediction of femoral fracture load using finite element models: an examination of stress- and strain-based failure theories." J Biomech 33(2): 209-214.

Keyak, J. H., et al. (1998). "Prediction of femoral fracture load using automated finite element modeling." Journal of Biomechanics 31(2): 125-133.

Klinbeil, K. (2006). Metallurgische Grundlagen für die gusstechnische Herstellung einer räumlichen Oberflächenstruktur. Ossärre Integration. R. Gradinger and H. Gollwitzer. Heidelberg, Springer Medizin Verlag: 46-52.

Kobayashi, S., et al. (2000). "Poor bone quality or hip structure as risk factors affecting survival of total-hip arthroplasty." Lancet 355(9214): 1499-1504.

Lee, W. C., et al. (2007). "Kinetics of transfemoral amputees with osseointegrated fixation performing common activities of daily living." Clinical Biomechanics 22(6): 665-673.

Martin, R. B. (1972). "The effects of geometric feedback in the development of osteoporosis." Journal of Biomechanics 5(5): 447-455.

Petersen, M. M., et al. (1995). "Changes in bone mineral density of the distal femur following uncemented total knee arthroplasty." Journal of Arthroplasty 10(1): 7-11.

Saari, T., et al. (2007). "Joint area constraint had no influence on bone loss in proximal tibia 5 years after total knee replacement." J Orthop Res 25(6): 798-803.

Sharma, G. B., et al. (2010). "Effect of glenoid prosthesis design on glenoid bone remodeling: adaptive finite element based simulation." J Biomech 43(9): 1653-1659.

Sherk, V. D., et al. (2008). "BMD and bone geometry in transtibial and transfemoral amputees." Journal of Bone and Mineral Research 23(9): 1449-1457.

Spittlehouse, A. J., et al. (1998). "Bone loss around 2 different types of hip prostheses." Journal of Arthroplasty 13(4): 422-427.

Sullivan, J., et al. (2003). "Rehabilitation of the trans-femoral amputee with an osseointegrated prosthesis: the United Kingdom experience." Prosthetics and Orthotics International 27(2): 114-120.

Tanck, E., et al. (2009). "Pathological fracture prediction in patients with metastatic lesions can be improved with quantitative computed tomography based computer models." Bone 45(4): 777-783.

Tarala, M., et al. (2011). "Balancing incompatible endoprosthetic design goals: a combined ingrowth and bone remodeling simulation." Med Eng Phys 33(3): 374-380.

Tomaszewski, P. K., et al. (2010). "A comparative finite-elelement analysis of bone failure and load transfer of osseointegrated prostheses fixations." Annals of Biomedical Engineering 38(7): 2418-2427.

Van Lenthe, G. H., et al. (1997). "Stress shielding after total knee replacement may cause bone resorption in the distal femur." J Bone Joint Surg Br 79(1): 117-122.

Van Rietbergen, B., et al. (2001). "Load transfer and stress shielding of the hydroxyapatite-ABG hip: a study of stem length and proximal fixation." J Arthroplasty 16(8 Suppl 1): 55-63.

Van Rietbergen, B., et al. (1993). "ESB Research Award 1992. The mechanism of bone remodeling and resorption around press-fitted THA stems." J Biomech 26(4-5): 369-382.

Ward, D. A., Robinson, K.P. (2005). Osseointegration for the skeletal fixation of limb prostheses in amputations at the trans-femoral level. The osseointegration book. P.-I. Brånemark, Quintessenz Verlags: 463-476.

Weinans, H., et al. (1992). "Effects of material properties of femoral hip components on bone remodeling." Journal of Orthopaedic Research 10(6): 845-853.

Weinans, H., et al. (1993). "Adaptive bone remodeling around bonded noncemented total hip arthroplasty: a comparison between animal experiments and computer simulation." J Orthop Res 11(4): 500-513.

Xu, W., et al. (2008). "X-ray image review of the bone remodeling around an osseointegrated trans-femoral implant and a finite element simulation case study." Annals of Biomedical Engineering 36(3): 435-443.

Chapter 4

Numerical analysis of an osseointegrated prosthesis fixation with reduced bone failure risk and periprosthetic bone loss

P.K. Tomaszewski[1], M. van Diest[1], S.K. Bulstra[2], N. Verdonschot[3,4], G.J. Verkerke[1,4]

[1] Department of Biomedical Engineering, University Medical Center Groningen, University of Groningen, The Netherlands.
[2] Department of Orthopaedics, University Medical Center Groningen, University of Groningen, The Netherlands.
[3] Radboud University Nijmegen Medical Centre, Orthopaedic Research Laboratory, Nijmegen, The Netherlands.
[4] Department of Biomechanical Engineering, University of Twente, Enschede, The Netherlands.

Journal of Biomechanics, 2012, Volume 45, Issue 11, pp. 1875-80.

Introduction

Osseointegrated prostheses fixation implants are available for rehabilitation of the transfemoral amputees since more than a decade. This direct attachment of an external leg prosthesis to the skeletal system allows overcoming common problems like poor fit and skin damage often experienced with conventional socket fixation (Meulenbelt et al., 2011). Additional benefits like better control of the prosthetic limb (Ward, 2005), more unrestricted hip joint motion and better sitting comfort (Hagberg et al., 2005; Hagberg et al., 2008), result in an improved quality of life and increased mobility of the patients.

Two types of direct fixation implants are currently clinically available, the OPRA system (Integrum, Göteborg, Sweden) and the ISP Endo/Exo prosthesis (ESKA Implants, Lübeck, Germany). The first implant consists of a type of intramedullary titanium screw, the second is a press-fit device composed of a cobalt-chromium alloy inner core covered by a layer of highly porous metal (Brånemark et al., 2001; Staubach and Grundei, 2001).

Recent reports about follow-up studies on 100 patients with the OPRA implant and 37 patients with the ISP prosthesis (Hagberg and Branemark, 2009; Aschoff, 2010) confirm the above-listed benefits of the osseointegrated fixations. Soft-tissue infections remain the most common complication, followed by implant and peri-prosthetic bone fractures (Sullivan et al., 2003; Ward, 2005; Buell, 2006; Aschoff, 2010; Lunow et al., 2010). Moreover, these implants are expected to change bone stresses (Gunterberg, 1998; Xu and Robinson, 2008), resulting in a progressive loss of bone mineral density (BMD), which reduces prosthetic support, decreases bone strength and ultimately may lead to implant loosening (Petersen et al., 1995; Spittlehouse et al., 1998; Kobayashi et al., 2000).

In the current rehabilitation programs percutaneous implants are mostly fitted in patients who have experienced problems with socket fixation. The reported mean time of socket prosthesis use is about 11 years (Aschoff et al., 2009; Hagberg and Branemark, 2009; Hagberg and Branemark, 2009; Aschoff, 2010). Hence, the bone has not been loaded to physiological levels for considerable time, resulting in considerable bone loss (Sherk et al., 2008).

Another recent clinical follow-up study reported bone remodeling around the OPRA implant in 11 patients with an average 8 years of socket use prior to implantation (Xu and Robinson, 2008). Clinical radiographs showed considerable bone loss around the distal end of the femur and bone deposition at the proximal end of the implant. Although up to now no clinical report of bone changes around the ISP prosthesis has been published, the same concept of cobalt-chromium alloy stem with a highly porous metal layer did not eliminate periprosthetic bone loss of hip implants (Götze et al., 2006). The decreased bone quality and its subsequent strength, prior to the implantation, might make the issue of periprosthetic bone remodeling even more critical for direct-fixation implants.

Previous numerical analyses have shown a non-physiological load distribution around generic models of the OPRA and the ISP implants, which leads to stress shielding in the distal regions and considerable stress peaks located at the tip of the stems

(Xu et al., 2006; Xu and Robinson, 2008; Tomaszewski et al., 2010). These stress peaks might lead to premature bone failure in case of adverse loading like during a fall.

The unphysiological, proximal load transfer of the current direct-fixation implants can be mainly attributed to their high stiffness in comparison to the surrounding bone. This effect, commonly referred to as stress shielding, was previously extensively studied for total hip replacements. To eliminate stress shielding around hip stems numerous shape and material modifications have been proposed and introduced to the designs throughout the past decades, i.e. proximally porous-coated stems (Rothman et al., 1996), composite implants (Glassman et al., 2001) or porous tantalum prostheses (Levine et al., 2006; Tarala et al., 2011).

To overcome the limiting issues of the current designs, a new concept of direct intramedullary fixation was developed. A multi-component system composed of a metallic core and an outer sleeve with an elastic modulus comparable to the cortex should restore the natural load transfer in the midshaft of a femur (Figure 1). To enhance distal load transfer in-between the implant and the osteotomy of the femur remnant, a collar with a layer of elastic material was added to the stem and further a low amplitude sliding motion between the inner and the outer part of the implant was enabled. To obtain osseointegration between the bone and the implant a porous titanium coating is applied on the implant's surfaces in direct contact with the cortex. Additionally, the new design is much shorter than the currently used implants to allow implantation in patients with shorter bone remnants.

The motivating hypothesis for this work states that the proposed alternative design of the direct fixation implant will provide more physiological bone stress distribution and thus reduce the peri-prosthetic bone failure risk and adverse bone remodeling as compared to the currently used implants. Hence, the new implant could increase mechanical safety and enable more patients to benefit from osseointegrated direct fixation implants.

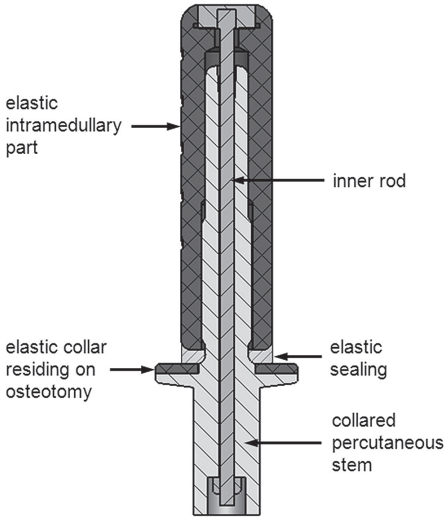

Figure 1. A schematic representation of the developed geometry.

Materials and Methods

Finite element analysis

Generic FE-models of intact femoral bone and amputated bones implanted with direct-fixation implants, with similar geometrical and mechanical characte-ristics as OPRA, ISP Endo/Exo prosthesis, and the new design were created. The FE-model of the femoral bone was based on computed tomography (CT) data of a femoral bone of an 81 year old male with normal bone quality (BMD_{neck}=0.87g/cm^2). The isotropic properties of cortical and trabecular bone were derived from the calibrated CT data. A calibration phantom was used to convert Hounsfield units to calcium-equivalent densities (ρ_{CHA}). With in-house created software a calcium-equivalent density was assigned to each element. The ash density (ρ_{ash}) was calculated using a relationship specific to the phantom $\rho_{ash} = 0.0633 + 0.887\rho_{CHA}$. The Young's modulus was derived for each element from the ash density using correlations for cortical and trabecular bone (Keyak and Falkinstein, 2003). The Poisson's ratio for all bone elements was set to 0.35.

The optimal mesh size for the bone model was determined by a mesh refinement test with 5% convergence error for the peak von Mises stress. The edge length for all meshes was 3 mm except for the interface region where it was further refined, leading to meshes of 150,000 - 190,000 four-noded tetrahedral elements.

The surface-shape contours of the implants were fitted in the femoral bone (amputated 250 mm above the knee) and implemented into the FE-models. The implants, which all had the same outer diameter (20 mm) were assumed to be bonded to represent full osseointegration. The lengths of the implants were 130, 110 and 75 mm for the ISP, the OPRA and the new design, respectively.

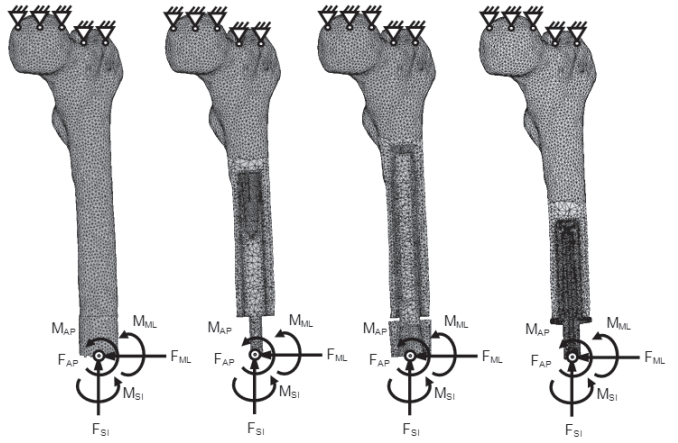

Load case	F_{SI} [N]	F_{AP} [N]	F_{ML} [N]	M_{SI} [Nm]	M_{AP} [Nm]	M_{ML} [Nm]
1	780	100	-20	-2.0	30.8	-7.2
2	180	120	40	0.0	37.3	4.1
3	547	367	-162	19.8	6.6	-101

Figure 2. Loads used in the analysis specific for a patient of 61 kg.

Characteristic elastic moduli for implant materials were as follows: ISP prosthesis stem (cobalt-chromium alloy) $210 \cdot 10^3$MPa, porous metal layer $1.0 \cdot 10^3$MPa (Klinbeil, 2006); the OPRA implant (commercially pure titanium) $110 \cdot 10^3$MPa; the elastic intramedullary part and collar of the new design $12.5 \cdot 10^3$MPa (glass-particle-reinforced PEEK), the stem $114 \cdot 10^3$MPa (titanium-aluminum-vanadium alloy). Poisson's ratio for all metallic materials was set to 0.3 and for PEEK to 0.4.

The models were subjected to two characteristic loading cases from a normal walking cycle at 25% (heel strike) and 55% (shortly before toe-off) and a forward fall loading (Figure 2).

All load values obtained from the experimental measurements with the OPRA device (Lee et al., 2007; Frossard et al., 2010) were recalculated to represent a patient with body mass of 61 kg. In all simulations the bone model was rigidly fixed at the proximal end and load was applied distally.

Bone failure risk assessment

Periprosthetic bone failure risk was evaluated by considering the von Mises stress (σ_{VM}) criterion (Keyak et al., 1998; Keyak and Falkinstein, 2003; Keyak et al., 2005). The bone strength (S) was calculated for each bone element $S = 137 \cdot \rho_{ash}^{1.88}$ for $\rho_{ash} < 0.317$ $S = 114 \cdot \rho_{ash}^{1.72}$ for $\rho_{ash} \geq 0.317$ (Keyak and Falkinstein, 2003) and bone failure risk was identified when $\sigma_{VM} / S \geq 1$.

Comparing solely the peak values of any stress or strain quantity obtained with the FE-modeling is often unreliable due to mesh dependency. Similarly as in our previous study (Tomaszewski et al., 2010), we therefore chose to define a 'failure risk parameter' (FRP). This defined the peak stress threshold beyond which one percent of the periprosthetic bone volume was exposed to. The periprosthetic bone volumes for stress assessment were selected from the osteotomy up to 10 mm above the proximal implants' end.

Bone remodeling simulation

The strain-adaptive bone remodeling theory was used to predict long-term changes in BMD. The theory assumes that during representative loading cycles bone cells react to local changes in elastic strain energy, which are provoked by the prosthesis relative to the normal physiological situation. The mathematical bone remodeling signal is determined in each element as the average strain energy per unit of mass. In each time step the rates of bone density adaptation are determined by comparing the signal values in the implanted model (s) to the pre-operative reference values (sref). In the locations where the remodeling stimulus (s-sref) is positive, bone is formed (BMD increases). Similarly, a negative stimulus indicates local bone loss (BMD decreases). A threshold level s=0.35sref is assumed, which leads to a stimulus zone where no bone reaction occurs. Furthermore, it is assumed that bone formation and loss occur more rapidly in bone with a higher amount of free surface as quantified in (Martin, 1972).

To calculate bone remodeling an iterative simulation procedure was integrated with the FE-program (MSC Software Corporation, Santa Ana, CA, USA). The simulation addressed the most common clinical situation when direct fixation prosthesis is

implanted after considerable time of socket prosthesis use. The original BMD-value at the femoral neck region of the bone used for modeling was assessed by in-house software to BMDneck = 0.87g/cm^2. Subsequently the BMD in the entire reference bone model representing intact bone was linearly increased to match the mean values (BMDneck = 1.01 g/cm^2) measured at the femoral neck of a 46 years old person (Sherk et al., 2008). For the amputated femur model the BMD was reduced by 30% (BMDneck = 0.72 g/cm^2) to represent a bone disuse caused by socket prosthesis (Sherk et al., 2008).

To relate simulation time to actual clinical time, the predictions were quantified by fitting a simulated case to clinical measurements of bone remodeling around an OPRA implant (Xu and Robinson, 2008).

Subsequently, the results were presented in the form of dual-energy X-ray absorptiometry (DXA) scans. The BMD and bone mineral content (BMC) around implants were measured in 7 zones (Figure 5), corresponding to Gruen zones defined for hip stems (Gruen et al., 1979).

Results

The analyzed implants presented considerable differences in the periprosthetic stress distribution patterns for both loading scenarios representing normal walking. The OPRA and the ISP implants induced high stress concentration in the proximal region (close to the implant tip). The stresses were decreasing in the distal direction to values below physiological levels of intact bone. The stresses around the new design were relatively more uniformly distributed along the cortex and resembled better to the intact case (Figure 3). A stress peak was present in the region where the collar was in contact with the bone.

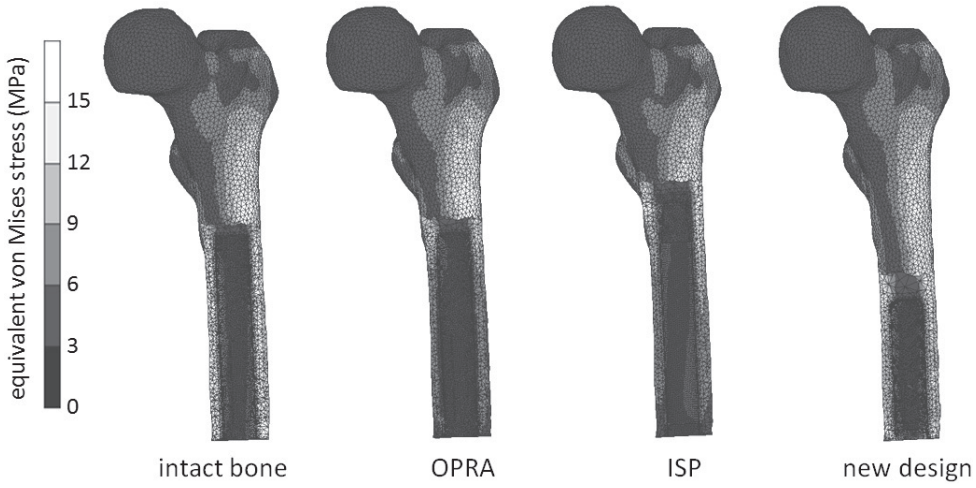

Figure 3. Equivalent von Misses stress distribution in the intact and implanted bones directly post-operative obtained for load case 2.

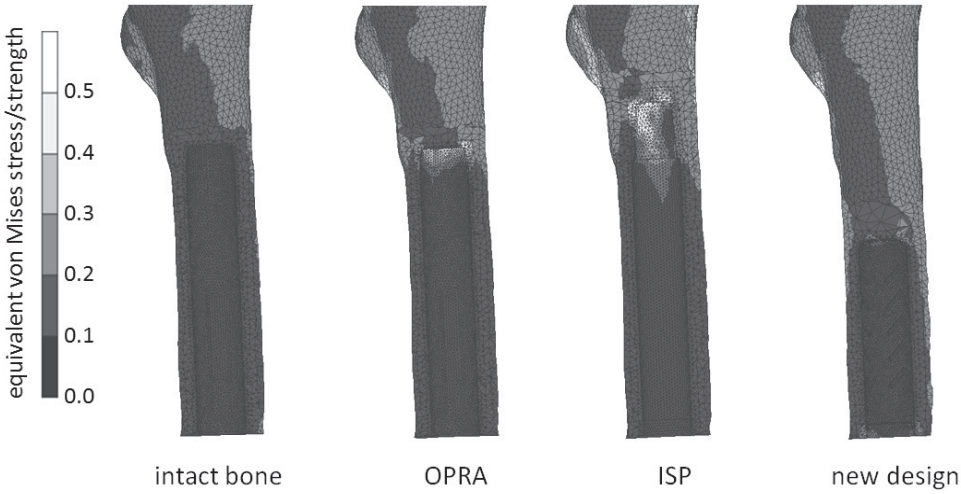

Figure 4. Periprosthetic bone failure risk (von Mises stress/strength) in the intact and implanted bones directly post-operative obtained for load case 2.

The highest failure risk for the OPRA and the ISP implant models was found in the bone region in contact with the proximal end of their stems for the second load configuration (toe-off). It did not indicate direct bone failure for the normal walking activities (load case 1 and 2). The new design presented considerably reduced bone failure risk in the proximal region with a maximum around the collar (Figure 4 and Table 1). Those results are consistent with the above described stress patterns. Concerning bone remodeling the OPRA and the ISP implants showed high bone resorption in the distal end of the femur (on average -15% OPRA, -17% ISP after 20 months and -75% ISP to -78% OPRA after 60 months). The bone remodeling simulation did not reveal any bone loss around the new design, even bone densification was seen. The highest increase of BMD was present proximally to the implants´ tips (zone 4), with values of 28%, 27% and 18% (after 60 months) for the OPRA, the ISP and the new design, respectively (Figure 5 and Figure 6).

In terms of total BMC the OPRA and the ISP implants induced only a short-term bone densification in contrast to the new design, which provoked a steady increase of the BMC over the whole analyzed period (Figure 7). Nevertheless, the BMC value throughout the whole considered period of the bone remodeling remained below the level of the intact healthy bone.

Subsequently, the periprosthetic bone failure risk was assessed for walking and forward fall loading of the implants both directly post-operative and after 60 months. As expected, the higher bone failure risk was found by falling than by normal walking both before and after remodeling (Table 1). Moreover, the bone turnover led to a reduction of the FRP for all considered implants and load configurations. The highest FRP during normal walking was present for the ISP implant (0.39 directly post-operatively and 0.15 after 60 months) and lowest for the new design (0.15 directly post-operatively and

0.11 after 60 months). Also during the forward fall the highest FRP was found for the ISP implant (0.41 directly post-operatively and 0.20 after 60 months). The forward fall with the new design and the OPRA implant resulted in the FRP values of 0.25 and 0.31 (directly post-operatively) and 0.18 and 0.25 (after 60 months), respectively.

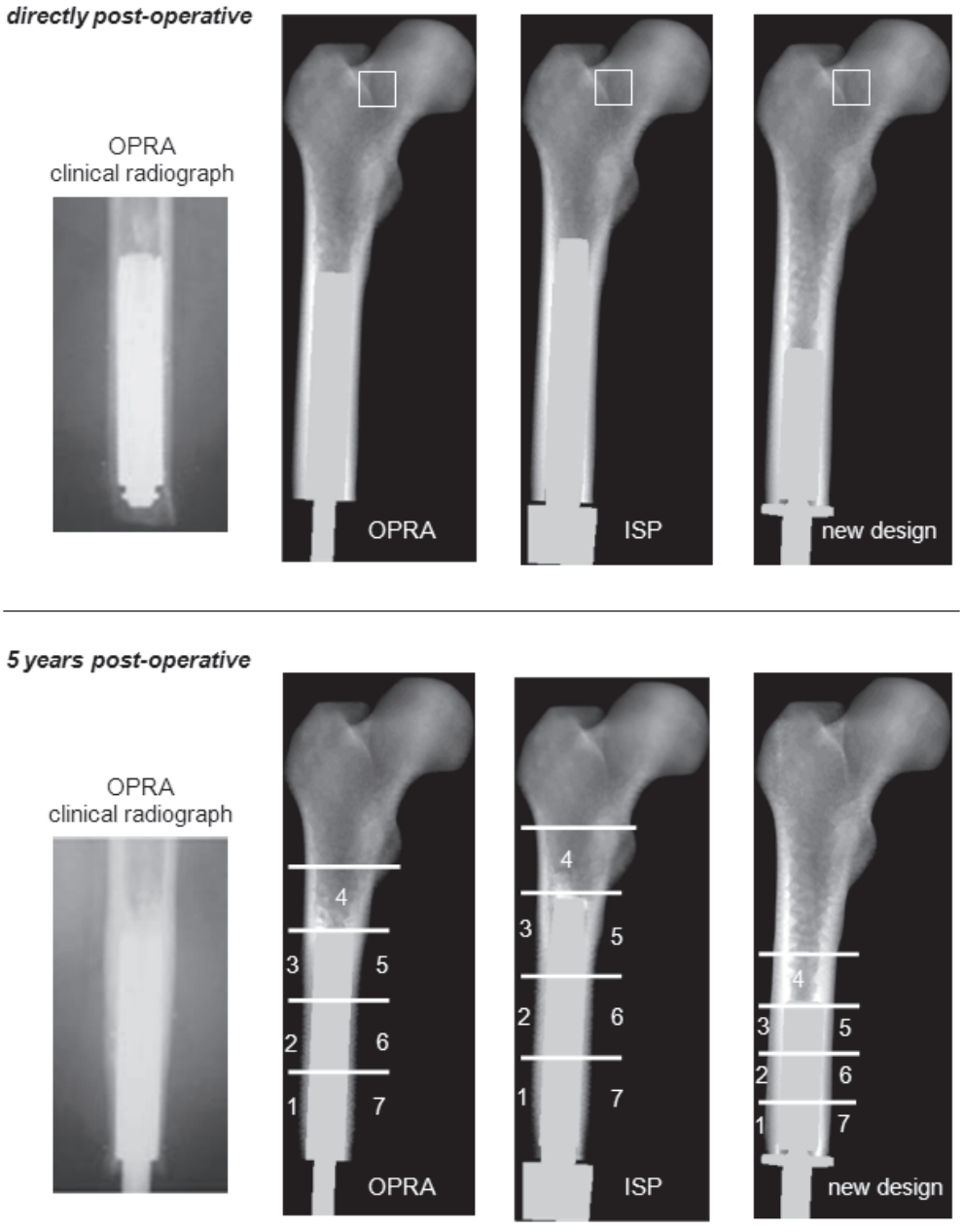

Figure 5. Computed periprosthetic bone remodeling presented in form of standard DXA scans.

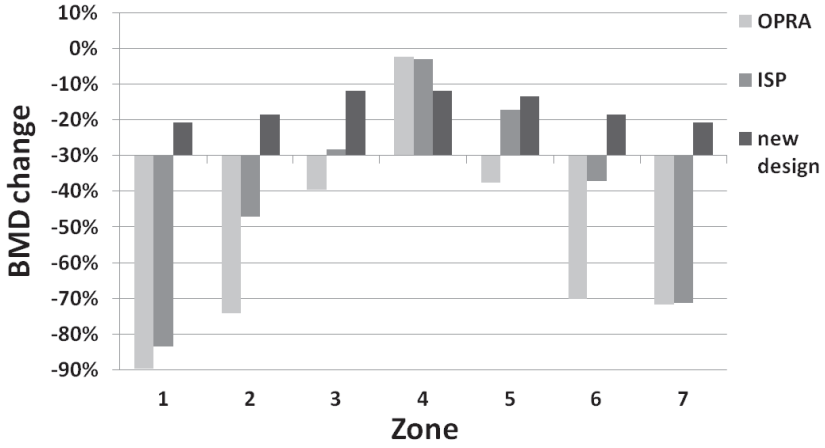

Figure 6. Bone mineral density change calculated in 7 zones around implants 60 months post-operative.

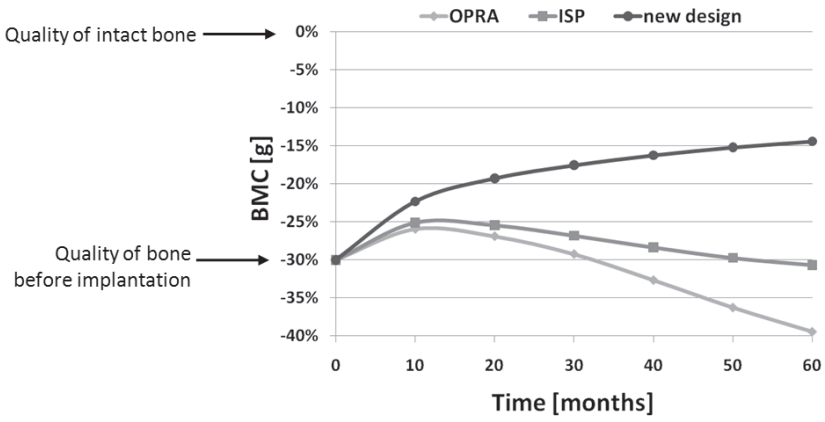

Figure 7. Change of the total bone mineral content (BMC) around implants during 60 months after operation.

Von Mises stress / Strength				
	Walking – Load 2 (1% limit)		Forward fall (1% limit)	
	Time = 0	Time = 60 months	Time = 0	Time = 60 months
OPRA	0.17	0.12	0.25	0.18
ISP	0.39	0.15	0.41	0.20
new design	0.15	0.11	0.31	0.25

Table 1. Periprosthetic bone failure risk parameter (FRP) during normal walking and forward fall directly after implantation and after bone remodeling.

Discussion and conclusions

In the present study we proposed an alternative design of a direct fixation implant for patients after trans-femoral amputation. Using FE-modeling we investigated if the new design can provide more physiological bone stress distribution and thus reduce the peri-prosthetic bone failure risk and the adverse bone remodeling as compared to the currently used implants.

The new design has shown a favorable, close to physiologic bone stress distribution during normal walking. This is attributed to the distal load transfer realized by means of a collared stem. The stress peaks located at the tip of the OPRA and ISP stems were effectively reduced and relocated to the bone resection level.

The bone remodeling simulations showed that the new design performed better in the long-term than the current implants, as it eliminates bone resorption present around the OPRA and the ISP implants.

The new design had lower bone failure risk during normal walking in comparison to the OPRA and the ISP implants both before and after the remodeling, which is surprising as the new design is much shorter. In case of a forward fall simulated immediately after implantation the FRP of the new implant was in between values obtained for the ISP and the OPRA. The forward fall simulation after remodeling resulted, however, in a slightly elevated FRP value as compared to the other implants, with the highest values found close to the collar. It indicates that the collared stem performs better during normal load regime (walking) than bending (fall). This effect was even more pronounced after remodeling, during which the bone structure is optimized for normal walking loads only.

Additionally, to check if the forward fall can actually induce any direct failure of the bone, the percentage volume of the failed elements was calculated. Before remodeling, local failure was found for 4.4% of the bone volume around the ISP and 0.2% around the OPRA implant. No direct bone failure was present around the new design. After 60 months of remodeling the forward fall did not provoke any direct bone failure around any of the analyzed stems. Interestingly, the stress peaks around the tips of the ISP and the OPRA stems were much higher and sharper than around the collar of the new design. The fact that the new design has a higher failure risk at the forward fall loading condition can be explained by its lower inherent resistance against bending moments due to its shorter length.

Remarkably, although remodeling optimized the bone only for normal walking, a reduction of the failure risk was observed also in case of forward fall loading. This indicates that the analyzed implants induce strengthening of the bone, previously disused after socket prosthesis.

Obviously the simulations embed several limitations which should be considered when interpreting the results. The simulations did not consider ingrowth properties of the implant surfaces, thus the whole implant area was in contact with the bone and the interface was not modeled. The bone model was based on CT-scans of an 81 year old male, which is not the common age for patients with osseointegrated implants. The reason for using this CT-data was no access to younger cadaver and the required high

dose of radiation to obtain high resolution images. Therefore the original BMD was re-scaled to fit with the clinical data reported for younger patients (Sherk et al., 2008). It allowed determining the time constant, which was based, however, only on one time point.

Another shortcoming is the application of the same loading conditions for both intact bone and implanted models. In this manner, only the effect of the implant is modeled and changes in the muscle loading due to amputation are not considered. This could be improved by incorporating musculoskeletal modeling into bone remodeling simulations.

Models used in this study were generic, rather than design-specific in a high degree of detail. Nevertheless, in our opinion they represent the most important geometrical and mechanical features of the current implants and were suitable for comparison of the bone changes.

In conclusion, we recognize that the new design offers much better bone maintenance and lower failure probability during normal walking than the current osseointegrated trans-femoral prostheses. Whether the new implant is more or less sensitive to adverse loading condition such as occurring during a falling incident needs to be further investigated. This positive outcome should encourage further developments of the presented concept, which in our opinion has a potential to considerably improve safety of the rehabilitation with the direct fixation implants and allow treatment of the patients with short stumps.

Conflict of interest statement

P.K. Tomaszewski, N. Verdonschot, S.K. Bulstra and G.J. Verkerke, University Medical Center Groningen and University of Groningen are inventors/applicants of the pending patent “Osseointegration system for a long bone”, WO2011037458A1.

References

Aschoff, H. H., et al. (2009). "The endo-exo femur prosthesis-a new concept of bone-guided, prosthetic rehabilitation following above-knee amputation." Zeitschrift für Orthopädie und Unfallchirurgie 147(5): 610-615.

Aschoff, H. H., Kennon, R.E., Keggi, J.M., Rubin, L.E. (2010). "Transcutaneous, Distal Femoral, Intramedullary Attachment for Above-the-Knee Prostheses: An Endo-Exo Device." Journal of Bone and Joint Surgery 92(Suppl 2): 180-186.

Brånemark, R., et al. (2001). "Osseointegration in skeletal reconstruction and rehabilitation: a review." Journal of Rehabilitation Research and Development 38(2): 175-181.

Buell, O. (2006). Theoretische aspekte und erste praktische ergebnisse von perkutanen exoprothesen bei oberschenkelamputationen. Munich, Ludwig-Maximilians-University.

Frossard, L. A., et al. (2010). "Load on osseointegrated fixation of a transfemoral amputee during a fall: loading, descent, impact and recovery analysis." Prosthetics and Orthotics International 34(1): 85-97.

Glassman, A. H., et al. (2001). "A low stiffness composite biologically fixed prosthesis. "Clinical Orthopaedics and Related Research 393: 128-136.

Götze, C., et al. (2006). "Long-term influence of the spongiosa metal surface prosthesis on the periprosthetic bone. A radiological and osteodensitometric analysis of implantation of the S&G (ESKA) hip prosthesis." Zeitschrift fur Orthopadie und ihre Grenzgebiete 144(2): 192-198.

Gruen, T. A., et al. (1979). ""Modes of failure" of cemented stem-type femoral components: a radiographic analysis of loosening." Clinical Orthopaedics and Related Research 141: 17-27.

Gunterberg, B., Branemark, P-I., Branemark, R., Bergh, P. and Rydevik, B. (1998). Osseointegrated prosthesis in lower limb amputation: the development of a new concept. IXth World Congress ISPO, Copenhagen, ISPO.

Hagberg, K., et al. (2009). "One hundred patients treated with osseointegrated transfemoral amputation prostheses--rehabilitation perspective." J Rehabil Res Dev 46(3): 331-344.

Hagberg, K., et al. (2009). "One hundred patients treated with osseointegrated transfemoral amputation prostheses-rehabilitation perspective." Journal of Rehabilitation Research and Development 46(3): 331-344.

Hagberg, K., et al. (2008). "Osseointegrated trans-femoral amputation prostheses: prospective results of general and condition-specific quality of life in 18 patients at 2-year follow-up." Prosthetics and Orthotics International 32(1): 29-41.

Hagberg, K., et al. (2005). "Socket versus bone-anchored trans-femoral prostheses: hip range of motion and sitting comfort." Prosthetics and Orthotics International 29(2): 153-163.

Keyak, J. H., et al. (2003). "Comparison of in situ and in vitro CT scan-based finite element model predictions of proximal femoral fracture load." Medical Engineering & Physics 25(9): 781-787.

Keyak, J. H., et al. (2005). "Predicting proximal femoral strength using structural engineering models." Clinical Orthopaedics and Related Research 437: 219-228.

Keyak, J. H., et al. (1998). "Prediction of femoral fracture load using automated finite element modeling." Journal of Biomechanics 31(2): 125-133.

Klinbeil, K. (2006). Metallurgische Grundlagen für die gusstechnische Herstellung einer räumlichen Oberflächenstruktur. Ossärre Integration. R. Gradinger and H. Gollwitzer. Heidelberg, Springer Medizin Verlag: 46-52.

Kobayashi, S., et al. (2000). "Poor bone quality or hip structure as risk factors affecting survival of total-hip arthroplasty." Lancet 355(9214): 1499-1504.

Lee, W. C., et al. (2007). "Kinetics of transfemoral amputees with osseointegrated fixation performing common activities of daily living." Clinical Biomechanics 22(6): 665-673.

Levine, B. R., et al. (2006). "Experimental and clinical performance of porous tantalum in orthopedic surgery." Biomaterials 27(27): 4671-4681.

Lunow, C., et al. (2010). "Endo-exo femoral prosthesis: clinical course after primary implantation of an intramedullary percutaneous endo-exo femoral prosthesis following upper leg amputation." Der Unfallchirurg 113(7): 589-593.

Martin, R. B. (1972). "The effects of geometric feedback in the development of osteoporosis." Journal of Biomechanics 5(5): 447-455.

Meulenbelt, H. E., et al. (2011). "Skin problems of the stump in lower limb amputees: 1. A clinical study." Acta Dermato Venereologica 91(2): 173-177.

Petersen, M. M., et al. (1995). "Changes in bone mineral density of the distal femur following uncemented total knee arthroplasty." Journal of Arthroplasty 10(1): 7-11.

Rothman, R. H., et al. (1996). "Hydroxyapatite-coated femoral stems. A matched-pair analysis of coated and uncoated implants." Journal of Bone and Joint Surgery 78(3): 319-324.

Sherk, V. D., et al. (2008). "BMD and bone geometry in transtibial and transfemoral amputees." Journal of Bone and Mineral Research 23(9): 1449-1457.

Spittlehouse, A. J., et al. (1998). "Bone loss around 2 different types of hip prostheses." Journal of Arthroplasty 13(4): 422-427.

Staubach, K. H., et al. (2001). "The first osseointegrated percutaneous prosthesis anchor for above-knee amputees." Biomedizinische Technik Biomedical engineering 46(12): 355-361.

Sullivan, J., et al. (2003). "Rehabilitation of the trans-femoral amputee with an osseointegrated prosthesis: the United Kingdom experience." Prosthetics and Orthotics International 27(2): 114-120.

Tarala, M., et al. (2011). "Balancing incompatible endoprosthetic design goals: a combined ingrowth and bone remodeling simulation." Medical Engineering & Physics 33(3): 374-380.

Tomaszewski, P. K., et al. (2010). "A comparative finite-elelement analysis of bone failure and load transfer of osseointegrated prostheses fixations." Ann Biomed Eng.

Tomaszewski, P. K., et al. (2010). "A comparative finite-elelement analysis of bone failure and load transfer of osseointegrated prostheses fixations." Annals of Biomedical Engineering 38(7): 2418-2427.

Ward, D. A., Robinson, K. P. (2005). Osseointegration for the skeletal fixation of limb prostheses in amputations at the trans-femoral level. The osseointegration book. P.-I. Brånemark, Quintessenz Verlags: 463-476.

Xu, W., et al. (2008). "X-ray image review of the bone remodeling around an osseointegrated trans-femoral implant and a finite element simulation case study." Annals of Biomedical Engineering 36(3): 435-443.

Xu, W., et al. (2006). "Three-dimensional finite element stress and strain analysis of a transfemoral osseointegration implant." Proceedings of the Institution of Mechanical Engineers, Part H: Journal of Engineering in Medicine 220(6): 661-670.

Chapter 5

Experimental assessment of a new direct fixation implant for artificial limbs

P.K. Tomaszewski[1], B.Lasnier[1], G. Hannink[2,3], G.J. Verkerke[1,4], N. Verdonschot[2,4]

[1] Department of Biomedical Engineering, University of Groningen, University Medical Center Groningen, Groningen, The Netherlands.
[2] Orthopaedic Research Laboratory, Radboud University Nijmegen Medical Centre, Nijmegen, The Netherlands.
[3] Department of Operating Rooms, Radboud University Nijmegen Medical Centre, Nijmegen, The Netherlands.
[4] Department of Biomechanical Engineering, University of Twente, Enschede, The Netherlands.

Submitted and under revision in Journal of Mechanical Behavior of Biomedical Materials

Introduction

Vascular disorders, trauma, tumors and congenital abnormalities are the main causes of amputation. Transfemoral amputation is a permanent disfigurement impacting patient's mobility, professional activity, lifestyle and quality of life. With an increasing number of amputations related both to diabetes (Anonymous, 1998; Anonymous, 2001; Cowie et al., 2010; Anonymous, 2011) and war related traumata (Fischer, 2010), it is important to explore improvements in the rehabilitation care and technology.

The current conventional method of artificial limb attachment is realized by a prosthetic socket, but this method very often causes skin irritation, a lack of appropriate control over the limb and pain (Meulenbelt et al., 2011). Moreover, it is not suitable for patients with short residual limbs.

An alternative solution is being offered by a direct attachment of the external prosthesis to the femur via a cementless implant. Currently, two so-called direct skeletal fixation devices exist and are referred to as 'osseointegrated devices': the OPRA system (Integrum, Göteborg, Sweden) (Brånemark et al., 2001), and the ISP Endo/Exo prosthesis (ESKA Implants, Lübeck, Germany) (Aschoff et al., 2009; Aschoff, 2010). Patients using these implants experience significant improvements such as a reduction of skin or residual limb problems associated with the prosthetic socket and an increased range of motion and mobility (Hagberg et al., 2005; Aschoff et al., 2009; Hagberg and Branemark, 2009). However, as the stiffness of these metal-based implants is higher than that of the periprosthetic bone, these implants will considerably change bone loading as compared to the intact situation. This inevitably leads to a bone remodeling response, which has been reported in a clinical follow-up study of the OPRA implant (Xu and Robinson, 2008). Radiographs presented considerable and progressive bone loss at the distal end of the femur and bone deposition at the proximal end of the implant. In general, this bone remodeling response is expected to reduce prosthetic support, decrease bone strength and ultimately may lead to peri-prosthetic fractures or implant loosening as previously studied for total hip implants (Petersen et al., 1995; Spittlehouse et al., 1998; Kobayashi et al., 2000; Stolk et al., 2002).

To overcome strain shielding a new concept of a direct fixation implant has been developed. A multi-component system composed of a metallic core and an outer sleeve with an elastic modulus comparable to the cortex should much better restore the natural load transfer in the midshaft of a femur (Figure 1). To enhance the distal load transfer in-between the implant and the osteotomy of the femur remnant, a collar with a layer of elastic material was added to the stem in combination with a low-amplitude sliding motion between the inner and the outer part of the implant. Osseointegration between the bone and the implant is realized by means of a porous titanium coating on the implant's surfaces, which are in direct contact with the cortex. The new implant is much shorter than the currently used implants to allow implantation in patients with shorter bone remnants.

The change in strains induced by a prosthetic design is usually evaluated by experimental testing using human cadaver bones (Aamodt et al., 2001; Kim et al., 2001; Decking et al., 2006; Ostbyhaug et al., 2009). Other methods include the use of

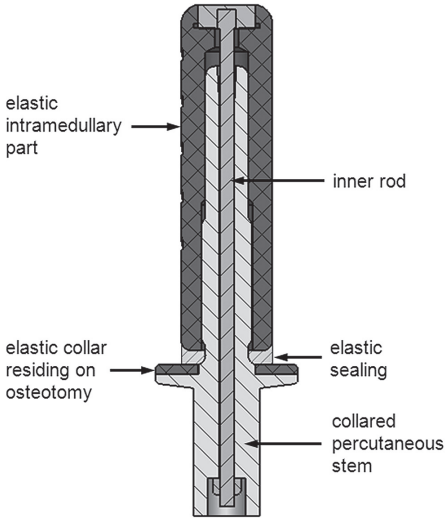

Figure 1. Schematic representation of the new direct fixation implant.

composite bone replicas, representing average adult bones with mechanical properties close to that of human bone (Cristofolini et al., 1996), and finite element (FE) analyses (Viceconti et al., 2001; Stolk et al., 2002; Completo et al., 2007). Subject-specific FE models of femoral bones, with the geometry and material properties derived from computed tomography (CT), have been described in several studies (Keyak et al., 2005; Schileo et al., 2007; Taddei et al., 2007). Recently, human subject-specific FE models for evaluating strain changes induced by the femoral stem have been validated by experimental strain gauge measurements (Pettersen et al., 2009).

Previous studies on direct fixation implants included FE analyses of the load distribution around a standard titanium implant (OPRA) using both simplified CT based models (Xu et al., 2006; Xu and Robinson, 2008) and generic 3-D CT based models of the OPRA and the ISP prostheses (Tomaszewski et al., 2010). Experimental studies on the load distribution and subsequent strain shielding in the human femur after insertion of any type of direct fixation implant have not been performed.

In this study we assessed if the design of a new direct fixation implant will reduce strain shielding in the femur as compared to a standard implant. For this purpose, we investigated the alteration in the pattern of cortical strains in the femur experimentally and in an FE simulation after insertion of a standard titanium implant and the new direct fixation implant.

Materials and Methods

Implants

A one-component generic model of a standard implant based on the OPRA implant was machined from commercially pure titanium with an outer thread of M15x1 and an intramedullary length of 110 mm (Figure 2). The dimensions of the new direct

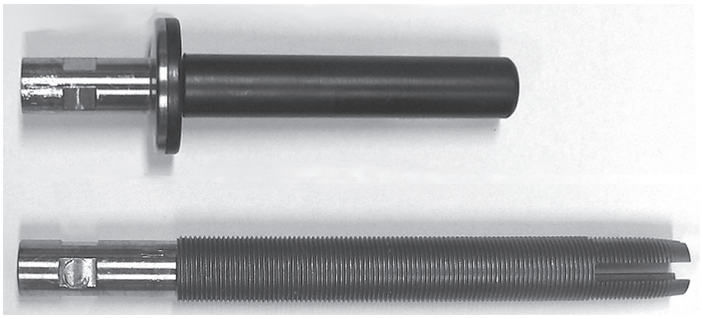

Figure 2. Implants used in the experiment: the standard titanium implant (below) and the new implant (above).

fixation implant were Ø14.6 mm and a 75 mm length. The core of the new implant was machined from Ti6Al4V alloy and the outer part from PEEK Motis polymer (Invibio, Lancashire, UK).

Specimens

Seven femurs from two male and two female donors aged 70-96 years (average 84 years) were used in the study. The femurs were examined with radiographs in two projections (antero-posterior and medio-lateral) to exclude skeletal pathologies and to confirm that the implants would fit into the bones. In addition, DEXA scanning was performed to measure bone quality. For this purpose bones were emerged in water and positioned in anatomical orientation in the scanner (Hologic QDR 4500W). T-scores based on the BMD of the femoral neck were calculated for all bones (Table 1). The femurs were stored at -25º C and thawed at room temperature prior to testing.

bone	BMD_{neck} [g/cm^2]	T-score
1	0.58	-2.4
2	0.52	-3.0
3	0.72	-1.6
4	0.77	-1.2
5	0.17	-5.7*
6	0.67	-1.9
7	0.68	-1.8

Table 1. Bone mineral density and T-scores of the bones used in the experiment as assigned by the DXA scanner or extrapolated (*).

The posterior femoral condyles and the posterior aspect of the greater trochanter defined the frontal plane of the femur. The femoral head was sectioned at the level of greater trochanter and cemented in a metal cylinder using a polymethyl methacrylate (PMMA) for load application purposes. Similarly, the distal part of the diaphysis was cemented in a metal cylinder after removing the condyles, so that the femoral shaft length between the cement blocks was standardized to 21.5 cm.

Test setup

After preparation, the femur was mounted in a servo-hydraulic MTS 458.20 machine (MTS Systems Corporation, Eden Prairie, Minnesota, USA). The distal cylinder was clamped in the setup and angled according to the desired load case. The load was applied vertically via a horizontally free-sliding jig (LWR 6150, SKF, Germany) to a 25 mm ball mounted on top of the proximal PMMA block (Figure 3). The loading characteristics were defined according to the forces measured in-vivo for a patient of 61 kg implanted with an OPRA implant (Lee et al., 2007). Three load cases were applied to the specimens, heel strike, toe off and one-leg stance. Loads and orientation (based on rotation in the hip joint) were as follows: heel strike (Load 1, 805 N, 10.5º flexion and 10º adduction), toe-off (Load 2, 720 N, 5.2º extension and 5º adduction), single-leg stance (Load 3, 800 N, vertical load).

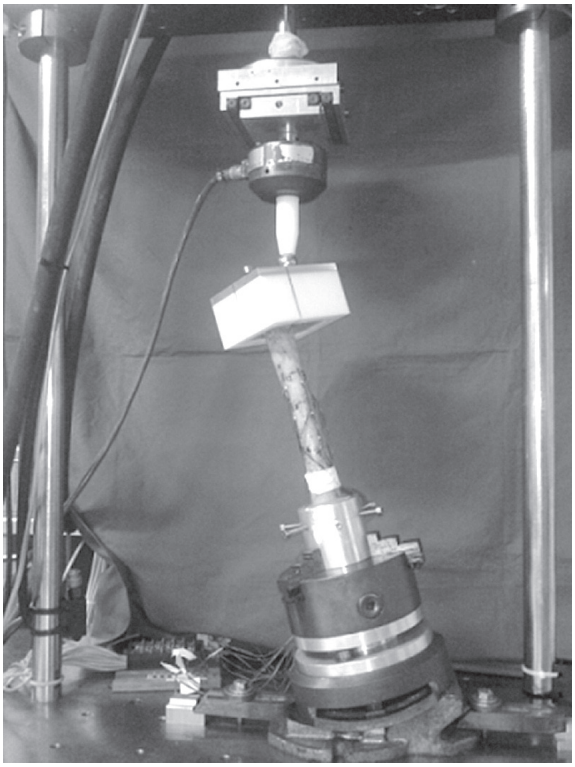

Figure 3. Experimental setup.

Every femur was tested three times: first the femur was tested intact followed by tests with the implants in-situ. The sequence of implant testing was alternated with a random start to eliminate the possibility that the results would be biased by the order of implant testing. The manually controlled load was slowly increased with increments of 10% until the required load was obtained. To prevent bone overload the load application was stopped if any strain gauge signal approached values corresponding to critical tensile strain levels (Bayraktar et al., 2004).

Strain measurement

For the measurements of the strains twelve unidirectional strain gauges (YFLA-5, Tokyo Sokki Kenkyujo, Tokyo, Japan) were attached at three different levels on the anterior, medial, posterior and lateral side of the proximal femur. Each strain gauge was oriented parallel to the longitudinal axis of the femur. Attachment levels were positioned at 15 mm, 75 mm and 110 mm above the osteotomy level (220 mm below the tip of greater trochanter). The locations were chosen to show strains at the distal femur and at the tips of both implants (Figure 4). At the sites of the attachments to the bone the surface was cleaned and smoothened with grinding paper. The gauges were bonded using a cyanoacrylate adhesive (Loctite 415, Henkel, EU) and covered with a waterproof sealing (M-Coat A, Vishay, USA).

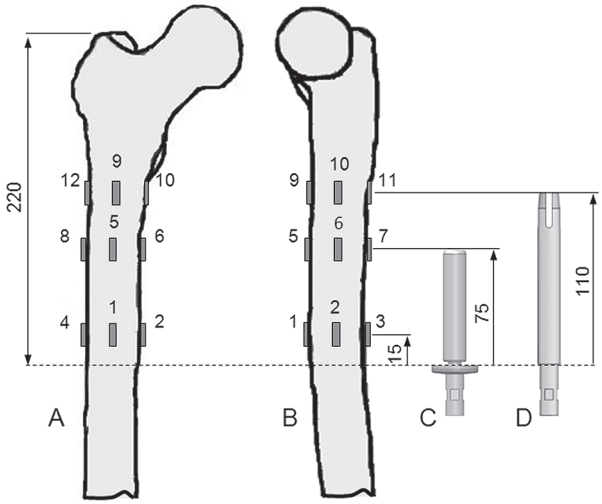

Figure 4. Locations of the strain gauges in the experiment.

Finite element analyses

Generic FE-models of an intact femoral bone and amputated bones fitted with both implant types, with similar geometrical and mechanical characteristics as the OPRA implant and the new design were created (Figure 5). The FE-model of the femoral bone was based on computed tomography (CT) data of a femoral bone of an 81 year old male with normal bone quality (BMDneck=0.87g/cm^2). The isotropic properties of cortical and trabecular bone were derived from the calibrated CT data. A calibration phantom was used to convert Hounsfield units to calcium-equivalent densities (ρ_{CHA}). With in-house created and validated software (Tanck et al., 2009) a calcium-equivalent density was assigned to each element. The ash density (ρ_{ash}) was calculated using a relationship specific to the phantom $\rho_{ash} = 0.0633 + 0.887\rho_{CHA}$. The Young's modulus was derived for each element from the ash density using correlations for cortical and trabecular bone (Keyak and Falkinstein, 2003). The Poisson's ratio for all bone elements was set to 0.35.

The surface-shape contours of the implants were fitted in the femoral bone and implemented into the FE-models. To represent the experimental situation the new implant was in friction contact (with a friction coefficient of 0.7) with the bone. The standard implant was assumed to be bonded with the bone, as its shape was represented without the thread in the model.

Characteristic elastic moduli for implant materials were as follows: standard implant 110 GPa (commercially pure titanium); the elastic intramedullary part and collar of the new design 12.5 GPa (PEEK Motis - Invibio, Lancashire, UK), and the stem 114 GPa (Ti6Al4V alloy). Poisson's ratio for all metallic materials was set to 0.3 and for PEEK to 0.4.

The original bone mineral density of the bone model assessed at the femoral neck ($BMD_{neck} = 0.87 g/cm^2$) was rescaled to match the mean BMD of the bones used in the experiment ($BMD_{neck} = 0.54\ g/cm^2$). The models were fixed distally at the level of the metal cylinders. Loads were applied proximally to a single node located at the top of the femoral head and connected with rigid link elements to the nodes at the bottom level of the upper PMMA block (Figure 5). The models were subjected to the same loading configurations as used in the experiment. After load application, the average of the axial component of the elastic strains from elements located within a 5 mm radius at the locations corresponding to the attachment sites of the strain gauges was calculated.

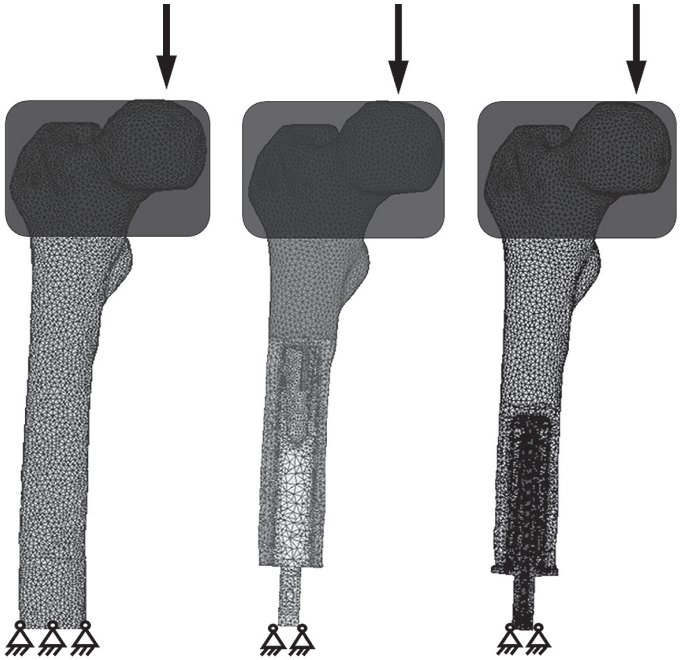

Figure 5. FE models with applied boundary conditions. Solid lines represent rigid link elements connecting load application node with the nodes at the bottom level of the PMMA block.

Statistical analysis

Strains measured in the intact bone, after implantation of the titanium screw implant and the new implant were compared using two-way repeated measurement ANOVA with within subject factors level (distal (15 mm), middle (75 mm), proximal (110 mm)) and implant type (intact, titanium screw, direct fixation implant). The results were presented as relative change in absolute strain value defined as the ratio of strain measured after implantation over strain measured in the intact situation. A value of 100% represents that the strain levels of the intact bone had been maintained. Linear regression analyses were performed to determine the overall correspondence between numerical and mean experimental strains.

Results

The standard implant presented a significant strain reduction at the distal ($p < 0.01$) and middle level ($p < 0.05$) for all three considered load cases (Figure 6). The lowest strains relative to the intact bone case were observed distally; on average: 8% for heel strike (L1), 20% for toe-off (L2) and 11% for one leg stance (L3). At the middle level the average relative strains were 55%, 61% and 67% for L1, L2 and L3, respectively. No significant strain change in comparison to the intact situation was measured in the proximal region ($p > 0.1$).

The new implant also caused a reduction in strains at the distal level in all of the load cases ($p < 0.008$); however as opposed to the OPRA implant no significant strain reduction was measured in the middle zones ($p > 0.3$ – strains remained higher than 84%). The average relative strain at the distal level was 37% for the heel strike (L1), 38% for the toe-off (L2) and 36% (L3) for the one leg stance load. No significant strain change in comparison to the intact situation was measured in the proximal region ($p > 0.2$).

Significant differences in strain shielding between both implant types were obtained for heel strike (L1) at the distal ($p < 0.04$) and the middle level ($p < 0.03$), as well as for the one leg stance (L3) at the middle level ($p < 0.03$) showing less strain shielding for the

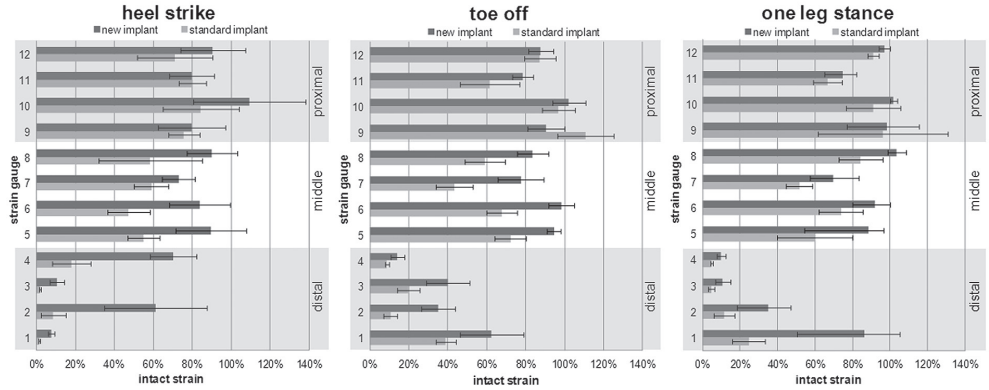

Figure 6. Changes in absolute values of strains (in % of the intact femur, mean value of seven bones) after insertion of two types of implants presented as a percentage of intact strains. The error bars indicate standard error.

new implant in these cases. The new implant presented on average 29% higher relative strains than the standard implant for L1 at the middle and distal level and 21% higher relative strains for the L3 at the middle level.

The FE predictions showed similar patterns as those measured in the experiments. All load cases produced comparable differences between measurements and FE analysis. The comparison of the measured strains with the FE results for heel strike is presented in Figure 7 and complete correlation results are given in Table 2 and Table 3. In general, the FE results, similarly as the experiments, showed a higher strain reduction for the standard implant as compared to the new implant. The numerical models tended to overestimate strain change after insertion of the new implant and more often underestimate strain change for the standard implant. While comparing the strain shielding pattern at heel strike, the largest discrepancies were found at the distal level around the new implant (Figure 7).

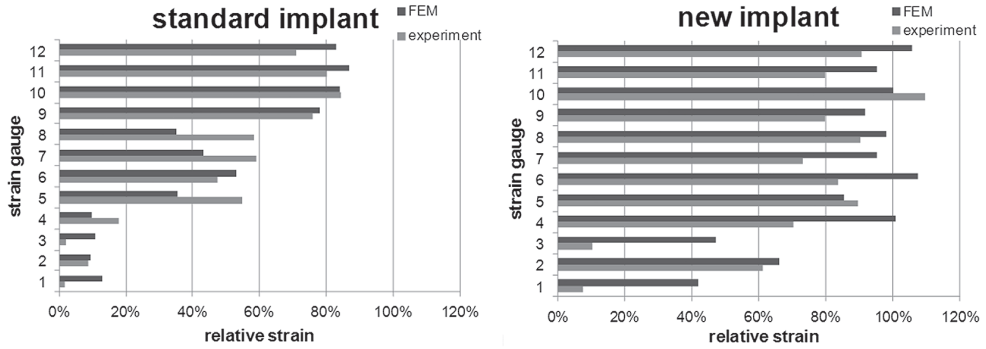

Figure 7. Measured and FE simulated strains for the load case 1 presented as a percentage of intact strains.

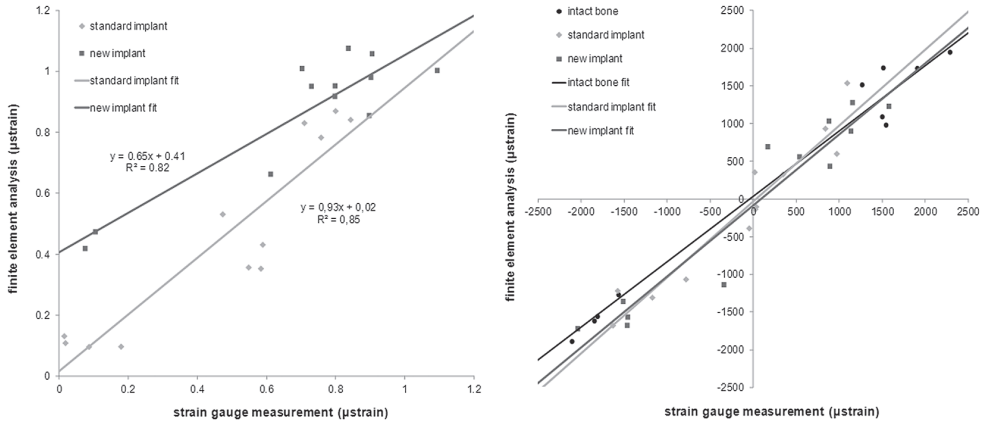

Figure 8. Comparison of intact and reconstructed strains (left) and relative strains (right) during heel strike.

load case	implant type	slope (95%CI)	intercept (95%CI)	R^2
1	intact bone	0.87 (0.79-0.94)	37 (-116 to 190)	0.99
	standard implant	0.97 (0.79-1.15)	-10 (-174 to 155)	0.93
	new implant	0.94 (0.74-1.14)	-78 (-319 to 162)	0.92
2	intact bone	1.06 (0.91-1.20)	91 (-173 to 355)	0.97
	standard implant	0.91 (0.74-1.07)	10 (-199 to 211)	0.94
	new implant	1.13 (0.86-1.40)	72 (-332 to 477)	0.90
3	intact bone	0.98 (0.83-1.12)	32 (-312 to 376)	0.96
	standard implant	0.84 (0.66-1.02)	13 (-261 to 287)	0.92
	new implant	1.13 (0.87-1.39)	60 (-413 to 533)	0.90

Table 2. Results of the linear regression analyses, comparing the mean experimental strains and the FE strains.

load case	implant type	slope (95%CI)	intercept (95%CI)	R^2
1	standard implant	0.93 (0.66-1.20)	0.02 (-0.13 to 0.17)	0.85
	new implant	0.65 (0.43-0.86)	0.41 (0.24 to 0.57)	0.82
2	standard implant	0.90 (0.67-1.13)	0.00 (-0.15 to 0.15)	0.88
	new implant	0.44 (0.19-0.70)	0.51 (0.31 to 0.70)	0.61
3	standard implant	0.90 (0.60-1.22)	-0.02 (-0.21 to 0.20)	0.81
	new implant	0.55 (0.33-0.76)	0.42 (0.25 to 0.60)	0.76

Table 3. Results of the linear regression analyses, comparing the mean relative experimental strain and the relative FE strain.

The linear regression analysis showed better correlation for the intact femurs (R^2=0.96 to R^2=0.99), than the operated femurs (R^2=0.90 to R^2=0.94) as presented in Figure 8 and Table 2. The numerical prediction of the cortical strain shielding yielded higher correlations with the experimental measurements for the standard (R^2=0.85 to R^2=0.88) than for the new implant (R^2=0.60 to R^2=0.82). The slopes of the standard implant were not significantly different from one and the intercepts were not different from zero. For the new implant, both slope and intercept were significantly different from one and zero (Table 3).

Discussion

The aim of the study was to determine if a new implant design has the capability to reduce strain shielding in the femur as compared to the standard implant. The new implant showed more physiological strain values at the middle level as opposed to significant reduction in strains for the standard implant. Significant strain shielding was found for the new implant as well as the standard implant at the distal level for all load cases. The direct experimental comparison between both implants presented significant differences at the middle and the distal level during heel strike and at the middle level during the one leg stance. In these cases the relative strain around the new implant was between 37% and 88% as compared to 8% and 67% around the standard titanium prosthesis, showing the merit of the novel concept.

The insertion of a standard implant showed high strain shielding at the distal level, much lower in the middle level and no significant change was observed proximally. This strain shielding pattern corresponds well with clinical BMD observations and numerical results (Xu et al., 2006; Xu and Robinson, 2008; Tomaszewski et al., 2010).

Obviously, both the experiment and FE model had a number of limitations. The loading conditions were a small selection of many possible ones and muscle forces were not taken into account. The experiment was performed with bones from elderly donors with a relatively large variation in bone mineral density. This made it sometimes difficult to obtain a stable fit of the implants, which is especially important to prevent implant rotation during loading. Additionally, because we wanted to use the same bone for both implants, special attention was paid not to fracture the bone while inserting the implants, which may have compromised tight fit between implant and bone.

Hardware limitations of our setup did not allow the use of multidirectional strain gauges. Multidirectional stain gauges would have provided additional information and additionally could have reduced the variability in the results due to misalignment of the gauges with respect to the long axis of the bones.

The main simplification of the FE modeling was related to the use of a generic model with averaged material properties. This meant that the original BMD of the model was linearly re-scaled to fit to the mean BMD value evaluated at the femoral neck of the used specimens.

In this study the alternate insertion of the implants for testing, instead of a pair wise comparison, was chosen in order to eliminate strain variations due to different local bone qualities in-between pairs and possible differences in alignment of the unidirectional strain gauges. To check the influence of exchanging implants in the same bone after one test we reimplanted the first implant and checked for differences in strains. The average values of 6% were found, which is acceptable.

The relative change in strain yielded a good correlation between FE models and experimental measurements (Table 3). The highest correlations were found for intact bone strains and the lowest for the relative strains around the new implant. In general, correlations between FE analysis and experiments obtained in this study were comparable to the level of correlation between subject-specific FE modeling and cadaver experiments (Pettersen et al., 2009) and clearly lower than in case of bone replicas (Stolk et al., 2002; Completo et al., 2007). The correlations were weaker when we simulated the implanted cases. This means that we introduced unknown aspects that we did not fully capture in our models. Most likely these aspects are related to the interface properties. For the OPRA we assumed a bonded assumption as it concerns a screw-fixation. For the new design we assumed frictional contact (with a friction coefficient of 0.7), with no gaps at the interface and with ideal contact between the collar and bone at the osteotomy level. By judging the strain gauge differences (see also Figure 8) it seems as if the load-transfer from collar to bone was over-estimated by the FE model. Hence, it seems that in the experiments we did not obtain ideal contact between the collar and the bone at the osteotomy level. This observation is highly probable as we did not have specialized instrumentation

to match the osteotomy to the collar plane. In a next generation of instruments this deserves more attention as the FE models show that by perfecting the collar-bone contact, a further idealized load transfer is obtained.

Conclusion

In conclusion, the study showed that the new implant has a potential to increase distal load transfer to the femur and reduce strain shielding as compared with the standard implant. Collar-cortex contact is an important aspect and requires further attention when developing the surgical technique. The encouraging results obtained in this study justify further development of this concept in order to improve the quality and applicability of direct skeletal fixation devices for patients requiring a transfemoral amputation.

Acknowledgements

We would like to thank Willem van de Wijdeven and Léon Driessen for technical support in the experimental setup preparation and measurements. The study was founded by the Fonds NutsOhra.

References

Aamodt, A., et al. (2001). "Changes in proximal femoral strain after insertion of uncemented standard and customised femoral stems. An experimental study in human femora." J Bone Joint Surg Br 83(6): 921-929.

Anonymous (1998). Diabetes-Related Amputations of Lower Extremities in the Medicare Population - Minnesota, 1993-1995. M.M.W.R. C. f. D. C. a. Prevention. Atlanta, GA, U.S., Department of Health and Human Services. 47: 649-652.

Anonymous (2001). Hospital Discharge Rates for Nontraumatic Lower Extremity Amputation by Diabetes Status - United States, 1997. M.M.W.R. C. f. D. C. a. Prevention. Atlanta, GA, U.S., Department of Health and Human Services. 50: 954-958.

Anonymous (2011). National diabetes fact sheet: national estimates and general information on diabetes and prediabetes in the United States, 2011. C. f. D. C. a. Prevention. Atlanta, GA, U.S., Department of Health and Human Services: 1-12.

Aschoff, H. H., et al. (2009). "The endo-exo femur prosthesis-a new concept of bone-guided, prosthetic rehabilitation following above-knee amputation." Zeitschrift für Orthopädie und Unfallchirurgie 147(5): 610-615.

Aschoff, H. H., Kennon, R.E., Keggi, J.M., Rubin, L.E. (2010). "Transcutaneous, Distal Femoral, Intramedullary Attachment for Above-the-Knee Prostheses: An Endo-Exo Device." Journal of Bone and Joint Surgery 92(Suppl 2): 180-186.

Bayraktar, H. H., et al. (2004). "Comparison of the elastic and yield properties of human femoral trabecular and cortical bone tissue." J Biomech 37(1): 27-35.

Brånemark, R., et al. (2001). "Osseointegration in skeletal reconstruction and rehabilitation: a review." Journal of Rehabilitation Research and Development 38(2): 175-181.

Completo, A., et al. (2007). "Finite element and experimental cortex strains of the intact and implanted tibia." J Biomech Eng 129(5): 791-797.

Cowie, C. C., et al. (2010). "Prevalence of diabetes and high risk for diabetes using A1C criteria in the U.S. population in 1988-2006." Diabetes Care 33(3): 562-568.

Cristofolini, L., et al. (1996). "Mechanical validation of whole bone composite femur models." J Biomech 29(4): 525-535.

Decking, R., et al. (2006). "Changes in strain distribution of loaded proximal femora caused by different types of cementless femoral stems." Clin Biomech (Bristol, Avon) 21(5): 495-501.

Fischer, H. (2010). U.S. Military Casualty Statistics: Operation New Dawn, Operation Iraqi Freedom, and Operation Enduring Freedom. CRS Report for Congress, Congressional Research Service: 1-8.

Hagberg, K., et al. (2009). "One hundred patients treated with osseointegrated transfemoral amputation prostheses-rehabilitation perspective." Journal of Rehabilitation Research and Development 46(3): 331-344.

Hagberg, K., et al. (2005). "Socket versus bone-anchored trans-femoral prostheses: hip range of motion and sitting comfort." Prosthetics and Orthotics International 29(2): 153-163.

Keyak, J. H., et al. (2003). "Comparison of in situ and in vitro CT scan-based finite element model predictions of proximal femoral fracture load." Medical Engineering & Physics 25(9): 781-787.

Keyak, J. H., et al. (2005). "Predicting proximal femoral strength using structural engineering models." Clinical Orthopaedics and Related Research 437: 219-228.

Kim, Y. H., et al. (2001). "Strain distribution in the proximal human femur. An in vitro comparison in the intact femur and after insertion of reference and experimental femoral stems." J Bone Joint Surg Br 83(2): 295-301.

Kobayashi, S., et al. (2000). "Poor bone quality or hip structure as risk factors affecting survival of total-hip arthroplasty." Lancet 355(9214): 1499-1504.

Lee, W. C., et al. (2007). "Kinetics of transfemoral amputees with osseointegrated fixation performing common activities of daily living." Clinical Biomechanics 22(6): 665-673.

Meulenbelt, H. E., et al. (2011). "Skin problems of the stump in lower limb amputees: 1. A clinical study." Acta Dermato Venereologica 91(2): 173-177.

Ostbyhaug, P. O., et al. (2009). "An in vitro study of the strain distribution in human femora with anatomical and customised femoral stems." J Bone Joint Surg Br 91(5): 676-682.

Petersen, M. M., et al. (1995). "Changes in bone mineral density of the distal femur following uncemented total knee arthroplasty." Journal of Arthroplasty 10(1): 7-11.

Pettersen, S. H., et al. (2009). "Subject specific finite element analysis of stress shielding around a cementless femoral stem." Clin Biomech (Bristol, Avon) 24(2): 196-202.

Schileo, E., et al. (2007). "Subject-specific finite element models can accurately predict strain levels in long bones." J Biomech 40(13): 2982-2989.

Spittlehouse, A. J., et al. (1998). "Bone loss around 2 different types of hip prostheses." Journal of Arthroplasty 13(4): 422-427.

Stolk, J., et al. (2002). "Finite element and experimental models of cemented hip joint reconstructions can produce similar bone and cement strains in pre-clinical tests." J Biomech 35(4): 499-510.

Taddei, F., et al. (2007). "The material mapping strategy influences the accuracy of CT-based finite element models of bones: an evaluation against experimental measurements." Med Eng Phys 29(9): 973-979.

Tanck, E., et al. (2009). "Pathological fracture prediction in patients with metastatic lesions can be improved with quantitative computed tomography based computer models." Bone 45(4): 777-783.

Tomaszewski, P. K., et al. (2010). "A comparative finite-elelement analysis of bone failure and load transfer of osseointegrated prostheses fixations." Annals of Biomedical Engineering 38(7): 2418-2427.

Viceconti, M., et al. (2001). "Pre-clinical validation of a new partially cemented femoral prosthesis by synergetic use of numerical and experimental methods." J Biomech 34(6): 723-731.

Xu, W., et al. (2008). "X-ray image review of the bone remodeling around an osseointegrated trans-femoral implant and a finite element simulation case study." Annals of Biomedical Engineering 36(3): 435-443.

Xu, W., et al. (2006). "Three-dimensional finite element stress and strain analysis of a transfemoral osseointegration implant." Proceedings of the Institution of Mechanical Engineers, Part H: Journal of Engineering in Medicine 220(6): 661-670.

Chapter 6

Analysis of different material couples for an optimal wear performance in a new design of a direct fixation implant

P.K. Tomaszewski[1], W. Lette[2], D.J. Schipper[2], G.J. Verkerke[1,3]

[1] Department of Biomedical Engineering, University of Groningen, University Medical Center Groningen.
[2] Surface Technology and Tribology Group, Faculty of Engineering, University of Twente.
[3] Department of Biomechanical Engineering, Faculty of Engineering, University of Twente.

Introduction

A new concept of a direct fixation implant for amputated patients has been developed to provide as close as possible a physiological load distribution in the periprosthetic bone. This multi-component system is composed of a metallic core and an outer sleeve with an elastic modulus comparable to the cortical bone (Figure 1).

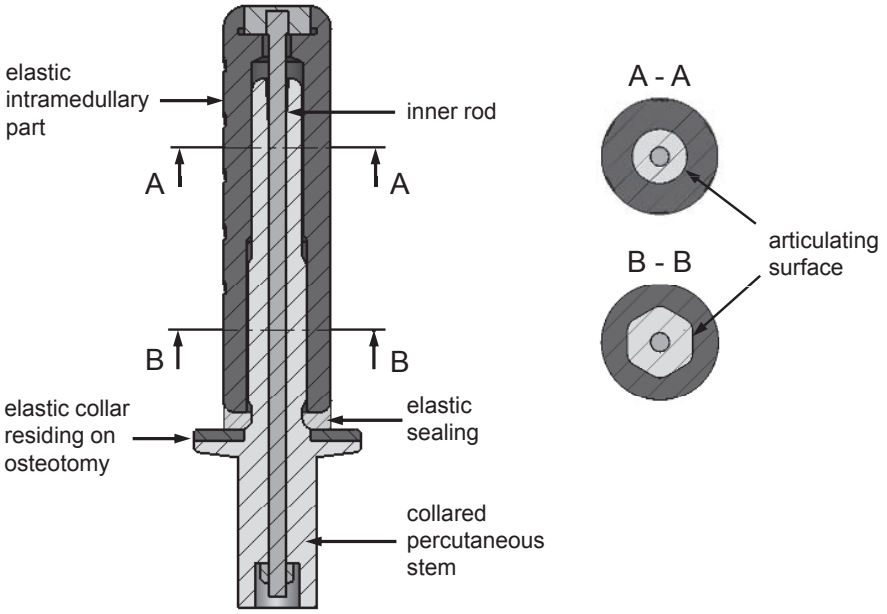

Figure 1. Schematic representation of the new implant.

To enhance distal load transfer from the implant to the osteotomy of the femur remnant, a collar with a layer of elastic material was added to the stem and a low-amplitude sliding motion between the inner and outer part of the implant was allowed. This sliding motion requires an appropriate bearing surface. The biomaterial couple should combine optimal bulk and surface properties. The materials should possess overall high mechanical strength, its interface should exhibit low friction and wear and the stiffness of the implant should be close to bone stiffness (especially the intramedullary part).

Low friction and wear has been important design objectives for prosthetic joints for two reasons. First, if large shear forces due to friction are applied to the articulating surface, the risk of implant loosening is increased. Second, the addition of frictional shear increases the stresses associated with surface damage due to contact, which can result in the release of wear debris to the surrounding tissue that also increases the risk of asceptic loosening. The search for a low-friction and low-wear articulation led to bearing combinations as metal against polyethylene, ceramic on polyethylene, ceramic on ceramic or metal on metal. All have potential advantages but metal and ceramic on ultra high molecular weight polyethylene (UHMWPE) continues to be the

most common bearing combination in artificial joint replacement implants. However, for the purpose of the new fixation implant the focus is set on materials with elastic modulus close to the cortical bone, thus with elastic moduli in the range of 11.5 to 17.0 GPa (Reilly and Burstein, 1975). For this reason, apart from widely used CoCrMo alloys (E=210-250 GPa) and UHMWPE (E≈1.0GPa), we considered application of PEEK polymer (E=4-150 GPa) and Ti6Al4V alloy (E=114 GPa) (Hallab et al., 2003; Kurtz, 2012). The PEEK polymer and Ti6Al4V alloy have been used in orthopaedic applications such as spinal implants, total hip and knee replacements (Kurtz and Devine, 2007).

Pure PEEK was found to have rather poor wear properties. Wear tests performed in a pin-on-plate setup, lubricated with dilute bovine serum at 37°C, against CoCrMo plates showed seven times higher wear rates (Scholes and Unsworth, 2009) than a UHMWPE/stainless steel couple in comparable tests (Joyce et al., 2000). The wear rates found in hip simulator studies (Wang et al., 1998) for PEEK against an alumina counter surface were approximately eight times higher than for UHMWPE cups (tests in bovine serum at 33°C).

To improve wear properties of the PEEK polymer, carbon fibre reinforced composites were created (CFR-PEEK). In general, the carbon fibres are classified based on its origin, that is polyacrylonitrile (PAN type) or petroleum pitch derived from oil processing (pitch type); and length (short and continuous). The short carbon fibre composites gained a wider scope of applications due to its extensive forming possibilities. A substantial reduction of both friction coefficient and specific wear rates related to addition of carbon fibres to PEEK was demonstrated in pin-on-disk tests against steel in dry circumstances (Lu and Friedrich, 1995) and lubricated with distilled water (Davim and Marques, 2001). When considering the CoCrMo alloy as a counterface, the pin-on-plate tests in bovine serum at 37°C with both PAN and pitch based CFR-PEEK composites show similar or lower wear rates than UHMWPE (Scholes and Unsworth, 2009). The difference was more pronounced in a hip joint simulator tests (in bovine serum at 33°C), which presented around four times lower wear rates for both pitch and PAN based PEEK composites as compared with UHMWPE articulating against CoCrMo (Wang et al., 1998). In the same study pitch based CFR-PEEK showed much lower wear rates than UHMWPE and PAN based CFR-PEEK when sliding against ceramic counterfaces.

Of all surgical metals, Ti6Al4V alloy has the best combination of biocompatibility, stiffness and fatigue properties, but its wear resistance is reported as inferior to that of stainless steel and CoCrMo alloys when sliding against UHMWPE (McKellop, 2001; Gutmanas and Gotman, 2004). To our knowledge no literature is available about wear performance of Ti6Al4V sliding against PEEK polymers, which would be of high interest for our application. Moreover, as friction and wear are not intrinsic material characteristics, but strongly depend on the test system (contact pressure, roughness, contact geometry, velocity, and temperature), it is difficult to extrapolate results from different setups to conditions expected in the designed implant.

In this study uni-directional fretting wear tests were performed on various combinations of PEEK and CFR-PEEK against CoCrMo and Ti6Al4V to assess the potential of this material combination for use in the new implant for direct prosthesis fixation.

Materials and methods

The following materials were used in the experiments: Polyetheretherketone (PEEK Optima, Invibio Ltd., Lancashire, UK), further referred to as PEEK; pitch based carbon fibre reinforced polyetheretherketone (PEEK Motis, Invibio, Lancashire, UK), further referred to as CFR-PEEK pitch; PAN based carbon fibre reinforced polyetheretherketone (PEEK LT1CA30, Invibio Ltd., Lancashire, UK), further referred to as CFR-PEEK PAN; Ultra-high-molecular-weight polyethylene (Multilene M1000, Eriks, Alkmaar, The Netherlands), further referred to as UHMWPE; Ti6Al4V alloy (Titanium Grade 5, Salomon's Metalen, Groningen, The Netherlands), further referred to as Ti6Al4V; CoCrMo alloy (Stellite21, Deloro Stellite, Swindon, UK), further referred to as CoCrMo. The average physical properties of these materials are presented in Table 1.

	Elastic modulus [GPa]	Tensile strength [MPa]	Poisson ratio	Density [g/cm^3]
PEEK	4	100	0.36	1.30
CFR-PEEK PAN	21	225	0.44	1.40
CFR PEEK pitch	12	155	0.41	1.42
UHMWPE	0.8	20	0.46	0.93
Ti6Al4V	114	900	0.34	4.43
CoCrMo	250	560	0.29	8.50

Table 1. Typical average physical properties of considered biomaterials (Kurtz, 2004; Kurtz, 2012).

The test setup (Figure 2) consisted of a polymer cylinder sample (radius = 10 mm, length = 34 mm) pressed against a reciprocating metal plate sample (55 mm wide, 150 mm long and 4 mm thick). The metal plate sample was fixed in a handle of a tensile testing machine (MTS Systems Corporation, USA) and the polymer sample was mounted in a holder with an integrated pneumatic system allowing to exert a pre-described normal force F_N.

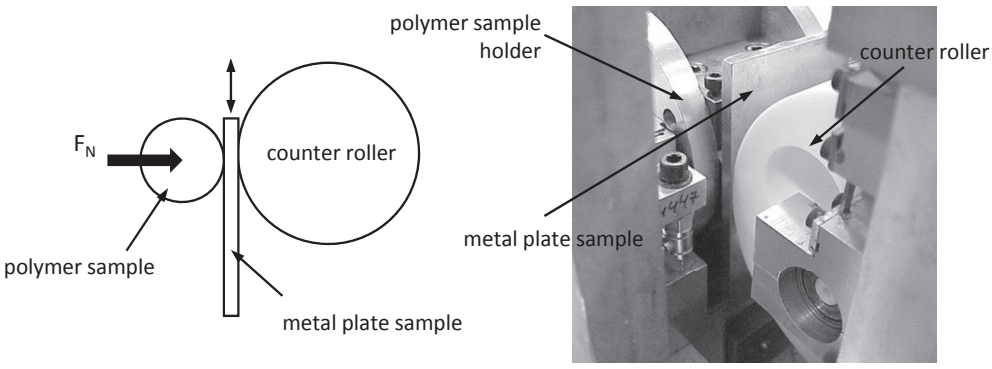

Figure 2. Experimental setup.

	CoCrMo		Ti6Al4V	
	p_{max} [MPa]	contact width [mm]	p_{max} [MPa]	contact width [mm]
PEEK	30.4	0.26	30.1	0.26
CFR-PEEK PAN	69.7	0.12	66.5	0.12
CFR PEEK pitch	52.9	0.16	51.5	0.16
UHMWPE	14.4	0.56	14.3	0.56

Table 2. The Hertzian maximum contact pressure between polymer cylinders (r = 10 mm and 55 mm width) and metal plates and contact width as load F_N=218N.

Based on the previous finite element analysis (FEA) (Chapter 3 and Chapter 4) the normal force acting on the polymer cylinder sample was set to FN=218N and a vertical movement amplitude of the metal plate sample A = 0.1 mm was prescribed. The reciprocating movement frequency was set to f = 10 Hz and the test was run for 106 cycles, which on average represent 6.5 months of implant use (Tudor-Locke et al., 2011). The maximum contact pressure and contact width was calculated using Hertz (line contact) and is presented in Table 2. The prescribed movement amplitude A was smaller than the contact width to represent fretting wear conditions as expected characteristic for the designed interface.

The metal plates were tested with two different surface finish, first, as delivered: CoCrMo alloy R_a = 0.26 μm, Ti6Al4V R_a = 0.50 μm, further called rough and afterwards in polished state: CoCrMo alloy R_a = 0.038 μm, Ti6Al4V R_a = 0.037 μm. The surface roughness of the polymer cylinders was in the range of R_a = 1.10 μm to R_a = 3.27 μm.

The tests were performed without any lubrication at room temperature (ca. 20°C). The friction force was recorded during the test and volumetric wear, ΔV, was measured by means of confocal microscopy (VK-9710, Keyence Corp., Japan) to obtain the specific wear rate by $k = \Delta V/(F_N \cdot s)$, in which FN and s are the normal load and sliding distance respectively.

Results

In the tests with rough metal surfaces the UHMWPE show a very low friction coefficient *CoF* = 0.17-0.18 (Table 3). Comparable friction coefficient values were found only for the Ti6Al4V and PEEK material couple, while CFR-PEEK PAN coupled with rough Ti6Al4V show moderate CoF=0.22 and the highest friction coefficient was found for rough CoCrMo sliding against both CFR-PEEK PAN composite (CoF=0.27) and PEEK (CoF=0.30). The lowest specific wear rates were measured for PEEK and CFR-PEEK PAN with CoCrMo and moderate specific wear rates with Ti6Al4V. The UHMWPE wear rates were very low when sliding against Ti6Al4V alloy and very high in contact with CoCrMo. It should be noted that both rough metal surfaces had a different surface roughness; tests with the CFR-PEEK pitch presented an irregular wear pattern along the sample and were not included in the Table 3.

	rough plates					
	CoCrMo (R_a=0.26µm)			Ti6Al4V (R_a=0.50µm)		
cylinder	Volume [mm^3]	k [$10^{-6}mm^3N^{-1}m^{-1}$]	CoF	Volume [mm^3]	k [$10^{-6}mm^3N^{-1}m^{-1}$]	CoF
CFR-PEEK PAN	0.0035	0.040	0.27	0.0196	0.2248	0.22
CFR-PEEK pitch	------	-------	0.26	-----	-------	0.21
PEEK	0.0038	0.044	0.30	0.0259	0.2970	0.16
UHMWPE	0.0393	0.451	0.17	0.0046	0.0521	0.18

Table 3. Measurements results using rough plates.

In general, polishing of the plates led to a decrease in both friction coefficient and specific wear rates (Table 3 and Table 4). Similar surface roughness allowed also a direct comparison between both metal counterfaces (Table 4). The lowest friction coefficient (CoF=0.18) was found again for UHMWPE sliding against both CoCrMo and Ti6Al4V. A slightly higher CoF=0.20 was recorded for CFR-PEEK PAN with both metal surfaces.

Further a moderate friction coefficient (*CoF*=0.26) was found for CFR-PEEK pitch/ CoCrMo couple and the highest (*CoF*=0.37) for CFR-PEEK pitch/Ti6Al4V. The lowest specific wear rate was obtained for CFR-PEEK pitch / Ti6Al4V couple and was more than twice lower than UHMWPE wear rates against both metal surfaces. Moderate specific wear rate was measured for CFR-PEEK pitch/CoCrMo and the highest for CFR-PEEK PAN/ Ti6Al4V. Once again an irregular wear pattern on a sample did not allow to measure reliable wear rate for the CFR-PEEK PAN/CoCrMo test. The PEEK material was not included in this series of measurements.

	polished plates					
	CoCrMo (R_a=0.038µm)			Ti6Al4V (R_a=0.037µm)		
cylinder	Volume [mm^3]	k [$10^{-6}mm^3N^{-1}m^{-1}$]	CoF	Volume [mm^3]	k [$10^{-6}mm^3N^{-1}m^{-1}$]	CoF
CFR-PEEK PAN	----	----	0.20	0.0095	0.1094	0.20
CFR-PEEK pitch	0.0028	0.0327	0.26	0.0010	0.0117	0.37
PEEK	----	----	----	----	----	----
UHMWPE	0.0023	0.0262	0.18	0.0020	0.0282	0.18

Table 4. Measurements results using polished plates.

Discussions and conclusions

The experiments were performed to compare wear and friction behaviour of several material couples considered for application in the new design of direct prosthesis fixation implant for amputated patients. The system characteristic test conditions were determined from FEA of the designed implant. The contacting surfaces in the implant experience cyclic tangential displacement of small amplitude, that is characteristic to fretting and was reproduced in the experimental setup.

Based on the *CoF*, combinations of CFR-PEEK PAN with both CoCrMo and Ti6Al4V perform slightly better than CFR-PEEK pitch/CoCrMo and much better than CFR-PEEK pitch/Ti6Al4V, while based on the wear results the performance of CFR-PEEK pitch/Ti6Al4V is slightly better than CFR-PEEK pitch/CoCrMo and considerably better than CFR-PEEK PAN/Ti6Al4V. From all tested material combinations the CFR-PEEK pitch/Ti6Al4V materials generated the lowest wear (even lower than the control UHMWPE/CoCrMo couple) but relatively high friction. Alternatively, CFR-PEEK pitch/CoCrMo material couple appears to be a reasonable compromise between low friction and wear under dry conditions (with only slightly higher values than the control UHMWPE/CoCrMo couple).

In this study dry conditions were considered for two reasons, namely, the implant can be assumed to be sealed (i.e. by means of a medical grade silicone) and if otherwise, the choice of lubricant in the case of this type of implant is disputable. In the literature different liquid media are used to represent hip and knee joint conditions, namely Ringers's solution (Gutmanas and Gotman, 2004), bovine serum (Wang et al., 1998; Scholes and Unsworth, 2009), distilled water (Dong et al., 1999; Davim and Marques, 2001; Onate et al., 2001), however these might not be representative for the direct fixation implant.

The measured friction coefficients for CFR-PEEK composites *CoF*=0.21-0.22 against Ti6Al4V and *CoF*=0.26-0.27 against CoCrMo were similar to the dry pin-on-disc measurements of CFR-PEEK against steel - CoF=0.22 (Lu and Friedrich, 1995). The surface roughness of used steel counterface (Ra=0.20-0.30 μm) was comparable to those used in our rough tests (R_a=0.26-0.50 μm), however, contact pressures for PEEK and CFR-PEEK in our tests were considerably higher (30-70 MPa as compared to 8 MPa). Tests with unfilled PEEK showed however lower friction coefficients for Ti6Al4V and CoCrMo *CoF*=0.16-0.30 than for steel *CoF*=0.40. When considering the specific wear, CFR-PEEK presented similar values $k=4.0\cdot10^{-8}$ $mm^3N^{-1}m^{-1}$ for CoCrMo and $k=2.2\cdot10^{-7}$ $mm^3N^{-1}m^{-1}$ for Ti6Al4V as compared to $k=1.0\cdot10^{-7}$ $mm^3N^{-1}m^{-1}$ steel (Lu and Friedrich, 1995). Similarly as for the friction coefficient the specific wear rates for unfilled PEEK were much lower in tests with CoCrMo ($k=4.4\cdot10^{-8}$ $mm^3N^{-1}m^{-1}$) and Ti6Al4V ($k=2.9\cdot10^{-7}$ $mm^3N^{-1}m^{-1}$) than steel ($k=1.0\cdot10^{-5}$ $mm^3N^{-1}m^{-1}$).

In our test we have observed that the values of the friction coefficient for CFR-PEEK grades have decreased with a decrease of surface roughness of metal counterface, which is in line with result reported in literature. This stays in agreement with abrasive wear measurements using pin-on-disc setup performed on CFR-PEEK (not reported if PAN or pitch based type was used) sliding against steel surface lubricated with distilled water (Davim and Marques, 2001). The specific wear rate for CFR-PEEK against steel found in the same study were slightly higher ($k=6.8\cdot10^{-8}$ $mm^3N^{-1}m^{-1}$) than in our measurements with CFR-PEEK pitch/CoCrMo ($k=3.3\cdot10^{-8}$ $mm^3N^{-1}m^{-1}$) and CFR-PEEK pitch/Ti6Al4V ($k=1.2\cdot10^{-8}$ $mm^3N^{-1}m^{-1}$). A similar surface roughness was used in both experiments (Ra=0.04 μm and R_a=0.05 μm) but in our setup the contact pressures for CFR-PEEK were considerably higher (50-70 MPa as compared to 10 MPa).

The friction coefficient for UHMWPE measured in this study was similar for both CoCrMo and Ti6Al4V materials *CoF*=0.18, which is higher than the reported average

CoF = 0.10 for CoCrMo (Saikko, 1993) and *CoF* = 0.11 for Ti6Al4V (Dong et al., 1999). The reduction in friction coefficient is most probably caused by lubrication used in the two latter studies. On the other hand the specific wear rates found for both metal surfaces in this dry fretting test: CoCrMo ($k = 3.3 \cdot 10^{-8}$ $mm^3N^{-1}m^{-1}$) and Ti6Al4V ($k = 1.2 \cdot 10^{-8}$ $mm^3N^{-1}m^{-1}$) were considerably lower than in the lubricated abrasive wear tests with CoCrMo ($k = 1.0 \cdot 10^{-7}$ $mm^3N^{-1}m^{-1}$) and Ti6Al4V ($k = 3.8 \cdot 10^{-6}$ $mm^3N^{-1}m^{-1}$) (Saikko, 1993; Dong et al., 1999). Also the specific wear of CFR-PEEK pitch vs. CoCrMo ($k = 3.3 \cdot 10^{-8}$ $mm^3N^{-1}m^{-1}$) obtained in our tests was lower than measured in lubricated pin-on-disc tests ($k = 1.2 \cdot 10^{-7}$ $mm^3N^{-1}m^{-1}$) (Scholes and Unsworth, 2009).

Apart from ranking the analysed material combinations, it is additionally useful to relate the measured wear volumes to the considered geometry and estimate if the expected wear values are acceptable or can compromise implant performance. Assuming steady state wear and desired performance of $55 \cdot 10^6$ cycles (as estimated for 30 years of operation, see Chapter 1) the maximum total wear volume is 0.523 mm^3 (polished Ti6Al4V and CFR-PEEK PAN) and minimum is 0.055 mm^3 (polished Ti6Al4V and CFR-PEEK pitch). Assuming further that due to the hexagonal cross-section effectively 1/6 of the total contact surface between metal stem and polymeric intramedullary part will be subjected to wear, the effective contact area is approximately 200 mm^2. Considering the above, the estimated reduction in thickness of the intramedullary part is <3 μm for CFR-PEEK PAN and <0.3 μm for CFR-PEEK pitch. These wear rates are rather unlikely to compromise the mechanical performance of the implant.

Obviously the performed study possessed some limitations, which need to be considered when interpreting the results. First, due to a long experimental time (28 hours per single experiment) and limited access to the measurement setup the number of tests had to be reduced to a minimum. For example PEEK was not included in the measurements with polished metal samples due to its low elastic modulus (as compared with bone) and considerably lower tensile strength as compared to the CFR-PEEK composites. Moreover, all the tests were performed once, thus measurements should be preferably repeated to ensure reproducibility of the data. Additionally, some tests failed due to misalignment of the samples in the setup.

In conclusion, the CFR-PEEK pitch/CoCrMo material couple appears to be the best compromise between low friction and wear under dry operating conditions in the new direct prosthesis fixation implant. Additionally, it is recommended to investigate possibilities of surface modifications i.e. titanium nitride or diamond like carbon coating (Dong et al., 1999; Gutmanas and Gotman, 2004; Dearnaley and Arps, 2005) to further decrease interfacial friction and wear.

Finally, if lubricated conditions are considered in the implant, it should be stressed that dry tests may give a different ranking of the material combinations tested, based on friction and wear rates, as in lubricated systems (Mens, 1991). Therefore, we would recommend including both CFR-PEEK composites and metal alloys in lubricated wear tests.

Acknowledgements

Invibio Ltd. (Lancashire, UK) for providing PEEK materials for testing. The study was founded by the Fonds NutsOhra.

References

Davim, J. P., et al. (2001). "Evaluation of tribological behaviour of polymeric materials for hip prostheses application." Tribology Letters 11(2): 91-94.

Dearnaley, G., et al. (2005). "Biomedical applications of diamond-like carbon (DLC) coatings: A review." Surface & Coatings Technology 200(7): 2518-2524.

Dong, H., et al. (1999). "Potential of improving tribological performance of UHMWPE by engineering the Ti6Al4V counterfaces." Wear 225: 146-153.

Gutmanas, E. Y., et al. (2004). "PIRAC Ti nitride coated Ti-6AI-4V head against UHMWPE acetabular cup-hip wear simulator study." J Mater Sci Mater Med 15(4): 327-330.

Hallab, N., et al. (2003). "Biomaterial optimization in total disc arthroplasty." Spine (Phila Pa 1976) 28(20): S139-152.

Joyce, T. J., et al. (2000). "A multi-directional wear screening device and preliminary results of UHMWPE articulating against stainless steel." Bio-Medical Materials and Engineering 10(3-4): 241-249.

Kurtz, S. M. (2004). The UHMWPE handbook : ultra-high molecular weight polyethylene in total joint replacement. Amsterdam ; Boston, Academic Press.

Kurtz, S. M. (2012). Peek Biomaterials Handbook. Amsterdam ; Boston, Academic Press.

Kurtz, S. M., et al. (2007). "PEEK biomaterials in trauma, orthopedic, and spinal implants." Biomaterials 28(32): 4845-4869.

Lu, Z. P., et al. (1995). "On Sliding Friction and Wear of Peek and Its Composites." Wear 181: 624-631.

McKellop, H. A., Rostlund, T., Ebramzadeh, E., Sarmiento, A. (2001). Wear of Titanium 6-4 Alloy in Laboratory Tests and in Retrieved Human Joint Replacements. Titanium in medicine: material science, surface science, engineering, biological responses, and medical applications. D. M. Brunette. Berlin ; New York, Springer: 748-767.

Mens, J. W. M., de Gee, A. W. J. (1991). "Fricton and wear behaviour of 18 polymers in contact with steel in environments of air and water." Wear 149: 255-268.

Onate, J. I., et al. (2001). "Wear reduction effect on ultra-high-molecular-weight polyethylene by application of hard coatings and ion implantation on cobalt chromium alloy, as measured in a knee wear simulation machine." Surface & Coatings Technology 142: 1056-1062.

Reilly, D. T., et al. (1975). "The elastic and ultimate properties of compact bone tissue." J Biomech 8(6): 393-405.

Saikko, V. (1993). "Wear and Friction Properties of Prosthetic Joint Materials Evaluated on a Reciprocating Pin-on-Flat Apparatus." Wear 166(2): 169-178.

Scholes, S. C., et al. (2009). "Wear studies on the likely performance of CFR-PEEK/CoCrMo for use as artificial joint bearing materials." Journal of Materials Science-Materials in Medicine 20(1): 163-170.

Tudor-Locke, C., et al. (2011). "How many steps/day are enough? For older adults and special populations." Int J Behav Nutr Phys Act 8(1): 80.

Wang, A., et al. (1998). "Carbon fiber reinforced polyether ether ketone composite as a bearing surface for total hip replacement." Tribology International 31(11): 661-667.

Chapter 7

Potential improvement of tribological performance of PEEK polymers by application of diamond-like carbon coating

P.K. Tomaszewski[1], Y.T. Pei[2], G.J. Verkerke[1,3], J.Th.M. De Hosson[2]

[1] Department of Biomedical Engineering, University of Groningen, University Medical Center Groningen.
[2] Department of Applied Physics, Materials Innovation Institute, University of Groningen, The Netherlands.
[3] Department of Biomechanical Engineering, Faculty of Engineering, University of Twente.

Introduction

To provide close to physiological load distribution in the periprosthetic bone, a new concept of a direct fixation implant for amputated patients has been developed. This multi-component system is composed of a metallic core and an outer sleeve with an elastic modulus comparable to the cortical bone. For this combination of materials optimal bulk and surface properties are needed. The materials should possess overall high mechanical strength and have an elastic modulus compatible with that of bones. Moreover, the contact interface should exhibit low friction and wear, which are crucial for implant stability and minimizing risk of debris-induced osteolysis.

As introduced in Chapter 5 low friction and wear have been important design objectives for prosthetic joints and thus have been extensively studied in the literature. Currently metal and ceramic on ultra high molecular weight polyethylene (UHMWPE) continues to be the most common bearing combination in joint replacement implants. However, for the purpose of the new fixation implant materials with elastic modulus close to the cortical bone, in the range of 11.5 to 17.0 GPa (Reilly and Burstein, 1975), are of higher interest. For this reason we focused on combinations of a PEEK polymer (E=4-150 GPa) and Ti6Al4V alloy (E=114 GPa) (Hallab et al., 2003; Kurtz, 2012). These materials have been successfully used in orthopaedic applications such as spinal implants, total hip and knee replacements (Kurtz and Devine, 2007), but never used together as an articulating couple up to now.

Poor wear properties of PEEK polymer as compared to UHMWPE (Wang et al., 1998; Joyce et al., 2000; Scholes and Unsworth, 2009), has been tackled by introduction of carbon fiber reinforced PEEK composites (CFR-PEEK). Two most common types of CFR-PEEK types are based on polyacrylonitrile (PAN) fibers or carbon fibers derived from petroleum pitch that is produced from oil processing (pitch). PAN–based carbon fibers are characterized by higher flexibility and higher tensile strength as compared to pitch-based fibers. Both types of CFR-PEEK were found to offer a substantial reduction of both: coefficient of friction (CoF) and specific wear rates (Lu and Friedrich, 1995; Davim and Marques, 2001) as compared to unfilled PEEK, when tested against steel. This results in similar or lower wear rates than UHMWPE (Scholes and Unsworth, 2009). Similarly as PEEK amongst biocompatible polymers, Ti6Al4V alloy has very good biocompatibility, stiffness and fatigue properties, but its wear resistance is reported as inferior to other metallic biomaterials such as stainless steel or CoCrMo alloys (McKellop, 2001; Gutmanas and Gotman, 2004).

In the previous study (Chapter 5) uni-directional fretting wear tests were performed on various combinations of PEEK and CFR-PEEK against CoCrMo and Ti6Al4V to assess the potential of this material combination for use in the new implant design. It was found that CFR-PEEK pitch/CoCrMo material couple appears to be the best compromise between low friction and wear under dry operating conditions (as compared to control UHMWPE/CoCrMo couple). The tests of Ti6Al4V presented very low specific wear rate with CFR-PEEK pitch (lower than any UHMWPE combination) and very low CoF with CFR-PEEK PAN (close to UHMWPE), but when considering both friction and wear CFR-PEEK and Ti6Al4V couples showed lower performance than the control UHMWPE/CoCrMo couple.

For the past years diamond-like carbon coatings have been explored as a mean for improving tribological properties of biomaterials. Diamond-like carbon (DLC) is a common name for amorphous carbon materials that contain at least some diamond sp^3–hybridized c-c bonds so referred as diamond-like. DLC coatings are considered for orthopaedic, cardiovascular and dental applications due to their high wear and corrosion resistance, chemical inertness and biocompatibility (Hauert, 2003; Dearnaley and Arps, 2005; Roy and Lee, 2007). Susceptibility of DLC coatings to microbial adhesion is similar to commonly used steel 316L, which suggests that DLC does not increase the risk of implant-related infections (Soininen et al., 2009).

First DLC coatings were applied mainly on metal surfaces and demonstrated reduction of wear and corrosion in orthopaedic applications (Dowling et al., 1997; Onate et al., 2001; Platon et al., 2001; Tiainen, 2001). More recently stable flexible DLC films were deposited also on very flexible materials such as for example rubber (Pei et al., 2010). Up till now one study presented biological and mechanical characterization of DLC coatings deposited on unfilled PEEK (Wang et al., 2010), however to our knowledge tribological behavior of DLC coating on unfilled and CF filled PEEK polymers has not been tested.

The aim of this study was to examine if DLC coating can improve tribological performance of a sliding interface between Ti6Al4V alloy and different PEEK polymers. For this purpose DLC films were deposited on PEEK polymers and its tribological behaviour was studied using a ball-on-disc test setup with a Ti6Al4V ball.

Materials and Methods

The following materials were used in the experiments: Polyetheretherketone (PEEK Optima, Invibio Ltd., Lancashire, UK), further referred to as PEEK; pitch based carbon fibre reinforced polyetheretherketone (PEEK Motis, Invibio, Lancashire, UK), further referred to as CFR-PEEK pitch; PAN based carbon fibre reinforced polyetheretherketone (PEEK LT1CA30, Invibio Ltd., Lancashire, UK), further referred to as CFR-PEEK PAN; Ultra-high-molecular-weight polyethylene (Multilene M1000, Eriks, Alkmaar, The Netherlands), further referred to as UHMWPE; Ti6Al4V alloy (Titanium Grade 5, Salomon's Metalen, Groningen, The Netherlands), further referred to as Ti6Al4V. Table 1 presents average physical properties of these materials.

	Elastic modulus [GPa]	Tensile strength [MPa]	Poisson ratio	Density [g/cm^3]
Ti6Al4V	114	900	0.34	4.43
PEEK	4	100	0.36	1.30
CFR-PEEK PAN	21	225	0.44	1.40
CFR PEEK pitch	12	155	0.41	1.42
UHMWPE	0.8	20	0.46	0.93

Table 1. Typical average physical properties of materials used in tribological tests (Kurtz, 2004; Kurtz, 2012).

The polymer substrate discs were polished with #4000 SiC abrasive paper (equivalent of surface roughness Ra=0,02 µm on steel). Plasma cleaning treatment of the polymers substrates and deposition of DLC films were carried out in a Teer UDP400/4 closed-field unbalanced magnetron sputtering system, which was configured of four magnetrons that were all powered off. The substrates were cleaned by Ar plasma for 35 minutes at pulsed-DC (250 kHz, 87.5% duty cycle) bias voltage of -600 V. Immediately after the plasma cleaning treatment, DLC films were deposited by plasma CVD (p-CVD) at pulsed-DC bias voltage of -300 V and -400 V, respectively, for 210 min and 120 min to reach the same film thickness of 600±50 nm. To enhance the interfacial adhesion of DLC films, higher substrate bias voltage was used at the beginning of deposition for 2 minutes. The polymer substrates were rotated at a revolving speed of 3 rpm during the deposition.

The surface morphology and microstructure of DLC films on the polymers substrates were characterized by means of optical microscope (Olympus, Tokyo, Japan) and scanning electron microscope (SEM, Philips XL-30 FEG). Tribological tests of DLC coated polymers substrates were performed at room temperature (20-23°C) on a CSM high temperature tribometer (CSM Instruments, Peseux, Switzerland) with ball-on-disc configuration. The counterpart was a commercial ø6 mm Ti6Al4V ball. Coefficient of friction (*CoF*) was measured during the tribological tests with a high accuracy of 0.005. All the dry sliding tribotests were carried out at a sliding velocity of 10 cm/s and a constant humidity of 50±1 % kept with a humidity regulator. The lubricated tribological tests were done in a bath of 8 ml phosphate buffered saline (PBS) solution to simulate the working environment of the implant. The wear track of DLC film coated samples was investigated with SEM and confocal microscope.

The contact pressures found in the finite element simulations of an implant composed of a Ti6Al4V stem in contact with a CFR-PEEK pitch intramedullary sleeve (Chapter 3 and 4) were: σ_{peak}=90 MPa and $\sigma_{average}$=40 MPa. The normal load used in the tribological test was 1, 3 and 5 N, which are standard values used in tribological tests. As presented in Table 2, these loads raised much higher contact pressures with respect to the contact pressure obtained with finite element simulations (Chapter 3, 4). The normal load of 0.2 is closest to the numerical prediction, but 0.5 N normal load would be a good compromise between the stability of tribological tests and the contact pressure in real applications.

	0.2 N		0.5 N		1 N		3 N	
	pressure [MPa]	radius [µm]	pressure [MPa]	radius [µm]	pressure [MPa]	radius [µm]	pressure [MPa]	radius [µm]
PEEK	43.9	46.6	59.6	69.3	75.1	79.7	108.3	115.0
CFR-PEEK PAN	126.4	27.5	171.5	37.3	216.1	47.0	311.7	67.8
CFR-PEEK pitch	89.8	32.6	129.1	44.3	153.5	55.0	221.4	80.4
UHMWPE	16.3	76.5	22.2	103.8	27.9	130.7	40.3	188.6

Table 2. The Hertzian maximum contact pressure between ø6 Ti6Al4V ball and polymer discs at different normal force.

Results

Initial experiments performed against Ti6Al4V ball sliding in dry conditions on unpolished and uncoated polymer specimens showed the lowest CoF for UHMWPE and the highest for PEEK (0). At 1N load the CoF of CFR-PEEK PAN was slightly lower than CFR-PEEK pitch, however at higher loads (3N and 5N) both materials showed very similar CoF (0 b,c).

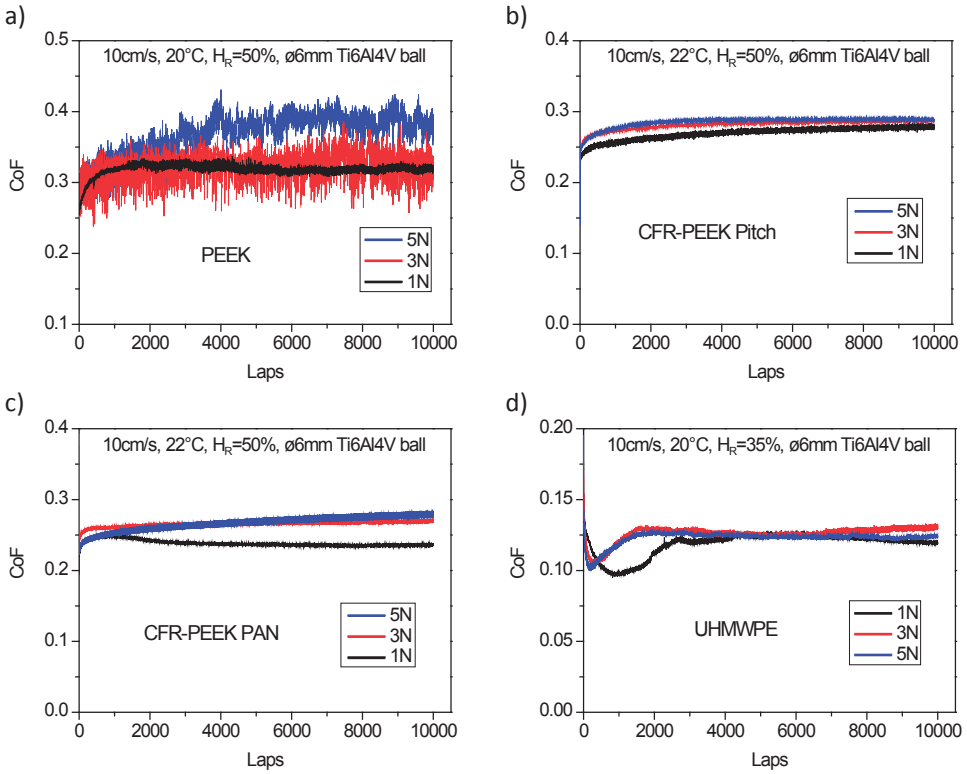

Figure 1. Friction coefficients measured at different loads for a) PEEK, b) CFR-PEEK pitch, c) CFR-PEEK PAN and d) UHMWPE.

Microscopic examination of the polymer samples after the test showed barely visible wear tracks on the UHMWPE surface (Figure 2). The wear track of CFR-PEEK pitch and CFR-PEEK PAN was smaller than of PEEK. The largest wear scar was present on the Ti6Al4V ball surface after tests with UHMWPE; a clearly smaller scar area was visible for PEEK materials. After tests with a UHMWPE disk a transfer film covering the Ti6Al4V ball was observed, which leads to self-lubrication and consequently a low CoF. During tests with PEEK material a large amount of PEEK debris was transferred to the Ti6Al4V surface that resulted in high oscillations of CoF measured for loads of 3N and 5N (Figure 1a). Stiff pitch based carbon fibers embedded in PEEK polymer caused slightly larger wear scar on the Ti6Al4V surface, as compared with the more flexible PAN based fibers.

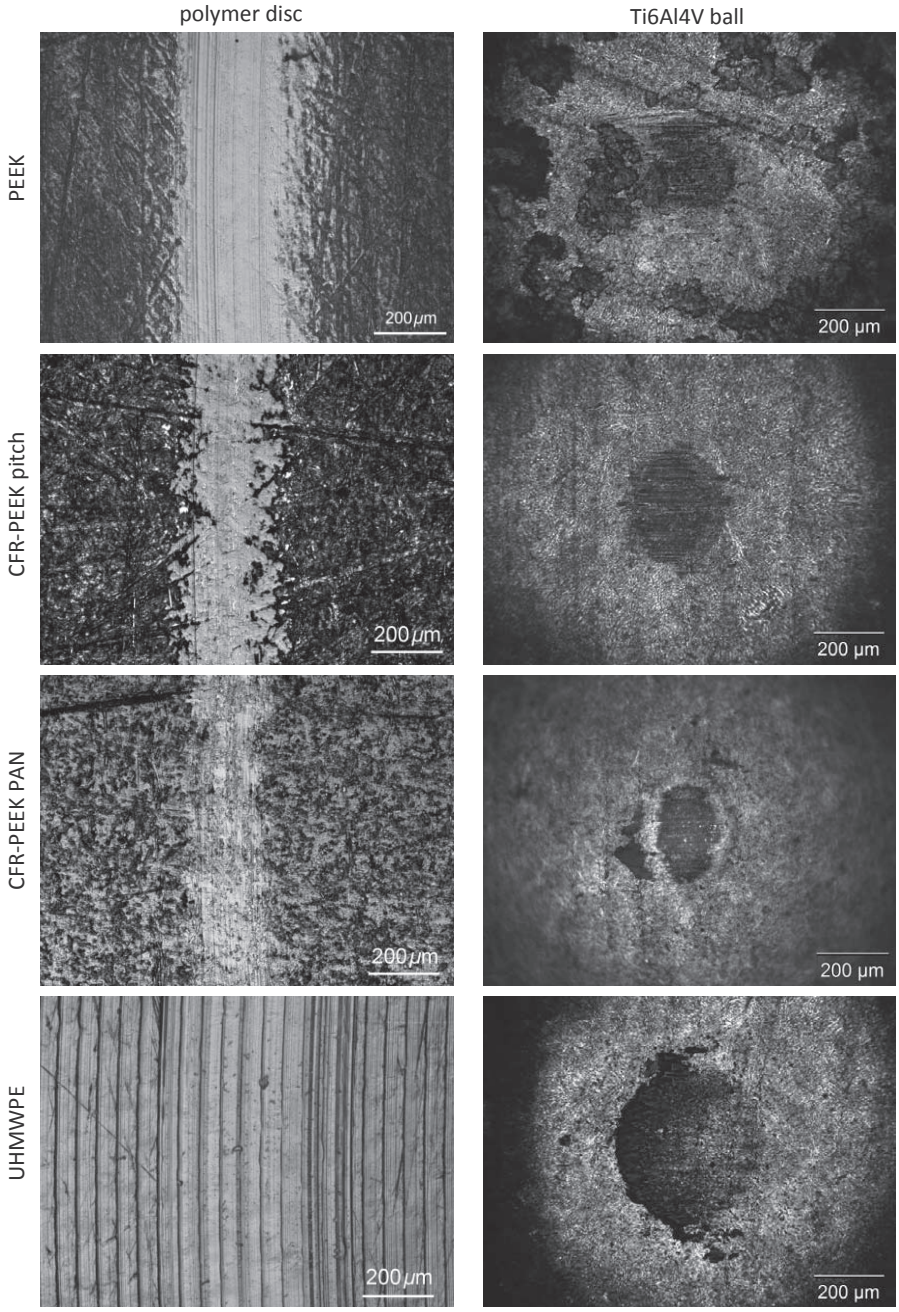

Figure 2. Micrographs of wear tracks on uncoated PEEK, CFR-PEEK pitch, CFR-PEEK PAN and UHMWPE discs and wear scar on Ti6Al4V ball surfaces after tests with 3N load.

Application of the DLC coating on the polymer samples highly reduced CoF for PEEK and both CFR-PEEK materials, as measured in dry conditions (Figure 3). The PEEK material showed larger reduction as compared to CFR-PEEK pitch and CFR-PEEK PAN. For loads of 3N and 5N measured CoF values of PEEK and CFR-PEEK discs were similar to those found for UHMWPE, while for 1N load DLC coated samples showed considerably lower CoF for PEEK and CFR-PEEK than UHMWPE (Figure 1).

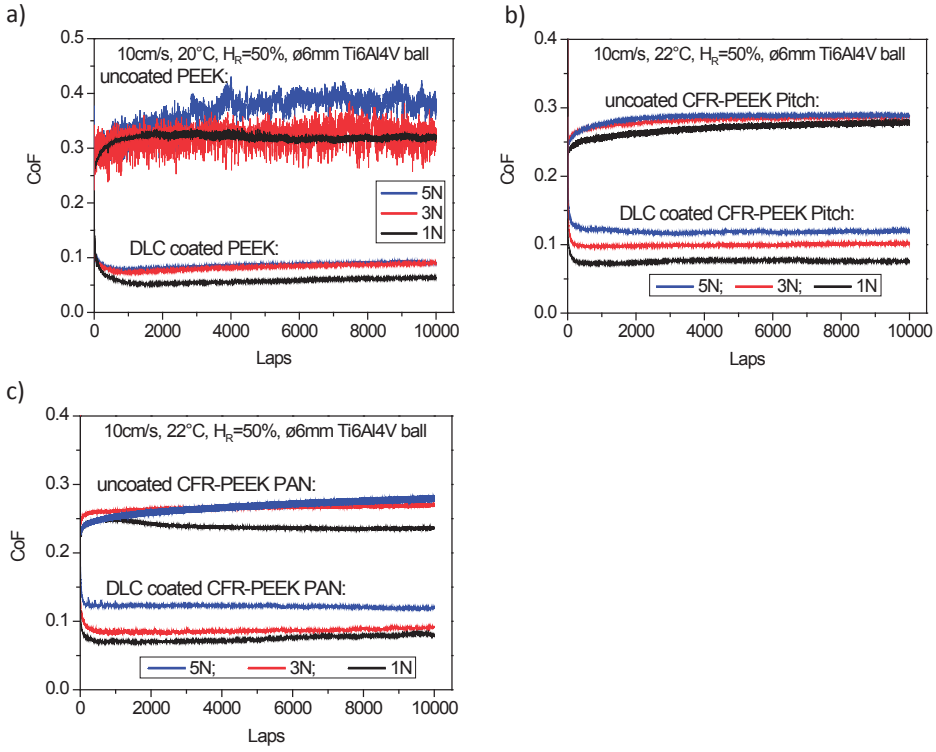

Figure 3. Friction coefficients measured at different loads before and after DLC coating for a) PEEK, b) CFR-PEEK pitch and c) CFR-PEEK PAN.

Examination of the DLC-coated samples after tests indicated only slight scratches on the coating surface, without any signs of film damage or delamination. The wear scars on the Ti6Al4V surface were larger as compared to sliding against uncoated PEEK discs but similar to UHMWPE. The largest wear was visually identified on the Ti6Al4V ball sliding against DLC coated CFR-PEEK pitch, which despite polishing had visibly higher surface roughness than other PEEK grades.

Similarly as in dry tests, CoF was measured under PBS lubrication first for uncoated and afterwards for DLC coated PEEK polymers. The lubrication considerably reduced CoF of uncoated PEEK and CFR-PEEK polymers (Figure 5a) as compared to dry sliding (Figure 1a,b,c). When considering lubricated conditions only, the application of the DLC-coating on PEEK surface resulted in reduced CoF, however no reduction of CoF was measured for CFR-PEEK pitch (Figure 5a, b).

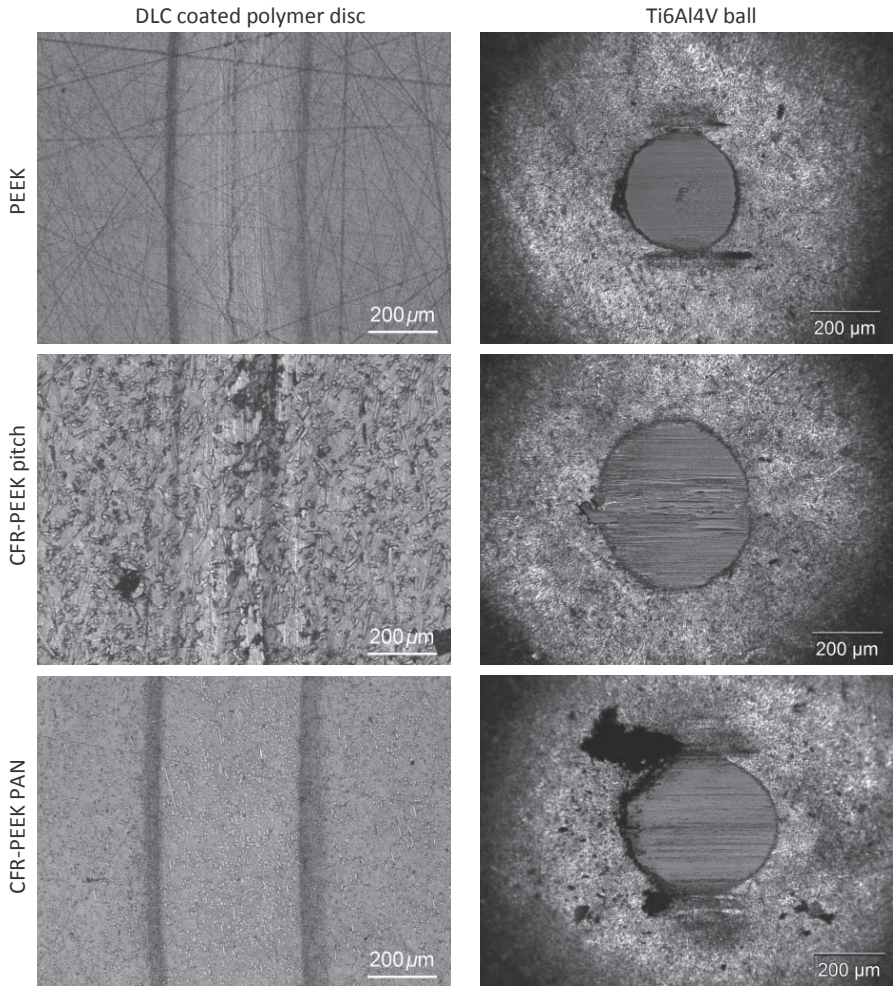

Figure 4. Micrographs of wear tracks on DLC coated PEEK, CFR-PEEK pitch and CFR-PEEK PAN discs and wear scar on Ti6Al4V ball surfaces after dry tests with 3N load

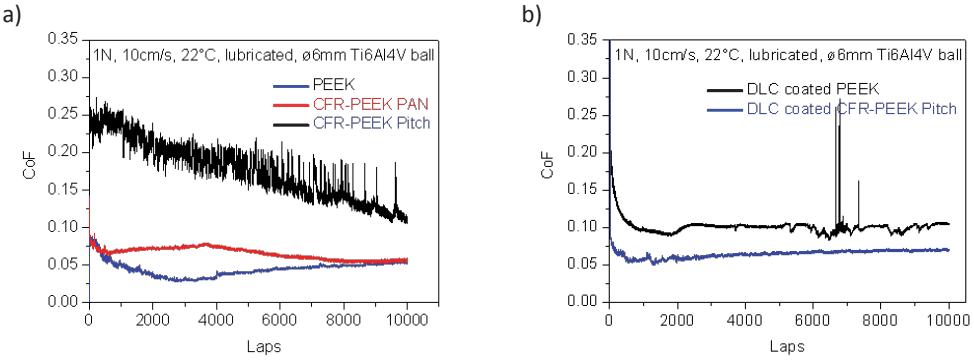

Figure 5. Comparison of CoF under PBS lubrication under 1N load: a) uncoated PEEK, CFR-PEEK PAN and CFR-PEEK pitch polymer discs and b) DLC coated PEEK and CFR-PEEK pitch.

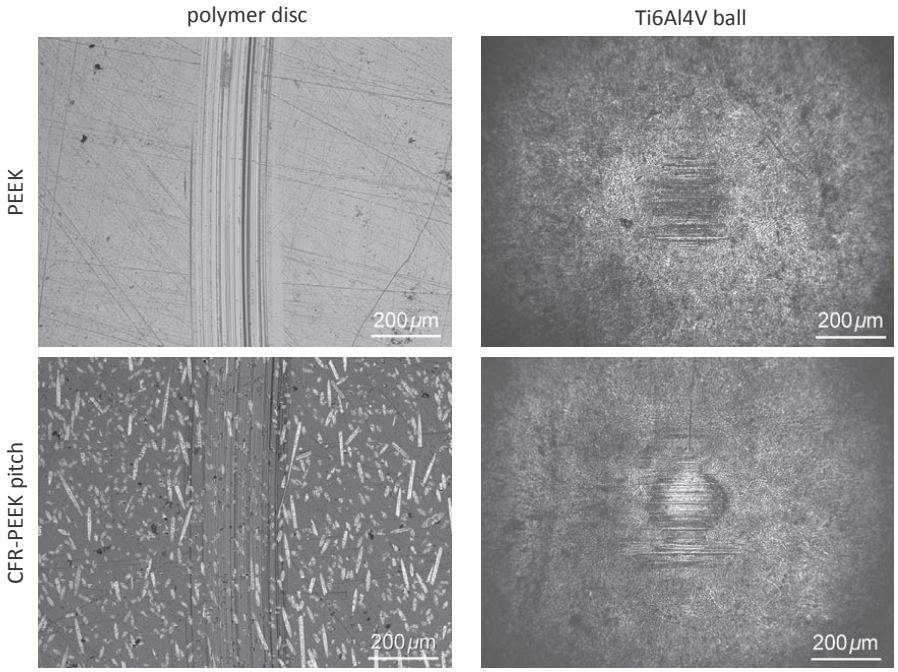

Figure 6. Micrographs of wear tracks on uncoated PEEK and CFR-PEEK pitch discs and wear scar on Ti6Al4V ball surfaces tested in PBS with 1N load.

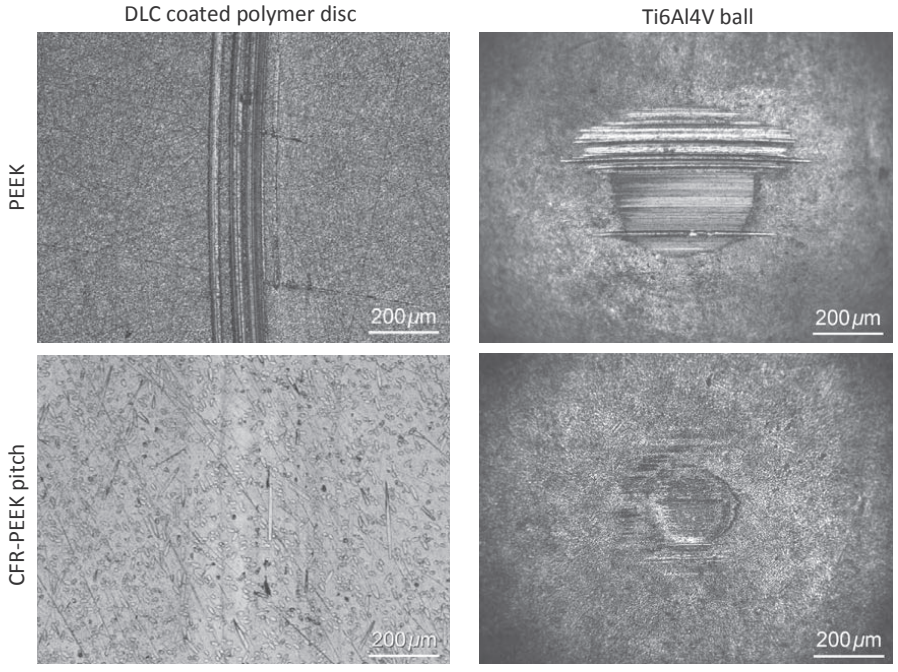

Figure 7. Micrographs of wear tracks on DLC coated PEEK and CFR-PEEK pitch discs and wear scar on Ti6Al4V ball surfaces tested in PBS with 1N load.

The PBS lubrication resulted in reduced wear of the PEEK and CFR-PEEK pitch discs (Figure 6) as compared to dry conditions (Figure 2). Also a slight reduction of the wear scar on the Ti6Al4V ball was observed (Figure 6) and no PEEK debris transfer to the counter surface was present when PBS was used (as opposed to dry sliding - Figure 2).

Differently from the dry tests with DLC coating, analysis of the disc surface tested in PBS lubrication showed some clear surface changes on the DLC-coated PEEK polymer (Figure 7). As no coating damage was observed, most probably a cohesive failure inside the PEEK substrate occurred. This led to uneven surface of the DLC-coating and resulted in highly increased wear of the Ti6Al4V ball - with some visible scratches (Figure 7). Also some high peaks in CoF were observed during the tests between 6 and 8 thousands laps (Figure 5b).

The DLC coating on CFR-PEEK pitch tested in PBS showed large improvement in wear resistance, similarly as in dry conditions. It was indicated by a barely visible wear track on DLC and relatively small wear scar on the Ti6Al4V ball (Figure 7), as compared to dry tests.

Discussion and conclusions

In this study we have examined the potential of deposition of DLC films on PEEK polymers on improving tribological performance of a sliding interface between Ti6Al4V alloy and different PEEK polymers. The tribological measurements using a ball-on-disc test setup in dry conditions showed considerable reduction of the CoF (to values similar or lower to UHMWPE) for all considered PEEK materials. Moreover, a microscopic evaluation of the DLC-coated polymer surfaces showed its very good resistance to wear during dry sliding. On the other hand, the DLC coating in the dry testing conditions caused some wear increase of the Ti6Al4V sphere.

Similar increase in wear resistance due to DLC coating was observed in PBS lubrication for CFR-PEEK pitch. Moreover, also the Ti6Al4V wear was very low in this case. The lubricated tests with DLC-coated PEEK showed however considerable surface changes of the DLC coating, which are probably caused by a cohesive material failure below the surface, as no coating damage was detected. This led to the highly increased wear (with visible scratching) of the Ti6Al4V sphere.

Consistently with the previous experiments (Chapter 5), the ball-on-disc tests in dry conditions with uncoated samples have shown higher friction coefficient for CFR-PEEK pitch than for CFR-PEEK PAN when articulating against Ti6Al4V.

While considering application of the protective DLC coating on a PEEK or any CFR-PEEK surface to improve wear properties of the interface with Ti6Al4V, it is important to stress that in dry conditions wear of the Ti6Al4V counterface was visibly increased. To overcome this limitation coating of the titanium surface with DLC layer might be considered, as DLC on DLC articulation has been demonstrated to have low interface wear and friction (Sheeja et al., 2003).

The presented here results poses some limitations, which should be considered before final selection of materials (and its surface treatment) for the application in the new direct fixation implant is chosen. Due to time restrictions, the results of the

tests with the DLC-coated CFR-PEEK PAN in PBS lubrication as well as other PEEK types under 3N and 5N loads could not be included in this chapter. Interestingly, during initial tests at 3N and 5N loads with DLC coated PEEK and CFR-PEEK pitch under PBS lubrication, a damage of the coating was observed. It might be caused by high adhesion forces between DLC and Ti6Al4V surfaces, but additional tests are needed to confirm these results. Moreover, it should be noted that the ball-on-disc setup was used in this experiment mainly for the sake of determination of influence of DLC coating on tribological properties of the proposed material couples. So it does not reflect the wear conditions expected in the new implant as the customized setup used in Chapter 5.

In this study PBS was chosen as the lubricant, as this solution is relatively easy to obtain and its properties do not change or degrade with time as for example bovine serum. It might be disputable if for example distilled water (Dong et al., 1999; Davim and Marques, 2001; Onate et al., 2001), bovine serum (Wang et al., 1998; Scholes and Unsworth, 2009), Ringers's solution (Gutmanas and Gotman, 2004) or phospholipids (Saikko and Ahlroos, 1997) are not more appropriate to simulate in-vivo environment of the direct fixation implant and this should be further investigated in the future studies.

In summary, the applied DLC coatings provided very good wear resistance to the PEEK and CFR-PEEK polymer surfaces and considerably reduced friction coefficient during dry sliding. Similar positive effect of the coating was observed for CFR-PEEK pitch in the PBS lubricated conditions. Therefore, it is recommended for the new direct fixation implant to use a DLC coating on CFR-PEEK pitch and further to consider use of DLC coating on the to Ti6Al4V to increase its wear resistance.

Acknowledgements

This study was supported by Fonds NutsOhra. Invibio Ltd. (Lancashire, UK) provided PEEK materials for testing.

References

Davim, J. P., et al. (2001). "Evaluation of tribological behaviour of polymeric materials for hip prostheses application." Tribology Letters 11(2): 91-94.

Dearnaley, G., et al. (2005). "Biomedical applications of diamond-like carbon (DLC) coatings: A review." Surface & Coatings Technology 200(7): 2518-2524.

Dong, H., et al. (1999). "Potential of improving tribological performance of UHMWPE by engineering the Ti6Al4V counterfaces." Wear 225: 146-153.

Dowling, D. P., et al. (1997). "Evaluation of diamond-like carbon-coated orthopaedic implants." Diamond and Related Materials 6(2–4): 390-393.

Gutmanas, E. Y., et al. (2004). "PIRAC Ti nitride coated Ti-6Al-4V head against UHMWPE acetabular cup-hip wear simulator study." J Mater Sci Mater Med 15(4): 327-330.

Hallab, N., et al. (2003). "Biomaterial optimization in total disc arthroplasty." Spine (Phila Pa 1976) 28(20): S139-152.

Hauert, R. (2003). "A review of modified DLC coatings for biological applications." Diamond and Related Materials 12(3-7): 583-589.

Joyce, T. J., et al. (2000). "A multi-directional wear screening device and preliminary results of UHMWPE articulating against stainless steel." Bio-Medical Materials and Engineering 10(3-4): 241-249.

Kurtz, S. M. (2004). The UHMWPE handbook : ultra-high molecular weight polyethylene in total joint replacement. Amsterdam ; Boston, Academic Press.

Kurtz, S. M. (2012). Peek Biomaterials Handbook. Amsterdam ; Boston, Academic Press.

Kurtz, S. M., et al. (2007). "PEEK biomaterials in trauma, orthopedic, and spinal implants." Biomaterials 28(32): 4845-4869.

Lu, Z. P., et al. (1995). "On Sliding Friction and Wear of Peek and Its Composites." Wear 181: 624-631.

McKellop, H. A., Rostlund, T., Ebramzadeh, E., Sarmiento, A. (2001). Wear of Titanium 6-4 Alloy in Laboratory Tests and in Retrieved Human Joint Replacements. Titanium in medicine : material science, surface science, engineering, biological responses, and medical applications. D. M. Brunette. Berlin ; New York, Springer: 748-767.

Onate, J. I., et al. (2001). "Wear reduction effect on ultra-high-molecular-weight polyethylene by application of hard coatings and ion implantation on cobalt chromium alloy, as measured in a knee wear simulation machine." Surface & Coatings Technology 142: 1056-1062.

Pei, Y. T., et al. (2010). "Flexible protective diamond-like carbon film on rubber." Scripta Materialia 63(6): 649-652.

Platon, F., et al. (2001). "Tribological behaviour of DLC coatings compared to different materials used in hip joint prostheses." Wear 250(1–12): 227-236.

Reilly, D. T., et al. (1975). "The elastic and ultimate properties of compact bone tissue." J Biomech 8(6): 393-405.

Roy, R. K., et al. (2007). "Biomedical applications of diamond-like carbon coatings: A review." Journal of Biomedical Materials Research Part B-Applied Biomaterials 83B(1): 72-84.

Saikko, V., et al. (1997). "Phospholipids as boundary lubricants in wear tests of prosthetic joint materials." Wear 207(1-2): 86-91.

Scholes, S. C., et al. (2009). "Wear studies on the likely performance of CFR-PEEK/CoCrMo for use as artificial joint bearing materials." Journal of Materials Science-Materials in Medicine 20(1): 163-170.

Sheeja, D., et al. (2003). "Tribological characterization of diamond-like carbon (DLC) coatings sliding against DLC coatings." Diamond and Related Materials 12(8): 1389-1395.

Soininen, A., et al. (2009). "Bacterial Adhesion to Diamond-like Carbon as Compared to Stainless Steel." Journal of Biomedical Materials Research Part B-Applied Biomaterials 90B(2): 882-885.

Tiainen, V.-M. (2001). "Amorphous carbon as a bio-mechanical coating — mechanical properties and biological applications." Diamond and Related Materials 10(2): 153-160.

Wang, A., et al. (1998). "Carbon fiber reinforced polyether ether ketone composite as a bearing surface for total hip replacement." Tribology International 31(11): 661-667.

Wang, H. Y., et al. (2010). "Mechanical and biological characteristics of diamond-like carbon coated poly aryl-ether-ether-ketone." Biomaterials 31(32): 8181-8187.

Chapter 8

In-vivo experiment with the new direct fixation implant

P.K. Tomaszewski[1], S.K. Bulstra[2], P. Buma[3], N. Verdonschot [3,4], G.J. Verkerke[1,4]

[1] Department of Biomedical Engineering, University of Groningen, University Medical Center Groningen, Groningen, The Netherlands.
[2] Department of Orthopaedics, University of Groningen, University Medical Center Groningen, Groningen, The Netherlands.
[3] Orthopaedic Research Laboratory, Department of Orthopaedics, Radboud University Nijmegen Medical Centre, Nijmegen, The Netherlands.
[4] Department of Biomechanical Engineering, Faculty of Engineering, University of Twente, Enschede, The Netherlands.

Introduction

A new design of the direct fixation device for amputated patients was presented in this thesis. The finite element analyses predicted more physiological bone stress distribution and reduced bone failure risk around the new implant as compared to the currently available devices. Cadaver experiments confirmed to a large extend the numerical predictions on reduced strain shielding induced by the new implant. Nevertheless, cadaver experiments and computer simulations are not able to show how non-cemented implants will respond under in-vivo conditions.

To verify in-vivo the theoretical predictions of strain-shielding and strain-adaptive bone remodeling around the new concept of the direct fixation implant we started an animal experiment, in which the stem is fixed in a relatively straight and circular bone. To our knowledge no literature data is available on pre-clinical in-vivo experiments with OPRA system (Integrum AB, Göteborg, Sweden) and ISP implant (ESKA Implants AG, Lübeck, Germany). Therefore animal model selection was based on the literature on testing of orthopaedic implants and available in-house experience (van Loon et al., 1992; Buma et al., 1997; Bullens et al., 2009; Bullens et al., 2010; Biemond et al., 2011; Biemond et al., 2011). A goat model is reported in literature to have a metabolic rate, bone remodelling rate (Spaargaren, 1994; Anderson et al., 1999) and comparable bone healing capacity similar to that of humans (Dai et al., 2005).

The aim of this experiment was to evaluate the overall biological response to the new implant and to verify our previous work relative to strain-adaptive bone remodeling around the new concept of the direct fixation implant.

Materials and methods

Implants

To allow an optimal comparison between the new design and the standard titanium screw fixation, the experiment was designed as an intra-animal comparison of bone response to the new implant and the standard titanium screw fixation implant (Figure 1). The femoral bone was chosen for implantation, as it offers a medullary canal diameter larger than 10 mm, which facilitates assembly of the developed multipart implant.

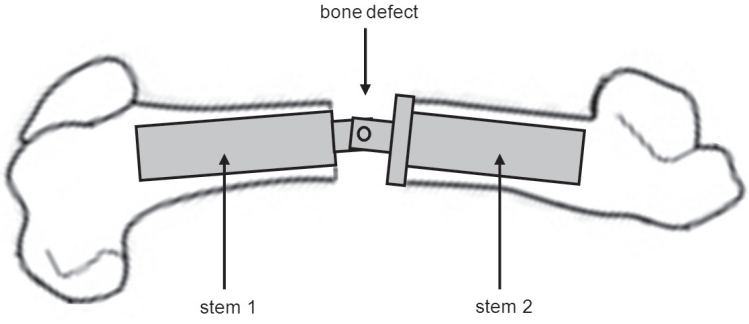

Figure 1. Schematic representation of the animal model. Stem 1 is the standard titanium screw fixation implant; stem 2 is the new design.

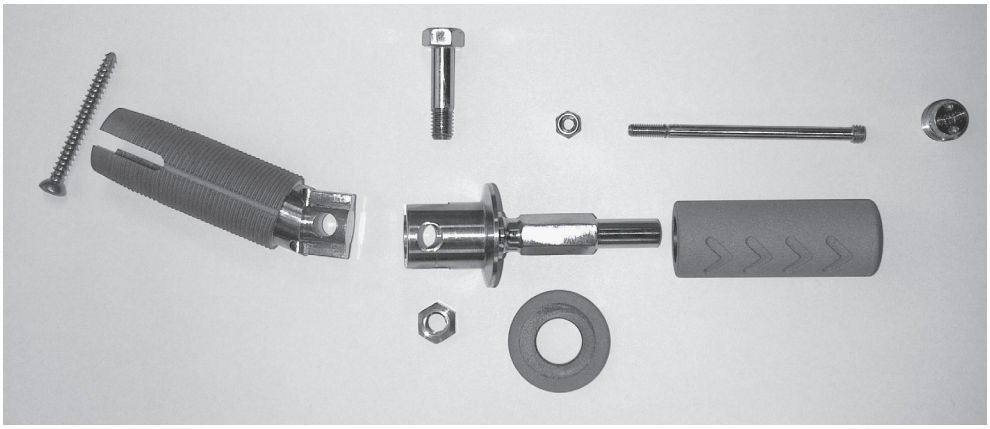

Figure 2. Disassembled goat implant system.

Both control and new implant design were rescaled and connected with a bolt joint (Figure 2). The range of implant sizes and angles between implants were determined based on a geometrical analysis of the goat femora obtained from other animal studies. Initial stability of the new implant was based on the press fit of the porous titanium coated intramedullary sleeve and the collar residing on the bone after osteotomy (Figure 3).

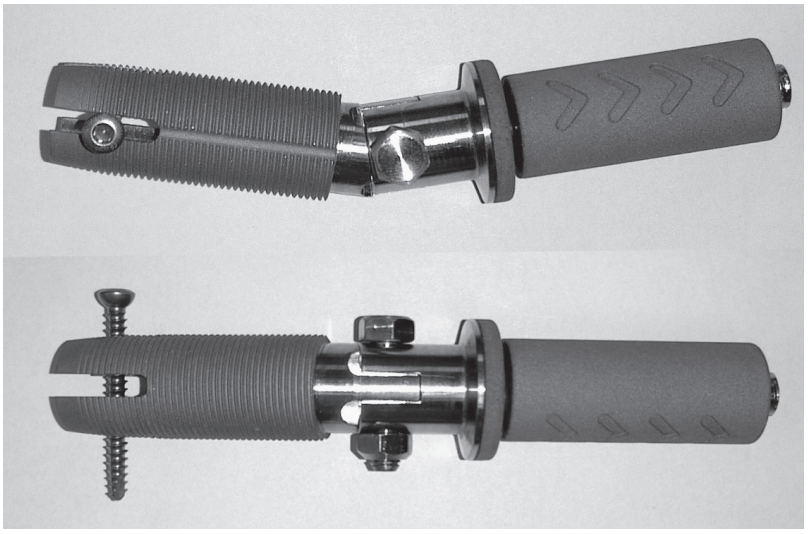

Figure 3. AP (up) and ML (down) view of the goat implant system. The standard titanium screw implant (left) was connected by bolt and nut with the new direct fixation implant (right).

The control titanium screw implant was sandblasted to obtain a realistic surface roughness, which was further comparable to the roughness of the titanium coating deposited on the new implant's surface. To increase initial stability in the bone, a transverse Ti-alloy cortical screw was used.

Surgery

Three Dutch milk goats (female, Capra Hircus Sana; weight: 68, 76 and 81 kg) were included in the study based on a preliminary radiological assessment of bone dimensions. The goats were anesthetized with Propofol (4 mg/kg, B.Brown, Melsungen, Germany) and an additional radiograph was taken to pre-plan the surgery. The animals were operated by an experienced surgeon (S.K.B.) unilaterally using a lateral approach. The right femur was exposed through a 10 cm skin incision. The middle of the femur was determined based on anatomical landmarks and the intra-operative X-ray, and a 2.5 cm segment was marked by small holes in the cortex. An oscillating saw was used to create the osteotomies. After removal of the segment the medullary canal was reamed with standard straight orthopaedic reamers to the desired diameter. Before insertion of the titanium screw implant, a custom tap was used to cut thread in the cortex. A cortical screw (Zimmer, Winterthur, Switzerland) was introduced through the cortex and implant slits to prevent its rotation. The new implant was press-fitted into the femur by slow-hammering into the femur (the distal/proximal orientation of the stems was alternated within the group). The soft tissue layers were placed over the implants and the wound was closed. The study was approved by the university animal ethical committee.

Post-operative treatment and evaluation

Directly after the surgery radiographs were taken to check implant position in the femur. Afterwards animals were placed in a hammock to support the animal's trunk and enable unloading of the operated leg. Two days after the surgery animals were transported to the farm where they were housed individually, while having visual contact with a herd. During four days after surgery animals received Ampicillin (7.5 mg/kg Intervet, Boxmeer, The Netherlands). General animal condition, wound healing and weight-bearing of the implanted leg were assessed on a daily basis. The animals were kept in the hammock for a minimum of 5 days after the surgery. Based on the observation of weight bearing capacity of the operated leg the animal was released to walk freely with other animals.

To asses new bone formation around implants, each goat received fluorochromes. The animals received subcutaneous injections of calcein green solution (25 mg/kg) at 4 weeks post-operatively for 2 days, xylenol orange (30 mg/kg) at 8 weeks post-operatively for 2 days and calceine blue (25 mg/kg) for two days before the goats were euthanized at 26 weeks. After animals were killed by an overdosis of pentobarbital (Euthesate, Ceva Santa Animale, Libourne, France) the operated femur was dissected and all soft tissues were removed. Specimens were fixated in buffered (0.1 M phosphate buffer, pH 7.4) paraformaldehyde (4%) for one week. First, 8 mm thick slices were made perpendicular to the femoral axis with a water-cooled sawing blade and the section surface was stained with fuxine to visualise soft tissues. Afterwards, 60 micrometer slices were embedded in polymethylmethacrylate and adjacent sections were stained with hematoxylin/eosine or were left unstained for fluorescence microscopy.

Results

Clinical observations

In two animals the cross-section of the medullary canal measured during the implantation was much more oval than expected based on previously analyzed goat femora of the same breed. In order to obtain proper initial stability of the control implant PMMA bone cement was used to create additional post-operative stability. In one out of three cases the experiment lasted for the planned period of 26 weeks. This animal returned to normal functional loading after 1 week. Some limited load bearing was observed temporarily 8 weeks after surgery. A radiographic follow-up was performed and tissue samples could be prepared for histological analyses. In the other two cases the goats were prematurely euthanized due to technological failure and implant loosening. In the goat with the technological failure proper fixation of the connecting bolt between implants was not possible, compromising its strength and leading to a mechanical failure at 2 weeks of follow-up. In the second failed case implant loosening and cortical fracture was observed; the animal was sacrificed at 6 weeks.

Radiological evaluation

In the animal with the complete follow-up period of 26 weeks, the positioning of the implant was checked on the radiograph taken directly after the surgery, showing a very accurate fit of the new implant in the proximal femur and some gaps between titanium control implant and the cortex in the distal femur (Figure 4). At week 9, some subsidence of the control titanium implant was observed. Radiographs of the retrieved bones showed complete callus bridging over the defect (Figure 5).

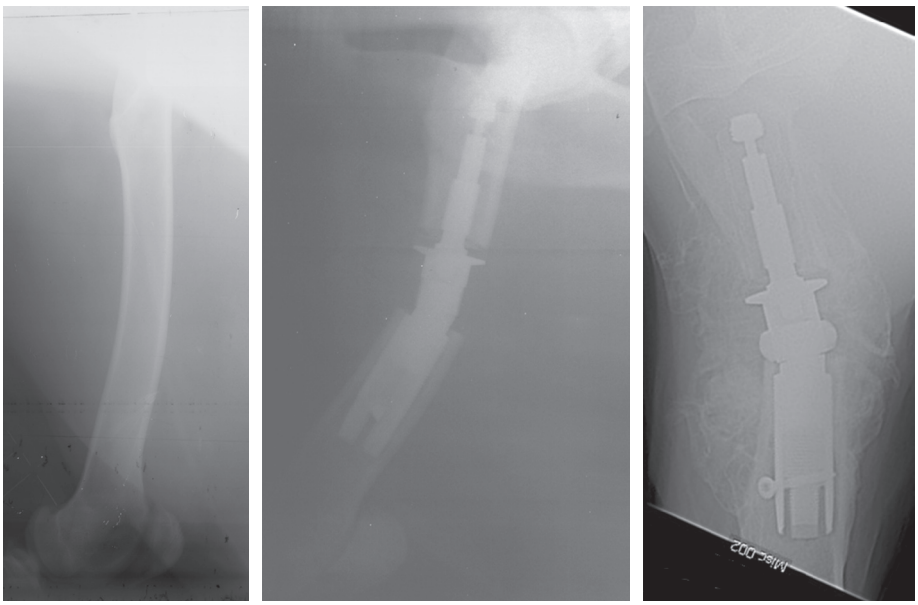

Figure 4. Femoral bone before surgery (left), directly after implantation (middle) and 9 weeks post-operative.

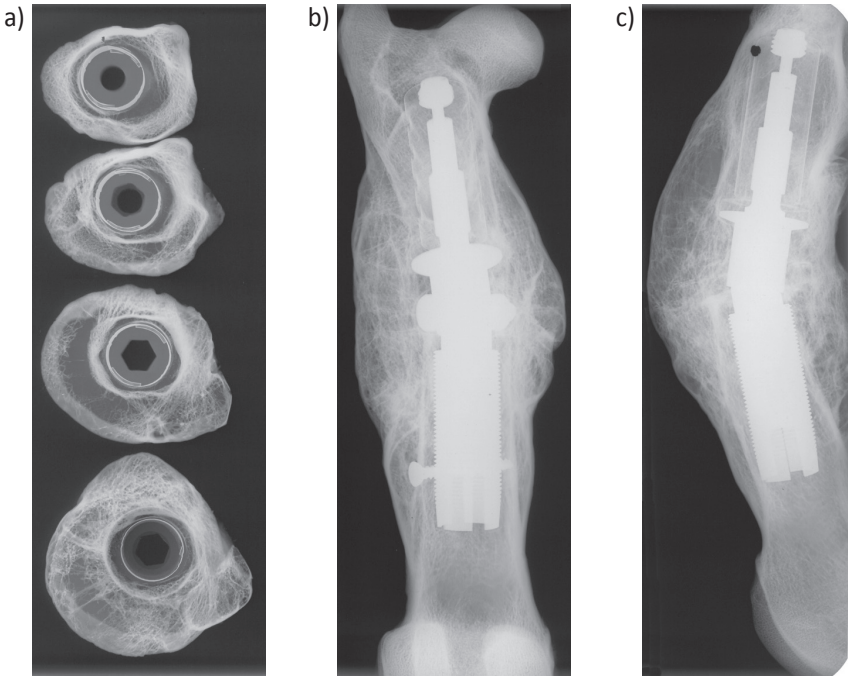

Figure 5. Implanted bone 26 weeks post-operatively: a) cross-section view of the new implant in the femur, b) AP view and c) ML view of the femur.

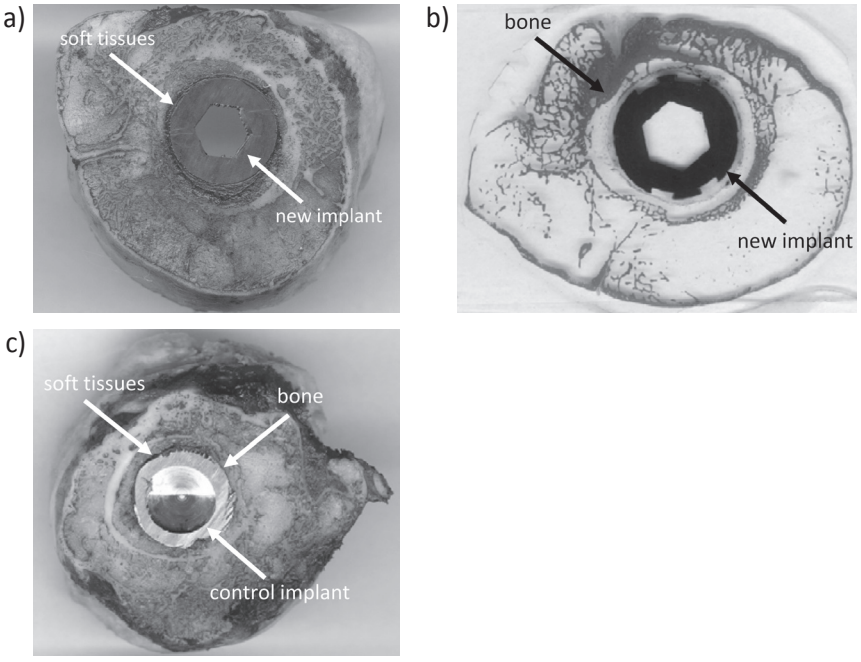

Figure 6. a) Fuchsine stained soft tissues layer around the new implant, b) HE-stained bone around the new implant, but not in direct contact with its surface; c) fuchsine stained soft tissues visible only in limited regions around the control titanium.

Histological evaluation

In all cross-sections the HE and fuchsine staining presented a layer of connective tissue completely surrounding the new implant (Figure 6 a, b). Fuchsine staining of the specimen with the control titanium implant showed both bone apposition around the implant, as well as regions of connecting tissue around the implant (Figure 6 c).

Unstained sections showed locally intense fluorochrome labelling around the new implant (Figure 7). In general the distribution of the calcein green and xylenol showed markedly similar distribution in more peripheral locations, indicating that during the first 8 weeks after implantation active callus formation and remodeling took place. Only at the later stage, 24 weeks post operatively; some bone formation was detected closer to the implant (gap of 600 μm).

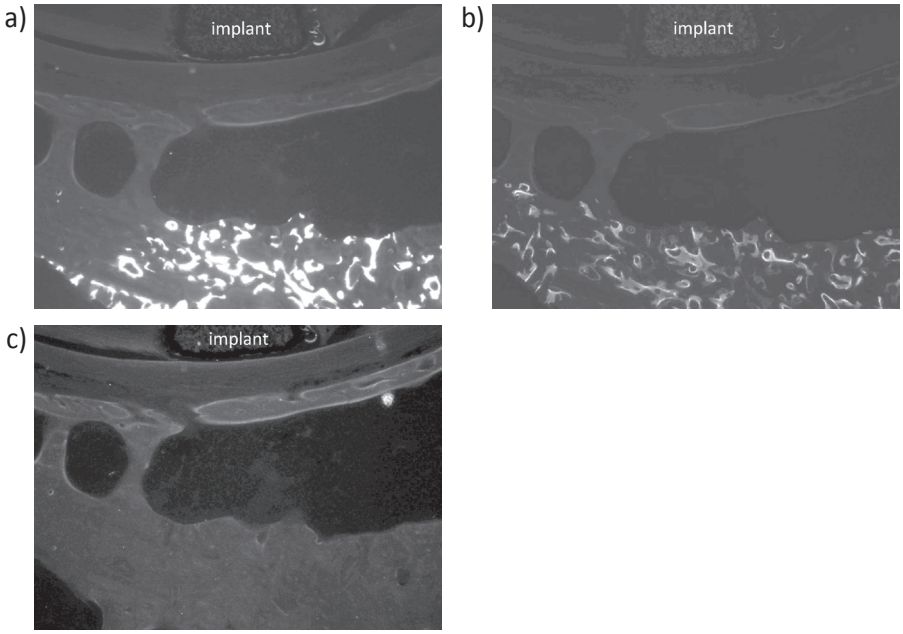

Figure 7. Ongoing bone remodelling of new bone around the new implant demonstrated with a) calceine green, b) xylenol orange and c) calceine blue.

Discussions and conclusions

In this study, we attempted to compare bone response to the new design of the direct fixation implant relative to the standard implant. The experimental design was chosen to enable direct intra-animal comparison of the standard and the new implant with minimized infection risk and animal discomfort. This was obtained by placing implant system in the femoral defect instead of using amputation model with percutaneous implant.

The encountered discrepancy between the sizes of the medullary canal determined from preliminary radiographs and intra-operative measurements, the highly oval cross-section of the medullary canal, and the relatively thin (around 3 mm) and brittle cortical

bone led to major difficulties in obtaining suitable fit and primary stability of the implants. Further, an unfavoured compromise between fit and the amount of removed bone was required, leading to compromised strength of the bone and implant stability. Based on these findings and the results of the animal experiment, further inclusions to the experiment were cancelled. Obviously, the obtained results are not sufficient for any comparison between standard and the new implant. In the single case when the complete follow-up was possible, no bone contact with the new implant surface was discovered during histological analyses. It is expected that large gaps between bone and implant surface and resulting large micromotions are responsible for the inferior osseointegration findings.

We conclude that the chosen animal model showed not to be suitable for this particular application and that another animal model needs to be found in order to proof the benefits of the new design under in-vivo conditions.

Acknowledgements

This study was supported by Fonds NutsOhra. Invibio Ltd. (Lancashire, UK) provided PEEK material for the implants. Eurocoating SpA (Trento, Italy) deposited the titanium coating on the PEEK parts of the implants and sandblasted surfaces of the titanium screw implants. The authors thank Willem van de Wijdeven and Léon Driessen for their technical assistance, Eric de Mulder, Gerjon Hannink and the staff of the central animal facility of the Radboud University Nijmegen for their assistance in the animal experiments.

References

Anderson, M. L., et al. (1999). "Critical size defect in the goat's os ilium. A model to evaluate bone grafts and substitutes." Clin Orthop Relat Res (364): 231-239.

Biemond, J. E., et al. (2011). "Frictional and bone ingrowth properties of engineered surface topographies produced by electron beam technology." Arch Orthop Trauma Surg 131(5): 711-718.

Biemond, J. E., et al. (2011). "Assessment of bone ingrowth potential of biomimetic hydroxyapatite and brushite coated porous E-beam structures." J Mater Sci Mater Med 22(4): 917-925.

Bullens, P. H., et al. (2010). "No effect of dynamic loading on bone graft healing in femoral segmental defect reconstructions in the goat." Injury 41(12): 1284-1291.

Bullens, P. H., et al. (2009). "The presence of periosteum is essential for the healing of large diaphyseal segmental bone defects reconstructed with trabecular metal: a study in the femur of goats." J Biomed Mater Res B Appl Biomater 92(1): 24-31.

Buma, P., et al. (1997). "Histological and biomechanical analysis of bone and interface reactions around hydroxyapatite-coated intramedullary implants of different stiffness: a pilot study on the goat." Biomaterials 18(18): 1251-1260.

Dai, K. R., et al. (2005). "Repairing of goat tibial bone defects with BMP-2 gene-modified tissue-engineered bone." Calcif Tissue Int 77(1): 55-61.

Spaargaren, D. H. (1994). "Metabolic rate and body size: a new view on the 'surface law' for basic metabolic rate." Acta Biotheor 42(4): 263-269.

van Loon, P. J., et al. (1992). "Intramedullary fixation with screwed, conical stems--unsolicited results from animal experiments." Clin Mater 10(4): 239-242.

Chapter 9

Discussion and Recommendations

In the United States, 30,000-40,000 lower limb amputations are performed annually. An estimated 1.6 million individuals had to live without a limb in 2005; this number is expected to more than double to 3.6 million by the year 2050 (Ziegler-Graham et al., 2008). High technological advancement in limb orthotics increased their functionality. However, the traditional principle of fixation around the amputation stump remains a limiting issue in patients' rehabilitation. In this respect this patient group can be considered as an under-served population.

An alternative is offered by osseointegration, which allows direct anchorage of the external orthosis to the skeletal system. The first generation of transfemoral osseointegrated direct fixation implants originates from different applications of osseointegration, such as dental implantology (OPRA system, Integrum AB, Sweden) or femoral THA component (ISP, ESKA Implants, Germany). These designs, however, are characterized by a sub-optimal biomechanical design, that results in unphysiological loading of the bone tissue leading to adverse bone remodeling and relatively high bone failure risk. Moreover long residual femur remnants are required for implantation. In order to overcome these limiting issues a new approach to realize direct anchorage of the external orthosis to the skeletal system was developed and investigated in this thesis.

Like every product development, the first activity was to evaluate if these problems and restricting issues of the current osseointegrated direct fixation implants, with underlying mechanical origin, indeed exist. It was the first goal of the thesis. For this purpose a FE analysis of the intact femur and femur implanted with models of the OPRA and ISP implants were performed (Chapter 2). The analyses revealed that implantation of percutaneous prostheses had considerable effects on stress and strain energy density levels in bone. This was caused by the implant itself, but also by changed loading conditions in the amputated leg. The ISP design promoted slightly more physiological strain energy distribution (favouring long-term bone maintenance), but the OPRA design generated lower bone stresses (reducing bone fracture risk). Both percutaneous designs showed relatively low safety factor against mechanical failure. Furthermore, we investigated long-term periprosthetic bone changes around both fixation implants using adaptive bone-remodeling simulations in case of immediate post-amputation implantation and implantation after considerable time of socket prosthesis use (Chapter 3). The bone loss caused by prolonged use of socket prosthesis had more severe effects on the ultimate bone quality than adaptation induced by the direct-fixation implants. Nevertheless, both implants showed considerable bone loss, which was more pronounced for the titanium screw implant (OPRA system) than for the porous coated CoCrMo stem (ISP implant). Based on the literature data on the performance of the current direct fixation implants (Chapter 1) and results of the numerical investigation on short and long term influence of the implants on the bone failure risk and remodeling, requirements for the new implant were formulated (Chapter 1).

Next the design of an improved osseointegrated implant was presented to solve the problems mentioned above and considering the formulated requirements as second goal of this thesis. A multi-component system, composed of a metallic core (Ti6Al4V alloy) and an outer sleeve (PEEK Motis – Invibio Ltd., Lancashire, UK) with an elastic modulus comparable to the cortex was proposed (Chapter 4).

The design should restore the natural load transfer in the midshaft of a femur. To enhance distal load transfer in-between the implant and the osteotomy of the femur remnant, a collar with a layer of elastic material was added to the stem (Figure 1). Further, a low amplitude sliding motion between the inner and the outer part of the implant aims to decouple axial and transverse load and minimize shear stresses at the bone implant interface. A porous titanium coating is plasma sprayed on the PEEK surface in direct contact with the bone. Additionally, the new design is much shorter than the currently used implants to allow implantation in patients with short residual femur remnants.

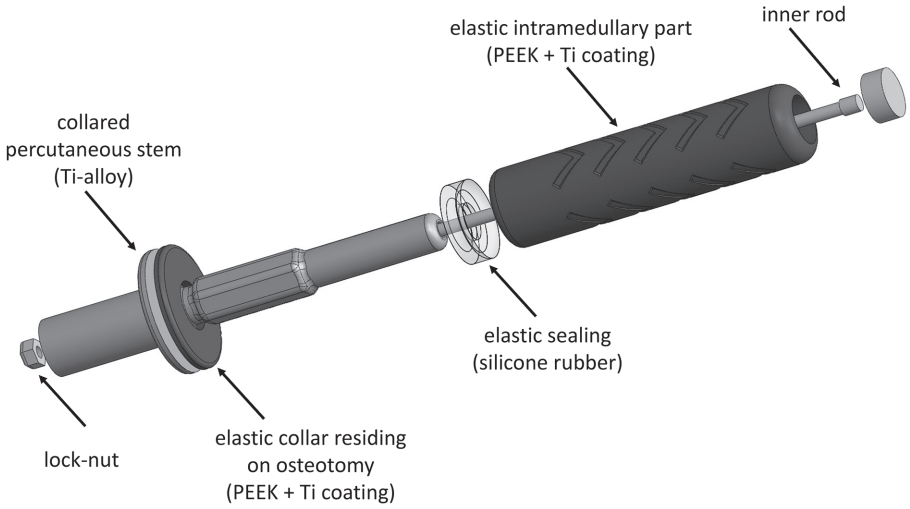

Figure 1. Design on the new direct fixation implant.

In the next development phase, according with the third aim of the thesis, we investigated if the defined requirements were met.

Requirement I states that the intramedullary stem should be fixed in the bone by means of direct bone ingrowth. Since the design is coated with a plasma-sprayed porous titanium coating, we expect a good osseointegration. The same type of coating on the PEEK polymer has been previously investigated and is applied as acetabular component, which currently undergoes an early clinical phase (Latif et al., 2008; Vedova, 2008; Robotti, 2009; Robotti, 2009).

According to requirement I all used materials must be biocompatible and suitable for a long-term application inside the human body. Both Ti6Al4V and PEEK Motis (plasma-sprayed with Ti) are already used in orthopaedics. Similarly, silicone rubber proposed as an elastic seal in the implant is also commonly used for medical applications. We performed an animal experiment to check this requirement and based on preliminary

results we expect that this requirement will be fulfilled. However, we cannot prove it yet; long-lasting animal and clinical experiments are required to investigate it.

Requirement II states that a close fitting of the stem and bone must be obtained to obtain initial implant stability and enable osseointegration. Similarly as the current osseointegrated implants, the intramedullary part of the new implant has a circular cross-section, which in combination with diameters between 13 and 23 mm (recommended are 11 different sizes in steps of 1 mm) will ensure accurate fit in the bone.

Requirement III states that the intramedullary part of the new implant should be not longer than 8 cm. As the intramedullary length of the new design is 7.5 cm, this requirement is fulfilled and the new implant will be applicable for patients with a short residual femur.

Requirement IV asserts that bone overload by the implant must be avoided. The FE analysis predicted that the new design provides a close to physiological distribution of stresses in the bone and a lower bone failure risk during normal walking as compared to the OPRA and the ISP implants (Chapter 4). These results indicate an improvement in the mechanical safety during normal walking as compared to the OPRA and the ISP devices. This improvement was not observed, when a forward falling load was applied to the device, which suggest that the shorter, collared design performs better during a normal loading regime (walking) than bending (fall). To minimize a potentially adverse effect of the bending overload on the periprosthetic bone, it is highly recommended to use a failsafe mechanism preventing excessive loads to be transferred from the external prosthesis to the implant.

Requirement V states that the design should minimize adverse periprosthetic bone remodeling. The simulated stress distribution around the new implant was close to physiological and consequently bone remodeling simulations did reveal a very favourable bone remodelling situation around the new design, which is in contrast to the OPRA and the ISP implants that induce considerable bone loss in the distal end of the femur (Chapter 3 and 4). Subsequent experimental measurement of cortical strains on human cadaver femora, both intact and implanted with a generic standard implant and the new implant (Chapter 5) revealed significantly less strain shielding around the novel implant design than around the standard implant. These findings indicate that the new implant will fulfil this requirement; however, it can be proven only in long-term animal and clinical studies.

Requirement VI states that the fixation implant should withstand fatigue loads characteristic for standard walking. A finite element analysis with normal walking loads (similarly as in Chapter 2) was performed to check this requirement. The implant was subjected to walking loads of a person with 100 kg body mass and stresses in its components were determined. As the resulting stress levels were below the endurance limits of the applied materials, it is expected that the implant will provide good long-term performance. Nevertheless, fatigue tests are necessary to confirm this prediction and to show implant endurance over the desired 36.5 million cycles (20 years of usage).

Requirement VII stated that the implant should be safe for patients with body mass up to 100 kg. For this purpose the failure risk was calculated for the new implant while normal walking loads were applied (similarly as in Chapter 2). The safety factor

appeared to be higher than 2. This indicates that the proposed implant should be safe for the patients with a body mass of 100 kg.

Requirement VIII involves minimization of wear debris generated by the new implant. Tribological measurements were performed on the fretting performance of various combinations of PEEK, CoCrMo and Ti6Al4V materials (Chapter 6). CFR-PEEK pitch/Ti6Al4V materials are capable to generate lower wear than the control UHMWPE/CoCrMo interface; however the friction coefficient is relatively high. As an alternative, a CFR-PEEK pitch/CoCrMo material couple was proposed due to its reasonable compromise between low friction and good wear properties. Aiming to further optimize tribological properties of the Ti6Al4V alloy and different PEEK polymers, potential application of diamond-like carbon coatings on the PEEK materials was examined (Chapter 7). The applied DLC coatings provided a very good wear resistance of the PEEK and CFR-PEEK polymer surfaces and a considerably reduced friction coefficient during dry sliding (comparable to UHMWPE). A similar positive effect of the coating was observed for CFR-PEEK pitch in PBS-lubricated conditions. It is important to notice however, that in dry conditions the DLC coating visibly increased the wear of the Ti6Al4V surface, whereas no difference was visible for lubricated tests. To minimize wear debris formation in the new direct fixation implant, it is recommended to use a DLC coating on CFR-PEEK pitch and further to consider the application of a DLC coating on Ti6Al4V as well. The above results give high confidence that generation of wear particles in the new design will not lead to aseptic loosening. Nevertheless, as it is very difficult to exactly represent the in-vivo conditions in the wear experiments, the final confirmation can only be obtained in-vivo.

Requirement IX states that the percutaneous connector should minimize the infection risk. This issue was, however, beyond the scope of this study, which focused on biomechanics of osseointegrated direct fixation implants. Current implants use a polished percutaneous part, so that soft tissue irritation is minimized and hygiene is facilitated. Further, it is recommended to investigate a concept of electrodes that apply a low current application to the percutaneous pin, as has been previously introduced and investigated with pin-track devices (van der Borden et al., 2007). It appears that this system combined with a concept of a perforated structure allowing a permanent soft tissue closure around the percutaneous pin (Pendegrass et al., 2006) can be capable of minimizing the infection risk around the new implant.

Requirement X states that implantation of the prosthesis must be possible by means of a surgical procedure that should not be more complex than that of total hip arthroplasty. The surgical procedure was analyzed during the in-vivo experiments (Chapter 8). The complexity of implantation of the new device is comparable to standard orthopaedic practice. From a technical point of view, the new implant can be placed either in a single or two stage implantation procedure. The former could considerably reduce clinical effort, patient burden and rehabilitation time, therefore it is recommended to investigate the clinical feasibility of this single stage implantation procedure.

According to **requirement XI** the manufacturing of the new implant must be economical. The in-vivo experiment allowed valuable insight into the feasibility of the

manufacturing of the new implant. Based on the cost of the implant prototypes for animal use, the economical cost of the implant is comparable to standard total joint replacement prostheses.

This thesis presented the early pre-clinical development phase of a new osseointegrated direct fixation implant, in which its feasibility and potential improvement over the existing solutions was investigated. The following tasks are recommended to complete this phase of development.

Firstly, a fatigue test, equivalent to the one used in case of hip stems (Standardization, 2010), is necessary to test the endurance properties of the implant.

In parallel, it is recommended to investigate the skin penetrating part of the implant, which must assure minimal infection risk and discomfort of the patient.

Finally, to present efficacy of the new direct fixation implant, an in-vivo experiment is recommended. For this purpose, an amputation animal model could be used to model closely the clinical situation. An alternative to the applied goat model, might be offered by a sheep model as presented in recent amputation studies (Shelton et al., 2011).

We are convinced that the new osseointegrated implant, developed within the frame of this thesis has a potential to overcome the limiting biomechanical issues of the current fixations and will allow more patients to benefit from a direct fixation of external prosthetic systems.

References

Latif, A. M., et al. (2008). "Pre-clinical studies to validate the MITCH PCR Cup: a flexible and anatomically shaped acetabular component with novel bearing characteristics." J Mater Sci Mater Med 19(4): 1729-1736.

Pendegrass, C. J., et al. (2006). "Development of a soft tissue seal around bone-anchored transcutaneous amputation prostheses." Biomaterials 27(23): 4183-4191.

Robotti, P., Vedova, A., Fabbri, A., Zappini, G., Migliaresi, G. (2009). Static and Fatigue Tensile Properties of Titanium-Coated Carbon Fibre-Reinforced PEEK. 22nd European Conference on Biomaterials. Lausanne, CH.

Robotti, P., Vedova, S., Fabbri, A., Migliaresi, C., Fontanari, V. (2009). Plasma Spray Deposition of Titanium and Hydroxyapatite on PEEK and CFR-PEEK. Society for Biomaterials Annual Meeting. San Antonio, Texas.

Shelton, T. J., et al. (2011). "Percutaneous osseointegrated prostheses for amputees: Limb compensation in a 12-month ovine model." J Biomech 44(15): 2601-2606.

Standardization, I. O. f. (2010). Implants for surgery - Partial and total hip joint prostheses Part 4: Determination of endurance properties and performance of stemmed femoral components. 7206-4:2010.

van der Borden, A. J., et al. (2007). "Prevention of pin tract infection in external stainless steel fixator frames using electric current in a goat model." Biomaterials 28(12): 2122-2126.

Vedova, S., Robotti, P., Fabbri, A., Zeni, D., D'Amato, M., Monelli, B. (2008). Effects of Plasma Spray HA coating process onto mechanical properties of PEEK and Carbon Fiber Reinforced PEEK. 8th World Biomaterials Congress 2008. Amsterdam, The Netherlands.

Ziegler-Graham, K., et al. (2008). "Estimating the prevalence of limb loss in the United States: 2005 to 2050." Arch Phys Med Rehabil 89(3): 422-429.

Summary

Leg amputation is a permanent disfigurement, which has a big impact on patients' mobility, professional activity, lifestyle and quality of life. Prosthetic systems allow to overcome a part of the functional loss of the leg. High technological advancement in limb orthotics has increased prosthetic functionality. However, the traditional principle of a fixation around the amputation stump remains a limiting issue in patients' rehabilitation. Stump pain, soft-tissue damage, lack of appropriate control and fitting problems are common complications experienced by socket prostheses users.

An alternative solution to the conventional stump-socket attachment of external leg prostheses is to fixate the prosthesis directly to the bone of the remnant of the leg, commonly referred to as fixation by osseointegration. Direct attachment of an artificial limb to the skeletal system allows overcoming skin problems and fitting difficulties characteristic to the conventional socket fixation. Furthermore, it provides a better control of the prosthetic limb and consequently leads to increased prosthetic use, better mobility and lower energy consumption. For those reasons osseointegrated implants gain more clinical and scientific attention. Available literature indicates, however, that rehabilitation with osseointegrated direct fixation implants still remains a challenging treatment due to restraining issues such as: periprosthetic bone loss, bone or implant failures and - infections around the percutaneous pin.

In Chapter 1, based on the overview of the available literature about direct fixation implants for amputated patients, goals of the project and requirements for an improved design were formulated.

The first goal of this thesis was to evaluate mechanical problems and restricting issues of the current osseointegrated direct fixation implants.

In Chapter 2 two percutaneous trans-femoral implants, the OPRA system (Integrum A.B.) and the ISP Endo/Exo prosthesis (ESKA Implants A.G.) were assessed by means of finite element (FE) analysis on the probability of bone failure and stem-bone interface mechanics both early post-operative (before bony ingrowth) and after full bone ingrowth. Moreover, mechanical consequences of implantation of those devices in terms of changed loading pattern within the bone and potential consequences on long-term bone remodeling were studied using finite element models that represented the intact femur and implants fitted in amputated femora. Two experimentally measured loads from a normal walking cycle were applied. The analyses revealed that implantation of percutaneous prostheses had considerable effects on stress and strain energy density levels within the periprosthetic bone. This was caused by the implant itself, but also by changed loading conditions in the amputated leg. The ISP design promoted slightly more physiological strain energy distribution (favouring long-term bone maintenance), but the OPRA design generated lower bone stresses (reducing bone fracture risk). Both percutaneous designs showed relatively low safety factors against mechanical failure.

Subsequently, in Chapter 3, we investigated long-term periprosthetic bone changes around currently used types of fixation implants using two different initial conditions, namely immediate post-amputation implantation and the conventional implantation

after considerable time of socket prosthesis use. We assessed the difference in bone remodelling response the implants provoked and if it could lead to premature bone fracture. Generic CT-based FE models of an intact femoral bone and amputated bone implanted with models of the OPRA system and the ISP Endo/Exo prosthesis were created for this study. Adaptive bone-remodeling simulations used the heel-strike and toe-off loads from a normal walking cycle. The bone loss caused by prolonged use of a socket prosthesis had more severe effects on the ultimate bone quality than adaptation induced by the direct-fixation implants. Both implants showed considerable bone remodeling; the titanium screw implant (OPRA system) provoked more bone loss than the porous coated CoCrMo stem (ISP implant). The chance of the peri-prosthetic bone fracture remained higher for the post-socket case as compared to the direct amputation cases. We concluded that both direct- fixation implants lead to considerable bone loss and that bone loss is more severe after a prolonged period of post-socket use. Hence, from a biomechanical perspective it is better to limit the post-socket time and to re-design direct fixation devices to reduce bone loss and the probability of peri-prosthetic bone fractures.

In accordance with the second aim of the thesis, the results of the analysis of the currently available direct fixation implants were used to develop a concept of the improved osseointegrated implant, which was presented in Chapter 4. A multi-component system, composed of a metallic core and an outer sleeve with an elastic modulus comparable to the cortex, will restore the natural load transfer in the midshaft of a femur better than traditional designs. To enhance distal load transfer in-between the implant and the osteotomy of the femur remnant, a collar with a layer of elastic material was added to the stem. Further, a low amplitude sliding motion between the inner and the outer part of the implant was designed to decouple axial and transverse load and minimize shear stresses at the bone implant interface. To obtain osseointegration between the bone and the implant a porous titanium coating is plasma sprayed on the polyetheretherketone (PEEK) polymer surface in direct contact with the bone. Additionally, the new design is much shorter than the currently used implants to allow implantation in patients with short residual femur remnants. We hypothesized that this design would reduce the peri-prosthetic bone failure risk and adverse bone remodeling by an improved load transfer from prosthesis to femur. Generic CT-based FE models of an intact femur and amputated bones implanted with the new implant and (two traditional designs and one new design) were created and loaded with a normal walking and a forward-fall load. The strain adaptive bone remodeling theory was used to predict long-term bone changes around the implants and the periprosthetic bone failure risk was evaluated by the von Mises stress criterion. The results showed that the new design provides closer to physiological distribution of stresses in the bone and lower bone failure risk for normal walking as compared to the OPRA and the ISP implants. Consequently, the bone remodeling simulations did not reveal any overall bone loss around the new design, as opposed to the other two implants, which induce considerable bone loss in the distal end of the femur.

In Chapter 5 we used experimental and FE models to verify that the novel concept produce a more physiological strain distribution in the bone as compared to a standard

titanium implant. Cortical strains were measured experimentally on human cadaver femora, both intact and implanted with a generic standard implant and a prototype of the new implant. Three load configurations were considered, simulating heel strike, toe off and one leg stance. A FE model derived from computed tomography data was used to calculate strains in the intact bone and the bone with the two implant types. Significant strain shielding occurred around both implant types, albeit that for the novel design strain shielding was generally less. Significant differences in strain shielding between both implant types were obtained for heel strike at the distal ($p < 0.04$) and the middle level ($p < 0.03$), as well as for the one leg stance at the middle level ($p < 0.03$) showing 21-29% less strain shielding for the new implant in these cases. FE model results were in agreement with the experimental findings: more strain shielding for the standard implant as compared to the novel design. In fact, the benefit of the new design was bigger in the simulations as compared to the experimental measurements, which was attributed to the idealized collar-cortex fit in the FE model of the new design which was not obtained in the experiments. The conclusion of the study was that the new implant has a potential to increase distal load transfer to the femur and reduce strain shielding as compared with the standard implant.

In Chapter 6, we investigated wear debris generation related to the new implant. Tribological measurements of the fretting performance of various combinations of the PEEK polymers, with CoCrMo alloy and Ti6Al4V alloy indicated that CFR-PEEK pitch/Ti6Al4V materials are capable to generate lower wear than the control UHMWPE/CoCrMo interface, however with relatively high friction. As an alternative, CFR-PEEK pitch/CoCrMo material couple was proposed due to its reasonable compromise between low friction and good wear properties.

Chapter 7 aimed to investigate the potential of diamond-like carbon (DLC) coatings on the PEEK materials to optimize the tribological performance of the Ti6Al4V alloy articulating against different PEEK polymers. The applied DLC coatings provided a very good wear resistance to the PEEK and CFR-PEEK polymer surfaces and a considerably reduced friction coefficient during dry sliding (to values similar or lower than UHMWPE). A similar positive effect of the coating was observed for CFR-PEEK pitch in PBS lubricated conditions. Therefore, it is recommended for the new direct fixation implant to use a DLC coating on CFR-PEEK pitch and further also to consider use of DLC coating on Ti6Al4V to increase its wear resistance.

In Chapter 8, an in-vivo experiment was performed to evaluate overall biological response of bone tissue and to verify FE predictions relative to strain-adaptive bone remodeling around the new implant. Although the outcomes of the experiment did not allow to realize this goal, the experiment gained valuable insight into manufacturing feasibility of the new implant and the complexity of the surgical procedure involving implantation of the new fixation device.

The last chapter (Chapter 9) discussed the results obtained in this thesis in the context of the defined design requirements (Chapter 1). The performed studies demonstrate the feasibility to realize the new osseointegrated direct fixation implant, which offers improvements over the existing devices, in terms of reduced bone failure risk and adverse bone remodeling. It also allows to treat patients with short bone

remnants due to reduced stem length. In order to complete this phase of development it is recommended to perform fatigue tests of the implant, to investigate the infection risks due to the skin penetrating part of the implant and finally to study the efficacy of the new implant in-vivo.

In conclusion, the new osseointegrated implant, developed within the framework of this thesis has the potential to overcome many of the limiting biomechanical issues of the current fixations and will allow more patients to benefit from a direct fixation of external prosthetic systems.

Patent summary

Patent summary

Title: OSSEOINTEGRATION SYSTEM FOR A LONG BONE

Application number: WO2010NL50614 20100921

Priority number: EP20090171013 20090922; US20090250886P 20091013

Date of publication: 23.03.2011

Date of filling: 22.09.2009

Inventor(s): Tomaszewski Pawel Krzysztof [NL]; Verkerke Gijsbertus Jacobus [NL]; Verdonschot Nicolaas Jacobus Joseph [NL]; Bulstra Sjoerd Klaas [NL]

Applicant(s): Rijksuniversiteit Groningen [NL]; Academisch Ziekenhuis Groningen [NL]; Stichting Katholieke Universiteit [NL]; Tomaszewski Pawel Krzysztof [NL]; Verkerke Gijsbertus Jacobus [NL]; Verdonschot Nicolaas Jacobus Joseph [NL]; Bulstra Sjoerd Klaas [NL]

Representative: Hatzmann, Martin et al., Vereenigde

Abstract: An osseointegration system (1) for a long bone (2) comprises: - a sleeve system comprising at least two osseointegrated sleeves (4,) being mutually uncoupled in the sense that respective ones of the sleeves do not prevent one another to perform transverse displacements relative to one another; - a stem (6) arranged for being, in said operation condition, received within the at least two osseointegrated sleeves in such manner that at least low amplitude to-and-fro axial sliding displacements of the stem relative to said sleeves are allowed; - at least one fitting collar (7); and - retaining means (9) arranged for realizing that in said operation condition the stem is retained by the long bone.

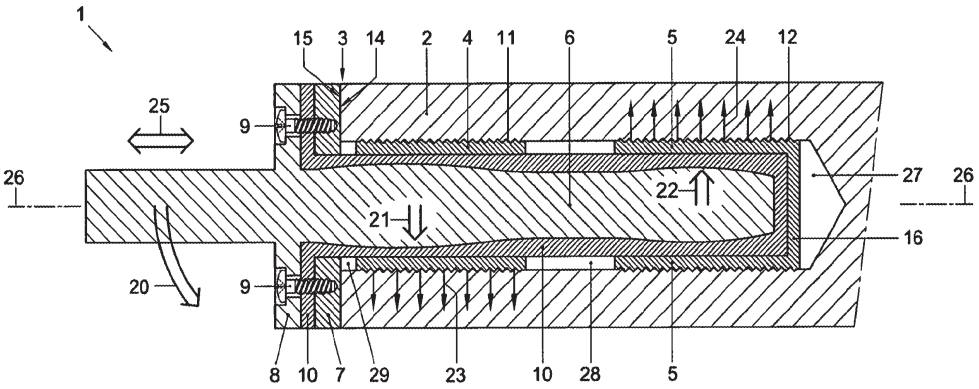

Figure 1

Samenvatting

Een beenamputatie betekent een permanente misvorming van het lichaam, met een grote impact op de mobiliteit, mogelijkheden tot werken, de lifestyle en de kwaliteit van leven van patiënten. Prothesesystemen kunnen het functieverlies van het been deels compenseren. Door de grote technologische vooruitgang op het gebied van externe beenprothesen is de functionaliteit van dergelijke systemen sterk toegenomen. Echter, het traditionele principe van een fixatie rondom de amputatiestomp beperkt de revalidatie. Stomppijn, beschadiging van de zachte weefsels, het gebrek aan adequate bewegingscontrole en montageproblemen zijn daarbij veelvoorkomende problemen.

Een alternatief voor de conventionele stomp-kokerbevestiging van externe beenprothesen is de directe bevestiging van de prothese aan het bot van de stomp. Deze bevestingsmethode door middel van botingroei wordt vaak aangeduid met de term 'osseointegratie'. Direct bevestiging van kunstmatige ledematen aan het skelet minimaliseren de huidproblemen en montagemoeilijkheden die zo kenmerkend zijn voor de conventionele kokerfixatie. Deze methode biedt bovendien een betere controle over de prothese en leidt daardoor tot toename van het prothesegebruik, en dus tot hogere mobiliteit van de patiënt bij een lager energieverbruik. Daarom krijgen osseointegratie-implantaten steeds meer klinische en wetenschappelijke aandacht. Uit de literatuur blijkt echter nog steeds dat revalidatie met zo'n implantaat een uitdagende behandeling is. Complicaties zoals botverlies, breuk van bot of implantaat en infecties rond de percutane pin spelen daarbij een grote rol. In Hoofdstuk 1 worden op basis van een overzicht van relevante beschikbare literatuur over osseointegratie-implantaten, de doelen voor het project en de vereisten aan een verbeterd ontwerp geformuleerd.

Het eerste doel van dit proefschrift was om de mechanische problemen van de huidige osseointegratie-implantaten te evalueren.

In Hoofdstuk 2 zijn twee osseointegratie-implantaten, het OPRA systeem (Integrum AB) en de ISP Endo / Exo prothese (ESKA Implantaten AG) beoordeeld op de kans op het falen van de prothese-bot-interface, zowel in de vroege post-operatieve fase (vóór integratie, net na de implantatie) als na volledige botingroei. Bovendien zijn de veranderde belastings-patronen in het bot en de mogelijke gevolgen daarvan op de lange termijn bestudeerd met behulp van eindige elementen modellen. Hierbij zijn twee experimenteel gemeten belastingen van een normale loopcyclus toegepast. De analyses tonen aan dat de mate van botingroei bij osseointegratie-implantaten een aanzienlijke invloed op de spanningsniveaus en energiedichtheden van het bot rond de prothese hebben. Dit wordt veroorzaakt door het implantaat zelf, maar ook door de veranderde belastingstoestand van het geamputeerde been. Het ISP-ontwerp resulteert in een meer fysiologisch spanningpatroon en een betere energiedistributie (wat gunstig is voor de lange termijn botremodelering), maar het OPRA ontwerp gegenereert lagere botspanningen (minder risico op botbreuken). Beide osseointegratie-implantaten lieten relatief lage mechanische veiligheidsfactoren zien ten aanzien van het breukrisico.

Vervolgens is in Hoofdstuk 3 onderzoek gepresenteerd naar veranderingen in het bot dat grenst aan de twee bestaande osseointegratie-implantaten. Hiervoor

zijn twee verschillende initiële condities gebruikt: implantatie direct na amputatie en de conventionele implantatie na gebruik van een kokerprothese. We hebben het verschil in botremodellering rondom de implantaten onderzocht en vervolgens beoordeeld of dit tot een fractuur zou kunnen leiden. Generieke, op CT-gebaseerde eindige elementen modellen van een intact en een geamputeerd femur met daarin modellen van het OPRA systeem en de ISP Endo/Exo prothese, zijn voor deze studie gecreëerd. Bij de botremodelleringsimulaties zijn de belastingen van het begin en het eind van de standfase van een normale loopcyclus gebruikt. Botverlies veroorzaakt door langdurig gebruik van een kokerprothese was ernstiger dan botverlies rondom de osseointegratie-implantaten. Rondom beide implantaten was botremodellering te zien, maar het titanium schroefimplantaat (OPRA systeem) veroorzaakte meer botverlies dan de poreus gecoate CoCrMo steel (ISP implantaat). De kans op een fractuur was hoger voor de conditie waarbij er eerst een kokerprothese was gebruikt vergeleken met de implantatie direct na amputatie. Beide osseointegratie-implantaten leiden tot aanzienlijk botverlies en dit wordt alleen maar erger na initieel gebruik van een kokerprothese. Vanuit biomechanisch oogpunt is het derhalve goed om het gebruik van een kokerprothese te beperken en om het ontwerp van osseointegratie-implantaten aan te passen om zo het botverlies te verminderen en fracturen te voorkomen.

In overeenstemming met het tweede doel van dit proefschrift zijn de resultaten van de analyse van de momenteel beschikbare, osseointegratie-implantaten gebruikt om een concept te ontwikkelen voor een verbeterde osseointegratie-implantaat, zoals beschreven in Hoofdstuk 4. Een systeem met meerdere componenten, bestaande uit een metalen kern omgeven door een huls met een elasticiteitsmodulus vergelijkbaar met het corticale bot, is beter in staat de natuurlijke krachtsoverdracht in het midden van een femur te herstellen dan de traditionele ontwerpen. Om de krachtsoverdracht tussen het implantaat en de osteotomie van het resterende femur te verbeteren, is een kraag, bedekt met een laag van zacht, elastisch materiaal aangebracht rondom de schacht. Daarnaast is een glijbeweging met kleine amplitude tussen de binnenste en buitenste laag van het implantaat toegevoegd aan het ontwerp, om de axiale en transversale krachten van elkaar los te koppelen en de afschuifspanningen tussen het bot en het implantaat te verminderen. Om osseointegratie van het implantaat te verkrijgen is een poreuze titanium coating aangebracht op het polyetheretherketone (PEEK) polymeer oppervlak dat in direct contact staat met het bot. Bovendien is het nieuwe ontwerp verkort ten opzichte van de bestaande implantaten, zodat ook fixatie mogelijk is in patiënten waarbij slechts een klein deel van het femur resteert. We hebben als hypothese aangenomen dat dit ontwerp het risico op botfalen rondom het implantaat zal verlagen en schadelijke botremodellering zal tegengaan, door de verbeterde krachtsoverdracht tussen de prothese en het femur. Op basis van CT-scans zijn generieke eindige elementen modellen gecreëerd van een intact femur en van geamputeerde botten geïmplanteerd met zowel het nieuwe implantaat als de twee bestaande protheses zoals ook bestudeerd in Hoofdstuk 3. Deze eindige elementen modellen zijn vervolgens getest onder belastingscondities horende bij wandelen en een voorwaartse val. De adaptive botremodelleringstheorie is gebruikt om te voorspellen welke veranderingen in het bot rondom het implantaat zullen optreden op de langere

termijn. Daarnaast is het risico op het falen van het bot rondom het implantaat geëvalueerd middels een von Mises spanningscriterium. De resultaten lieten zien dat bij het nieuwe ontwerp de spanningsverdeling in het bot dichter bij de fysiologische situatie ligt en dat er een lager risico op botfalen wordt gegenereerd in vergelijking met de OPRA en ISP implantaten. Als gevolg hiervan treedt er, zoals bleek uit de botremodelleringssimulaties, nauwelijks botverlies op rondom het nieuwe ontwerp, terwijl de twee andere implantaten beide aanmerkelijk botverlies veroorzaken aan de distale zijde van het femur.

In Hoofdstuk 5 werd met behulp van experimenten en eindige elementen modellen aangetoond dat het nieuwe implantaat een meer fysiologisch rekpatroon laat zien in vergelijking met het standaard titanium implantaat. In mechanische experimenten werden femora getest in 3 situaties. Bij de eerste situatie werden de femora intact gelaten, in de tweede situatie werd een standaard generisch implantaat geplaatst en in de derde situatie werd een prototype van het nieuwe implantaat geplaatst. Tijdens de experimenten werden rekken op de cortex van de femora gemeten. Er werden drie verschillende belastingscondities opgelegd die verschillende momenten uit de loopcylus simuleerden, namelijk: hielcontact, teenafzet en de monopedale fase. Met behulp van eindige elementen modellen die gegenereerd werden op basis van computed tomography (CT) data werden rekken berekend in de intacte femora en de beide situaties met de geimplanteerde femora. Zowel in de modellen met een standaard implantaat als die met het nieuwe implantaat werd 'strain shielding' (een verlaging van rek in de cortex rondom het implantaat) gedetecteerd, maar dit effect was groter in het geval van het standaard implantaat. Distaal ($p<0.04$) en halverwege de steel ($p<0.03$) werd een significant geringere strain shielding gevonden voor het nieuwe implantaat tijdens hielcontact. Verder zagen we significant minder strain shielding (21-29%) halverwege de steel van het nieuwe implantaat ($p<0.03$) tijdens de monopedale fase. De resultaten van de eindige elementen simulaties kwamen overeen met de experimentele resultaten, waarin de standaard implantaten ook meer strain shielding lieten zien. De afname in strain shielding als gevolg van het nieuwe design was groter in de simulaties dan in de experimenten, waarschijnlijk vanwege het feit dat er een perfecte fit tussen de kraag en de cortex werd gemodelleerd. Deze perfecte fit kon in de experimenten niet bereikt worden, door gebrekkig instrumentarium. Uit deze studie blijkt dat het nieuwe ontwerp de distale belastingsoverdracht lijkt te verhogen ten opzichte van het traditionele ontwerp, waardoor de strain shielding verminderd.

In Hoofdstuk 6, onderzochten we het ontstaan van slijtagepartikels in verband met het nieuwe implantaat. Tribologische metingen van de slijtage ten gevolge van cyclische microbeweging van verschillende combinaties PEEK polymeer met cobalt legering (CoCrMo) en titanium legering (Ti6Al4V) werden uitgevoerd. Resultaten lieten zien dat koolstofvezel versterkte PEEK (CFR-PEEK pitch) en Ti6Al4V minder slijtage vertonen in vergelijking met de controle ultra-high-molecular-weight polyethylene (UHMWPE) en CoCrMo interface, echter met relatieve hoge wrijving. Een compris zou CFR-PEEK pitch/CoCrMo kunnen zijn, vanwege een lagere wrijving in combinatie met een iets hogere slijtage.

Het doel van Hoofdstuk 7 was te onderzoeken of diamant-achtig carbon coatings (DLC) op PEEK materialen de tribologische prestaties van Ti6Al4V legeringen in combinatie met PEEK polymeren verbeteren. De toepassing van DLC coatings zorgde voor een goede slijtageweerstand met de PEEK en CFR-PEEK oppervlakken en een verminderde

wrijvingscoefficent tijdens droog glijden (tot waarden gelijk aan, of lager dan, UHMWPE). Een vergelijkbaar positief effect van de coating was te zien bij CFR-PEEK pitch in PBS gesmeerde condities. Daarom raden we aan om voor de nieuwe direct gefixeerde implantaten een DLC coating te gebruiken op CFR-PEEK pitch. Ook zou er overwogen moeten worden om DLC coatings te gebruiken op Ti6Al4V om slijtage te verlagen.

In Hoofdstuk 8 zijn biologische reacties van botweefsel geëvalueerd aan de hand van een in-vivo dierexperiment. Met de resultaten van het experiment is waardevolle informatie verkregen voor de productie van het implantaat en is meer inzicht gekregen in de complexiteit van het fixeren van het implantaat tijdens een operatieve ingreep. Vervolgens zouden de experimentele data worden gebruikt om de Eindige Elementen modellen te valideren die het spanningsafhankelijke adaptatievermogen van bot rondom het implantaat simuleren, maar helaas bleek dat de data voor dit laatste doel niet geschikt was.

In het laatste Hoofdstuk (Hoofdstuk 9) worden de resultaten uit dit proefschrift geplaatst in de context van de gestelde ontwerpeisen (Hoofdstuk 1). De uitgevoerde studies demonstreren de mogelijkheden van het nieuwe osseointegratie-implantaat. Het nieuwe concept is een verbetering ten opzichte van bestaande implantaten door het verlaagde risico op botfalen en het tegengaan van ongunstige botvervormingen. Daarnaast is het door de korte steel nu ook mogelijk om patiënten te behandelen waarbij de femurstomp relatief kort is. Om deze fase van het ontwikkelingsproces te voltooien, wordt aanbevolen vermoeiingstesten met het implantaat uit te voeren. Vervolgens zal het risico op infecties door de huidpenetratie moeten worden onderzocht en uiteindelijk kan de toepassing van het nieuwe implantaat in-vivo worden getest.

Het nieuwe osseointegratie-implantaat dat is ontwikkeld tijdens dit promotietraject, heeft de potentie om beperkende biomechanische factoren van bestaande ontwerpen op te lossen en zal ervoor zorgen dat een grotere patiëntengroep gebruik kan gaan maken van de voordelen van directe fixatie van uitwendige amputatieprotheses.

Streszczenie

Amputacja nogi jest trwałym uszczerbkiem na zdrowiu, który ma duży wpływ na mobilność pacjenta, styl i komfort życia. Systemy protetyczne pozwalają przezwyciężyć utratę funkcji części nogi, a dzięki wysokiemu zaawansowaniu technologicznemu współczesnej protetyki znacznie podnoszą sprawność pacjentów. Jednak tradycyjne mocowanie protezy do ciała za pomocą leja protezowego pozostaje ograniczającym aspektem w rehabilitacji. Ból kikuta, uszkodzenia tkanek miękkich, brak właściwej kontroli i trudności z odpowiednim dopasowaniem są częstymi problemami.

Alternatywnym rozwiązaniem dla standardowego mocowania protezy nogi (opartym na leju protezowym obejmującym kikut) jest bezpośrednie zamocowanie protezy z kością w oparciu o osseointegrację. Bezpośrednie połączenie protezy kończyny dolnej do układu kostnego pozwala uniknąć charakterystycznych dla leja protezowego problemów z obrażeniami skóry i dopasowaniem leja do kikuta. Ponadto ta metoda zapewnia lepszą kontrolę nad sztuczną kończyną i w konsekwencji pozwala na bardziej intensywne korzystanie z protezy, zwiększoną mobilność, a także pozwala na mniejsze zużycie energii przy chodzeniu. Z tych powodów cieszy się coraz większym zainteresowanie lekarzy i naukowców. Dostępna literatura wskazuje jednak, że rehabilitacja z tego typu przezskórnymi implantami wciąż pozostaje znacznym wyzwaniem z powodu różnego rodzaju ryzyka jakie ze sobą niesie, a mianowicie infekcji wokół implantu, okołoimplantowej utraty kości oraz mechanicznego uszkodzenia kości, a także implantu.

W rozdziale 1, w oparciu o systematyczny przegląd dostępnej literatury na temat implantów oferujących pacjentom po amputacjach bezpośrednie połączenie protezy z kością, zostały sformułowane cele projektu i wymagania dla ulepszonej konstrukcji osseointegrowalnego implantu.

Pierwszym celem tej pracy było zbadanie mechanicznych problemów i ograniczeń współczesnych implantów do bezpośredniego połączenia protezy z kością.

W rozdziale drugim dwa przezskórne implanty udowe, OPRA system (Integrum AB) i ISP Endo/Exo (ESKA Implant AG) zostały przeanalizowane za pomocą analizy metodą elementów skończonych pod względem prawdopodobieństwa uszkodzenia kości i zjawisk mechanicznych na styku kości z implantem zarówno bezpośrednio po operacji (przed wzrostem tkanki kostnej) jak i po pełnej osseointegracji. Ponadto analizowano mechaniczne następstwa wszczepiania implantów, takie jak zmiany w strukturze naprężeń wewnątrz kości i ewentualnych ich skutków dla długotrwałej przebudowy kości. W tym celu wykorzystano symulacje komputerowe oparte o metodę elementów skończonych, w których użyte zostały modele reprezentujące nienaruszoną kość udową i implanty wszczepione w te same kości udowe po amputacji. Do tego celu zostały zastosowane dwa obciążenia eksperymentalnie zmierzone podczas normalnego chodu pacjenta z bezpośrednim zamocowaniem protezy w kości.

Analizy wykazały, że wszczepienie protezy przezskórnej miało znaczący wpływ na poziom naprężeń i gęstości energii odkształcenia w kości wokół protezy. Było to spowodowane obecnością implantu, a także zmienionymi warunkami obciążenia kości

po amputacji na skutek utraty aktywności znacznej części mięśni. Implant ISP oferował bardziej fizjologiczny rozkład gęstości energii odkształcenia (sprzyjający długotrwałemu zachowaniu gęstości kości), natomiast implant OPRA generował niższe naprężenia w kości (oznaczające zmniejszenie ryzyka złamania kości). Oba implanty wykazały relatywnie niskie współczynniki bezpieczeństwa przed mechanicznym uszkodzeniem kości.

Następnie w rozdziale 3, zbadaliśmy długoterminowe zmiany kostne wokół implantów OPRA i ISP uwzględniając dwa różne warunki początkowe, a mianowicie implantację bezpośrednio po amputacji kończyny i implantację po znacznym okresie używania konwencjonalnego mocowania protezy nogi za pomocą leja protezowego. Przeanalizowaliśmy różnice w przebudowie kości wywołanej obecnością implantów i badaliśmy czy mogłyby one powodować uszkodzenie kości. Na podstawie tomografii komputerowej (CT) stworzone zostały generyczne (uogólnione) modele kości udowej przed amputacją i po amputacji z wszczepionymi oboma obecnie używanymi implantami do bezpośredniego mocowania protezy nogi.

Symulacje adaptacyjnej przebudowy kości wykorzystywały obciążenia charakterystyczne dla fazy zetknięcia pięty z podłożem i oderwania palców podczas normalnego chodu pacjenta. Odwapnienie kości (utrata kości) wywołane przez długotrwałe użycie leja protezowego miało poważniejsze skutki dla ostatecznej jakości kości niż adaptacja wywołana przez implanty. Oba implanty wywołały znaczną przebudowę kości, implant OPRA w kształcie tytanowej śruby wywołał większą utratę masy kostnej niż implant ISP pokryty porowatą powłoką ze stopu kobaltowo-chromowego (CoCrMo). Ryzyko okołoprotezowego złamania kości pozostawało wyższe w przypadku wcześniejszego użycia leja protezowego niż w przypadku implantacji bezpośredio po amputacji. Podsumowując, oba implanty służące do bezpośredniego połączenia protezy z kością prowadziły do znacznej utraty kości, która jest bardziej wyraźna po długim okresie używania leja protezowego. Dlatego też, z biomechanicznego punktu widzenia, zaleca się ograniczyć okres używania leja protezowego i przeprojektować implanty w celu zminimalizowania okołoprotezowej utraty masy kostnej oraz prawdopodobieństwa mechanicznego uszkodzenia kości.

Zgodnie z drugim celem tej pracy, wyniki analizy obecnych implantów zostały wykorzystane przy rozwijaniu konceptu ulepszonego osseointegrowalnego implantu, który został przedstawiony w rozdziale 4. Wieloczęściowy system składający się z rdzenia i zewnętrznej tulei o module sprężystości porównywalnym do kości zbitej ma za zadanie przywrócić naturalne obciążenia w trzonie kości udowej w znacznie lepszym stopniu niż w przypadku współczesnych konstrukcji. W celu zwiększenia dystalnego przenoszenia obciążenia pomiędzy implantem i osteotomią kości udowej po amputacji, do trzpienia dodano kołnierz z warstwą z elastycznego materiału. Ponadto, możliwość ruchu posuwnego pomiędzy wewnętrzną i zewnętrzną częścią implantu ma na celu oddzielenie naprężeń osiowych i poprzecznych i zminimalizowanie naprężeń stycznych na granicy implantu z kością.

Aby uzyskać osteointegrację pomiędzy kością a implantem, zastosowana została porowata tytanowa powłoka natryskiwana plazmowo na powierzchnię polietereterkenotu (PEEK) znajdującą się w bezpośrednim kontakcie z kością. Dodatkowo nowa

konstrukcja jest o wiele krótsza niż obecnie stosowane implanty, aby umożliwić wszczepienie u pacjentów z krótką pozostałością kości po amputacji. Postawiliśmy hipotezę, że tak zaprojektowany implant zmniejszy okołoprotezowe ryzyko uszkodzenia i niekorzystną przebudowę kości poprzez zmodyfikowany transfer obciążenia pomiędzy protezą, a kością udową umożliwiający bardziej fizjologiczne rozłożenie naprężeń w samej kości.

W celu zweryfikowania tej hipotezy zostały przeprowadzone obliczenia za pomocą metody elementów skończonych. Modele nienaruszonej kości udowej i kości po amputacji z wszczepionym modelem nowego implantu oraz implantów OPRA i ISP zostały stworzone na podstawie danych z tomografii komputerowej. Zastosowane zostały obciążenia charakterystyczne dla normalnego chodu oraz upadku do przodu. Długoterminowe zmiany kości wokół implantów zostały przewidziane na podstawie teorii adaptacyjnej przebudowy kości, a ryzyko uszkodzenia kości wokół protezy zostało wyznaczone na podstawie kryterium von Misesa. Wyniki wykazały, że nowa konstrukcja w porównaniu z implantami obecnie używanymi OPRA i ISP zapewnia bliższy fizjologicznemu rozkład naprężeń w kości i mniejsze ryzyko uszkodzenia kości podczas chodzenia. W konsekwencji, symulacje przebudowy kości nie wykazały ogólnej utraty kości wokół nowego implantu, w przeciwieństwie do obu współczesnych implantów, które wywołują istotne straty kości w dystalnej części kości udowej.

W rozdziale 5 zastosowano techniki eksperymentalne i porównano je z analizą przeprowadzoną metodą elementów skończonych, aby zweryfikować czy nowy implant wywołuje bardziej fizjologiczny rozkład naprężeń w kości, w porównaniu ze standardowym implantem z tytanu. Naprężenia na powierzchni kości zostały zmierzone najpierw bez, a następnie z implantami.

Trzy konfiguracje obciążenia zostały zastosowane w pomiarach: zetknięcie pięty z podłożem, oderwanie pięty i stanie na jednej nodze.

Dane uzyskane za pomocą tomografii komputerowej zostały użyte do symulacji odkształceń nienaruszonej kości i kości z modelami dwóch rodzajów implantów za pomocą metody elementów skończonych. Znacząca redukcja odkształceń w porównaniu z nienaruszoną kością (tzw. ekranowanie odkształceń) nastąpiła wokół obu typów implantów, jednakże znacznie mniej w przypadku prototypu nowego implantu.

Statystycznie znaczące różnice w ekranowaniu odkształceń pomiędzy oboma implantami uzyskano podczas zetknięcia pięty z podłożem w dystalnej części kości ($p<0,04$) i w regionie powyżej ($p<0,03$), również podczas stania na jednej nodze ($p<0,03$). Nowy implant wykazał od 21 do 29 procent mniejsze ekranowanie odkształceń niż standardowy implant. Wyniki symulacji pozostawały w zgodzie z pomiarami doświadczalnymi, a mianowicie znacznie większe ekranowanie odkształceń w kości było wywołane przez standardowy niż nowo zaprojektowany implant. Wyniki symulacji były bardziej korzystne dla nowego implantu w stosunku do pomiarów doświadczalnych na wskutek założenia o dokładnym przyleganiu kołnierza protezy do kości w modelu numerycznym. Taki kontakt nie był możliwy do osiągnięcia w doświadczeniach, a w praktyce wymagałby wrostu kości w powierzchnię implantu. Badania wykazały, że nowy implant ma możliwość dystalnego przenoszenia obciążeń do kości udowej i zmniejszenia ekranowania odkształceń w porównaniu ze standardowym implantem.

W rozdziale 6 badano potencjalne powstawanie produktów tarcia w odniesieniu do nowego implantu. Zachowania się różnych kombinacji par materiałów takich jak polimery oparte na PEEK-u w zestawieniu ze stopem kobaltowym (CoCrMo) i tytanowym (Ti6Al4V), poddanych tarciu suwnemu zostało wyznaczone w badaniach trybologicznych. Wyniki pokazały, iż para materiałów CFR-PEEK pitch i Ti6Al4V jest zdolna do generowania mniejszego zużycia niż polietylen ze stopem kobaltowym (UHMWPE/CoCrMo) użyty jako kontrola. Z powodu wysokiego współczynnika tarcia, jako alternatywę, zaproponowano parę materiałów PEEK CFR pitch/CoCrMo, które oferują dobry kompromis pomiędzy oporami tarcia i odpornością na ścieranie.

Rozdział 7 miał na celu zbadanie możliwości zastosowania diamentopodobnej powłoki węgla (DLC) na PEEK-u w celu zoptymalizowania właściwości trybologicznych na styku stopu Ti6Al4V i różnych rodzajów PEEK-ów. Nałożone powłoki DLC zapewniały bardzo dobrą odporność na ścieranie powierzchni polimerowych i znaczne obniżenie współczynnika tarcia w czasie suwu w warunkach suchych (wartości zbliżone lub niższe niż UHMWPE). Podobne pozytywne działanie powłoki zaobserwowano dla testowanego w buforowanym roztworze soli fizjologicznej (PBS) materiału CFR-PEEK. W związku z tym, zaleca się stosowanie powłoki diamentopodobnej w nowym implancie na powierzchni CFR-PEEK pitch i również rozważenie możliwości wykorzystania podobnej powłoki na powierzchni stopu tytanu Ti6Al4V.

W rozdziale 8 przeprowadzone zostały badania in-vivo w celu oceny ogólnej odpowiedzi biologicznej tkanki kostnej na implant oraz zweryfikowania wyników symulacji adaptacyjnej przebudowy kości wokół nowego typu implantu.

Pomimo napotkanych problemów z dopasowaniem rozmiarów implantów do kształtu kości udowych kóz, zebrane zostały cenne informacje dające wgląd w możliwości produkcji nowego implantu i złożoności zabiegu chirurgicznego wszczepienia nowego implantu.

Ostatni rozdział (rozdział 9) omawia wyniki uzyskane w ramach tej pracy w kontekście wymagań postawionych w rozdziale 1 dla ulepszonej konstrukcji osseointegrowalnego implantu. Przeprowadzone badania potwierdzają możliwości opracowania nowego implantu, który oferuje ulepszenia w stosunku do istniejących urządzeń, w postaci zmniejszenia ryzyka uszkodzenia i niekorzystnej przebudowy kości. Pozwala również na rehabilitację pacjentów z krótkimi pozostałościami kości po amputacji z powodu ograniczonej długości implantu. W celu sfinalizowania obecnej przedklinicznej fazy rozwoju nowego implantu zaleca się wykonywanie badań zmęczeniowych implantu, zbadanie ryzyka zakażeń skóry wokół elementu przezskórnego i ostatecznie także zbadanie zachowania się nowego implantu in-vivo.

Podsumowując, opracowany w ramach tej tezy nowy osseointegrowalny implant ma potencjał przezwyciężyć wiele ograniczeń biomechanicznych obecnych implantów i pozwoli większej liczbie pacjentów skorzystać z zalet bezpośredniego mocowania zewnętrznych systemów protetycznych.

Acknowledgements
Dankwoord
Podziękowania

It has been almost five years since this project started and now I am writing the very last pages of this thesis book (what a strange feeling to write a book at all...). Time to take a short look back and give credit to all of you, who directly or indirectly helped to get things done.
First of all I would like to thank my promoters for their expertise, advice and support:

Prof. dr. ir. Bart Verkerke, dear Bart, five years ago I entered your office and you gave me opportunity to do this research. It is funny that our paths have crossed already for the second time since then :), though we both realized it much later. It was a pleasure to learn from you; I am impressed by your creativity and persistency in realizing your ideas and plans. I always enjoyed your easygoing attitude and calm (which I managed to disturb at least once...). Good luck with the SPRINT initiative; it would be certainly nice to work on a project again with you.

Prof. dr. ir. Nico Verdonschot, dear Nico, your deep knowledge, analytical skills in combination with „contagious" enthusiasm and energy makes you an inspiring promoter. Your open attitude made it a pleasure to work and travel with you. Thank you for your input into this project and also giving me opportunity to develop further in the ORL. You and Pieter made this lab a great place to work. Fingers crossed for the JOINt initiative.

Prof. dr. Sjoerd Bulstra, dear Sjoerd, your clinical input and insights into the project were very valuable. Thank you for taking time from your busy schedule to come to Nijmegen for experiments and to proofread manuscripts and the thesis.
Of course, a PhD cannot be done without networking and I would like to thank all my collaborators and co-authors:

Prof. dr. Jeff de Hosson and dr. Yutao Pei, dear Jeff and Yutao, thank you for the invaluable input into this thesis, it was a pleasure to collaborate with you!

Prof. dr. ir. Dik Schipper and ing. Walter Lette, dear Dik and Walter, thank you for guiding me in the field of tribology, for your patience and performing experimental work, which supplied me with data for an important chapter in this book.

Prof. dr. Pieter Buma, dear Pieter, thank you for your contribution to the in-vivo study and making ORL such a nice environment to work in.

Mike van Diest, MSc, dear Mike, you performed great during your master project and congratulations for the prizes you got for your work. Your optimism and sense of humour made it very enjoyable to work with you. I am glad that you liked the research and wish you good luck with your PhD project, I am sure you will make the best out of it!

Dr. Gerjon Hannink, dear Gerjon, thanks for your cheerful attitude and advice and teaching me some statistics, it is always nice to hear you "maestro". Veel succes met JOINt!

Bastien Lasnier, BSc, thanks for your company during long experimental hours spent in the ORL's basement.

Prof. dr. Hans Rietman, thank you for your enthusiasm towards the project and that you are always ready to help.

Ward, Anne, Loes, René, Eric, Astrid, Nico en Bart, hartelijk bedankt voor jullie hulp met Nederlandse samenvatting!

Elk concept tijdens de ontwikkeling moet gematerialiseerd worden en hiervoor wil ik de verspaningsspecialisten bedanken voor het fantastische werk: **Jeroen, Wolter, Mark**. Alvast bedankt!

Gianpaolo and **Pierfrancesco,** many thanks for the nice collaboration and your work, although the experimental results were not exactly as expected, you did a professional job and it would definitely be great if we could collaborate sometime.

Semme, Frits en **Frank,** bedankt voor het delen van jullie kennis en jullie inspanningen bij de commercialisering van dit project.

To my invaluable paranymphs, **Ward** and **Anita**, thank you for your support and assistance in preparations for the defence. Last months are always extremely busy but you made it much lighter for me, alvast bedankt!

Ward, many thanks for all the time spent together, your hospitality and friendship. You are an inspiring men with many passions, the long evening discussions with a 'glass' of jenever will be definitely missed! Good luck with your new job(s) and remember that you and Cristina are always welcome in Nijmegen.

Anita, your energy and enthusiasm seems to be endless and that is what makes you very special person. Good luck with your PhD, I am sure you will make it great and reach your goals!

A special thanks to all my roommates, both past and present, **Shanti, Marten, Oana, Punto, Stefan, Chris, Anne, Sanaz, René, Huub, Astrid, Tony, Mircea**, thank you for making my stay in our office so pleasant, nice talks and coffee-breaks.

Shanti, it was always a pleasure to learn from you about Indonesian culture and food (I know now that your mother's sambal is definitely the best!). Semoga kita dapat berjumpa lagi baik di Eropa ataupun di Indonesia.

Marten, thanks for introducing me to Bart (I think it was during the trip to Poland when you mentioned about a professor, who is looking for a PhD candidate...). It was a pleasure to share the office with you!

Punto, your regular treat with Indonesian food for lunch was truly great! terima kasih! All the best in your work back home in Indonesia!

René A, it was cool to share office with you man! I like the blast of energy that comes with your music. Fingers crossed for new records and tours and good luck with your new job!

Anne, you are the most organized person I have ever known, I could learn a lot from you. Thanks for nice chats and help with various things!

I would like to thank all the colleagues from the former Artificial Organ group and Biomedical Engineering Department, **Gerard, Gerwin, Gu, Reindert, Tjar, Ed, Marten, Sandra, Oana, Anita, Shanti, Stefan, Ward (and all his students), Adam, Katia P, Guru, Deepak, Agnieszka, Anton, Shariar, Łucja, Jesse, Arina, Prashant, Bastiaan, Ellen, Punto, Adi, Das, Titik, Mihaela, Katia O, Joana, Joop, Babs**, thanks for nice chats during coffee-breaks, overtime activities and always creating a nice atmosphere to work.

A special thanks to the whole Orthopaedic Research Lab, both former and current colleagues: **Nico, Pieter, Esther, Dennis, Gerjon, Ineke, Willem, René A, Léon, Huub, Jorrit, Daan, René vd V, Astrid, Loes, Anne, Sanaz, Erwin, Lisbeth, Marysia, Pieter H, Hendi, Eric, Wojtek, Veronica, Thom**. Many thanks for your help with various things, nice stays at conferences and making the lab a pleasant environment.

Marysiu, dzięki wielkie za wspólne kolacje i gościnność podczas moich wizyt w Nijemgen, a później przygarniecie nas na Steenhommelhof :) powodzenia w Mediolanie (super miasto) i pozdrowienia dla Michele.

Daan, you are great guy, regular dinners and chats will be definitely missed, but hope we can find some time to meet up from time to time. Good luck with your new position! Greetings to Nora and a hug to Merkel!

Willem, many, many thanks for your technical assistance in various experiments, your expertise is always invaluable for the lab and it was not different in case of my research!

Léon, thank you for your technical assistance in various lab works and always positive attitude.

Dennis, thanks for your help with multiple various things, your sharp comments are always appreciated, it is nice working with you!

Eric, you are a nice guy, always keen for social activities and ready to give a hand, thanks for that!

Ineke, during last couple of years you probably answered more my questions than anybody else, thank you for your assistance with all

Hendi, your friendliness and politeness constantly keeps on impressing me; it is not always easy but you are always motivated and I am sure you will make it! semoga sukses!

Wojtek, dzięki za wypady na siłownię („jest moc, nie ma lipy") i squasha, zawsze miło spotkać się z Tobą i Olą. Powodzenia w pracy naukowej!

Veronica, many thanks for correcting my English texts and congratulations on your new job! It will be nice to have you as a colleague in the ORL.

Groningen people (current and former), thank you for all the fun activities, meetings and chats during coffees and parties, that made my time in Groningen a memorable

experience, among others greetings to: **Antek, Kasia, Saskia, Deepak, Agnieszka, Magda, Henk, Szymon, Michał, Ola, Gosia, Jan, Andreas, Maria, Jesús, Elie, Emila, Mat, Monika, Adam** and many, many more... (so difficult to name all names at once).

Antek, dzięki za ciekawe dyskusje i mile spędzony czas, który zawsze pozwalał się oderwać od pracy i zrelaksować (może czasami aż za...). Zawsze super jest widzieć Ciebie i Kasię, samych sukcesów w pracy dla was obojga!

Saskia, hartelijk bedankt voor je hulp en bereidheid om mijn Nederlands altijd te corrigeren. Het was echt een plezier met je (en in het begin ook met Magda) elke week te babbelen. Succes met je werk en geniet om het wonen in de buurt van je familie.

Deepak it is always fun to meet up with you, your energy and enthusiasm makes you a great lad, I am sure you will succeed as an entrepreneur, thank you to you and **Agnieszka** for letting me and Gosia stay at your place. **Agnieszka**, dzieki za miłe spotkania i gościnność, powodzenia w kończeniu doktoratu.

Asia i Michał, dzięki za miłe spotkania, wspólne kolacje i weekendowe wypady na łono dzikiej holenderskiej przyrody! Fajnie, że zostajecie w Asmterdamie.

Serdeczne pozdrowienia dla wszystkich znajomych w Polsce, dzięki za miłe spotkania i rozmowy za każdym razem kiedy wpadamy na kilka dni w odwiedziny. **Michał i Dominka, Bartek i Agnieszka, Paweł, Malina, Piotrek, Agnieszka i Łukasz**.

Mamo i Tato, dziękuję Wam za to że zawsze jesteście i byliście dla mnie, waszą mądrość i wsparcie! Przez te rozjazdy trochę rzadko się widujemy ale zawsze są to bardzo miłe chwile. Dziękuję za wszystko!

Ania, hej siostra, dzięki za wszystko, powodzenia na studiach i być może do zobaczenia wkrótce w Holandii!? Trzymam kciuki!

Serdeczne podziękowania dla całej rodziny: drogie babcie **(Janka, Bronia, Hela i Rela)** i dziadkowie **(Zdzicho i Tadeusz)**, mamo **Aniu**, ciocie **(Basia, Zosia, Gosia, Todzia, Bożenka, Wiesia, Grażynka)** i wujkowie **(Czesiek, Heniek, Rysiek, Tadeusz, Mirek)**, **Łukasz, Agnieszka, Aneta, Marek, Ania, Jarek, Kasia, Zosia, Antoś, Piotrek, Paweł, Jacek, Aneta, Michał,** dziękuję za wiele miłych spotkań i zawsze ciepłe przyjęcie.

Gosiu i ... dziękuję za cierpliwość i wsparcie, wspólne podróże i doświadczenia, nie ma nic lepszego niż dzielić z Tobą każdy dzień, nie mogę się doczekać kiedy już będziemy we trójkę, kocham Cię:*

Nijmegen, September 5, 2012.